

Dear Dr. Zhang:

Please find below our itemized responses to the reviewer's comments. We have addressed the comments raised by both reviewers, and incorporated their comments / suggestions in the revised manuscript.

Thank you very much for your consideration.

Sincerely,

Xuejun Liu and Zhaozhong Feng

On behalf of all co-authors

Anonymous Referee #1

This paper presented spatial and temporal trends of reactive nitrogen species in air, precipitation and deposition in eastern China. Some of the spatial patterns described in the paper are interesting, such as the higher rural concentrations observed in the northern region compared to the southern region. The paper discusses the need for ammonia emissions policies to reduce reactive nitrogen in air and in deposition. The nitrogen datasets from this ground-based measurement network is valuable; however, a longer dataset needs to be collected before it is suitable for analyzing temporal trends. With only five years of data, this could be the main reason why most of the annual trends were not significant. Another concern that I have is a lack of explanation on the causes of the spatial and temporal trends, which requires analyzing the reactive nitrogen data with other datasets. The discussions seems biased towards ammonia emissions reductions as a more effective means of reducing reactive nitrogen than NO_x and SO₂ emissions reductions, but I don't think there is enough evidence in this study supporting this conclusion.

Response: Thanks for the referee's thoughtful and critical comments on our manuscript. Below we provide a point-by-point response to the reviewer' comments and how we have addressed them in the revised manuscript (in blue).

Specific comments

Line 77: Define Nr since this is the first time that it is mentioned in the paper.

Response: N_r has been defined as “reactive nitrogen” occurring in the first time in the text.

Line 83: Be more careful about linking deposition of N to increased greenhouse gas emissions. The referenced article only suggests that the nitrogen cycle is coupled with the carbon cycle and climate variation; however, the latter could be influenced by many factors.

Response: We have deleted “increased greenhouse gas emissions” and the referenced article in the revision.

Lines 110-111: The analysis presented by Xu et al. (2015) is quite similar to this study in terms of the measurement network, nitrogen species, time period, and site categories analyzed. The authors should discuss the previous study and explain how this study is different to avoid presenting a duplicate analysis.

Response: Thank you for this valuable suggestion. In the revised paper, we have added some sentences to discuss the study of Xu et al., (2015), and explain why the current study is different from the previous one. For details, please see our response to next comment (Lines 148-156).

Lines 148-156: This is where it might be appropriate to discuss the previous study, Xu et al. (2015), and emphasize the new work that will be shown in this study.

Response: The main purpose of this study was to reveal spatial-temporal (annual and seasonal) patterns of N_r concentrations and deposition based on a full 5-year (2011-2015) measurement at 27 NNDMN sites in eastern China and its northern and southern parts. It also should be noted that, although the study of Xu et al. (2015) and this study both examined the spatial patterns, the regions divided are different. In contrast, the study of Xu et al., 2015 mainly focused on spatial pattern of N deposition at six regions in China, and did not consider seasonal and annual trends. We have added the following sentences in the revision.

“Our previous work (Xu et al., 2015) used multiyear measurements (mainly from Jan. 2010 to Sep. 2014) at the 43 sites in the NNDMN, aiming to provide the first quantitative information on atmospheric N_r concentrations and pollution status across China, and to analyze overall fluxes and spatial variations of N deposition in relation

to anthropogenic N_r emissions from six regions”.

Reference:

Xu, W., Luo, X.S., Pan, Y.P., Zhang, L., Tang, A.H., Shen, J.L., Zhang, Y., Li, K.H., Wu, Q.H., Yang, D.W., Zhang, Y.Y., Xue, J., Li, W.Q., Li, Q.Q., Tang, L., Lu, S.H., Liang, T., Tong, Y.A., Liu, P., Zhang, Q., Xiong, Z.Q., Shi, X.J., Wu, L.H., Shi, W.Q., Tian, K., Zhong, X.H., Shi, K., Tang, Q.Y., Zhang, L.J., Huang, J.L., He, C.E., Kuang, F.H., Zhu, B., Liu, H., Jin, X., Xin, Y.J., Shi, X.K., Du, E.Z., Dore, A.J., Tang, S., Collett, J.L., Goulding, K., Sun, Y.X., Ren, J., Zhang, F.S., and Liu, X.J.: Quantifying atmospheric nitrogen deposition through a nationwide monitoring network across China, *Atmos. Chem. Phys.* 15 (13), 12345–12360, 2015.

Line 170: Suggest using “and” instead of “resulting in” because this sentence suggests there is a relationship between economic development and nitrogen emissions. If there is such relationship, please elaborate.

Response: Agree and done.

Lines 220-221: You need to be clearer about what type of deposition the open sampler collects. Why is it only “some” dry deposition? Isn’t the sampler open to the atmosphere which means it is collecting total deposition?

Response: We ensure that N deposition collected by continuously-open rain gauge refers to wet/bulk deposition, rather than total deposition. Wet/bulk deposition is generally defined as the sum of wet plus some dusts in non-precipitation period (i.e. sedimentary deposition); while dry deposition includes both gases and particles deposition (in which dust or sedimentary deposition is not included). In fact, the wet/bulk plus dry deposition consists of total N deposition without overestimation.

Although N-containing gases and fine particles can be deposited in the 'dry' form to the sampler funnel, the amount of N captured is negligible compared with the dry deposition to plant canopies (Dämmgen et al., 2005; Sutton and Bleeker, 2013). Thus, it is only “some” or small part dry deposition. To make it clearer, “some” was replaced by “incomplete” in the revision.

References:

Dämmgen, U., Erisman, J. W., Cape, J. N., Grünhage, L., and Fowler, D.: Practical

considerations for addressing uncertainties in monitoring bulk deposition, Environ. Pollut. 134(3), 535–548, 2004.

Sutton, M.A., and Bleeker, A.: Environmental science: the shape of nitrogen to come. Nature 494, 435–437, 2013.

Line 271: The dates here should be January 2011 to 30 September 2014 because you stated in the next sentence that the data after 30 September 2014 were not used.

Response: This was a wrong expression in the sentence. Actually, we used the daily IASI-NH₃ data from 1 January 2011 to 31 December 2015 for the spatial analysis, and from January 2011 to 30 September 2014 for temporal analysis.

We now state that “The daily IASI-NH₃ data (provided by the Atmospheric Spectroscopy Group at Université Libre De Bruxelles, data available at <http://iasi.aeris-data.fr/NH3/>) from 1 January 2011 to 31 December 2015 was used for the spatial analysis in the present study. For the temporal analysis, we used the IASI_NH₃ from 1 January 2011 to 30 September 2014 because an update of the input meteorological data on 30 September 2014 had caused a substantial increase in the retrieved atmospheric NH₃ columns.”

Lines 347-349: The concentration ranges are not clear. Is it the range of the mean concentration between sites or between years?

Response: The ranges of mean concentrations denote the minimum and maximum 5-year mean concentrations of measured five N_r species (i.e., NH₃, NO₂, HNO₃, pNH₄⁺, and pNO₃⁻) for each land use type (i.e., urban, rural and background), which can be derived from Table 1. For example, the values of 1.6 ± 0.2 and 10.2 ± 1.0 µg N m⁻³ are 5-year mean concentrations of HNO₃ and NO₂ at urban sites in eastern China, respectively.

To make it clear, in the revision we now state that “In eastern China, annual mean concentrations of NH₃, NO₂, HNO₃, pNH₄⁺, and pNO₃⁻ at the urban sites (averages for the 5-year, 1.6 ± 0.2 (for HNO₃) to 10.2 ± 1.0 (for NO₂) µg N m⁻³) increased by 18, 70, 33, 23, and 43%, respectively, compared with their corresponding concentrations at the rural sites (1.2 ± 1.0 (for HNO₃) to 7.2 ± 0.9 (for NH₃) µg N m⁻³); they also increased by 78-118% compared with the concentrations at the

background sites (0.9 ± 0.1 (for HNO_3) to 5.2 ± 0.3 (for NO_2) $\mu\text{g N m}^{-3}$) (Table 1).”

Lines 350-352: What is the reason for the lower concentrations at urban sites in the northern region?

Response: This is mainly due to the fact that the North China Plain (NCP, that is, the plain areas in Beijing, Tianjin, Hebei, Henan, and Shandong provinces) is located in the northern region. The Plain (i.e., NCP) is featured by intensive agricultural production in rural areas, which contributes 30-40% of the total annual NH_3 emissions in China (Huang et al., 2012). In addition, the north is dominated by calcareous soils, which favor high soil NH_3 volatilization from croplands (Huang et al., 2015). Those emitted NH_3 can directly enhance ambient NH_3 concentration and also particulate NH_4^+ concentrations via chemical reactions between NH_3 and acidic gases in the atmosphere (e.g., H_2SO_4 and HNO_3).

References:

Huang, X., Song, Y., Li, M. M., Li, J. F., Huo, Q., Cai, X. H., Zhu, T., Hu, M., and Zhang, H. S.: A high-resolution ammonia emission inventory in China, *Global Biogeochem. Cycles* 26, GB1030, 2012.

Huang, P., Zhang, J. B., Xin, X. L., Zhu, A. N., Zhang, C. Z., Ma, D. H., Zhu, Q. G., Yang, S., and Wu, S. J.: Proton accumulation accelerated by heavy chemical nitrogen fertilization and its long-term impact on acidifying rate in a typical arable soil in the Huang-Huai-Hai Plain, *J. Integr. Agric.* 14, 148–157, 2015.

Lines 359-365: I suggest analyzing which nitrogen species was particularly higher between urban and rural sites and between northern and southern regions because this would provide some insight whether the patterns are related to a specific type of emission source.

Response: Good point. In the old version, we have made a comparison of annual mean concentration of each N_r species between urban and rural sites, as shown in Table 1. In Results Section, we also stated that “In eastern China, annual mean concentrations of NH_3 , NO_2 , HNO_3 , $p\text{NH}_4^+$, and $p\text{NO}_3^-$ at the urban sites (1.6 ± 0.2 to $10.2 \pm 1.0 \mu\text{g N m}^{-3}$) were 18-70% and 78-118% higher than their corresponding concentrations at the rural (1.2 ± 1.0 to $7.2 \pm 0.9 \mu\text{g N m}^{-3}$) and background (0.9 ± 0.1

to $5.2 \pm 0.3 \mu\text{g N m}^{-3}$) sites, respectively.”. According to suggestion by the reviewer, the sentence was revised to make it clearer, and now reads as “In eastern China, annual mean concentrations of NH_3 , NO_2 , HNO_3 , $p\text{NH}_4^+$, and $p\text{NO}_3^-$ at the urban sites (averages for the 5-year, 1.6 ± 0.2 (for HNO_3) to 10.2 ± 1.0 (for NO_2) $\mu\text{g N m}^{-3}$) increased by 18, 70, 33, 23, and 43%, respectively, compared with their corresponding concentrations at the rural sites (1.2 ± 1.0 (for HNO_3) to 7.2 ± 0.9 (for NH_3) $\mu\text{g N m}^{-3}$); they also increased by 78-118% compared with the concentrations at the background sites (0.9 ± 0.1 (for HNO_3) to 5.2 ± 0.3 (for NO_2) $\mu\text{g N m}^{-3}$) (Table 1).”

As for comparisons between northern and southern regions, we added the following sentence in the revision.

“Averaged across three land use types, the annual mean N_r concentrations of five N_r species in the north increased to varying extent (by 84% for $p\text{NO}_3^-$, 63% for $p\text{NH}_4^+$, 57% for NH_3 , 47% for NO_2 , and 28% for HNO_3) compared with those in the south.”.

Lines 371-374: What is the reason for the higher precipitation concentrations in northern rural sites compared to southern rural sites? Is this related to the higher air concentrations of N_r species in northern rural sites?

Response: Yes, it is mainly due to significantly ($p < 0.05$) higher air concentrations of five N_r species at northern rural sites than at southern rural sites (Table 1), as $\text{NH}_4^+\text{-N}$ and $\text{NO}_3^-\text{-N}$ in precipitation primarily originates from reduced N (e.g., gaseous NH_3 and particulate NH_4^+) and oxidized N (e.g., gaseous NO_2 , HNO_3 , and particulate NO_3^-) in air (Wang et al., 2018). Another reason is the "concentration effect" because annual precipitation is much lower in the north (e.g. 400-600 mm per year) than in the south (e.g. 800-1400 mm per year).

Reference:

Wang, H.B., Shi, G.M., Tian, M., Chen, Y., Qiao, B.Q., Zhang, L.Y., Yang, F.M., Zhang, L.M., and Luo, Q.: Wet deposition and sources of inorganic nitrogen in the Three Gorges Reservoir Region, China, *Environ. Pollut.*, 233, 520-528, 2018.

Lines 383-401: Presenting only the annual trends in the N_r concentrations is not enough. I think that additional analysis with other variables is necessary to attempt to

explain the trends in N_r concentrations (e.g. emissions data). As stated in the introduction, one of the goals of this study is to assess the effectiveness of emissions control measures.

Response: We partly agree with the referee. Given that N_r (NH_3 and NO_2) emissions and concentrations are in different units, and higher N_r concentrations generally result in higher N deposition on an annual timescale, the comparison of N_r emissions with deposition (both are calculated in the unit of $kg\ N\ ha^{-1}\ yr^{-1}$) is more reasonable relative to the comparison between N_r emissions and concentrations. As the main objective of this study is to spatial-temporal patterns of atmospheric inorganic N concentrations and deposition, we presented relevant results of N_r concentrations and deposition in the Results, and put the comparison between N_r emission and deposition in the Discussions (please see Section 4.5 in the old version). Therefore, we keep the analysis as it is.

According to the referee's suggestion, here we also attempt to make the corresponding comparisons using the annual average values on N_r emissions (NH_3 and NO_x) and air concentrations of NH_3 and NO_2 at the sixteen sites (details are given in Section 4.5). As shown in Figure 1 below, across all the sites annual mean NH_3 emissions and concentrations showed increases of 4 and 20% in 2013-2015 compared with those in 2011-2015, respectively. Correspondingly, annual mean NO_x emissions and NO_2 concentrations showed reductions of 18 and 2%, respectively. In addition, there were no significant ($p>0.05$) correlations between NH_3 emissions and concentrations, and between NO_x emissions and concentrations during 2011-2015.

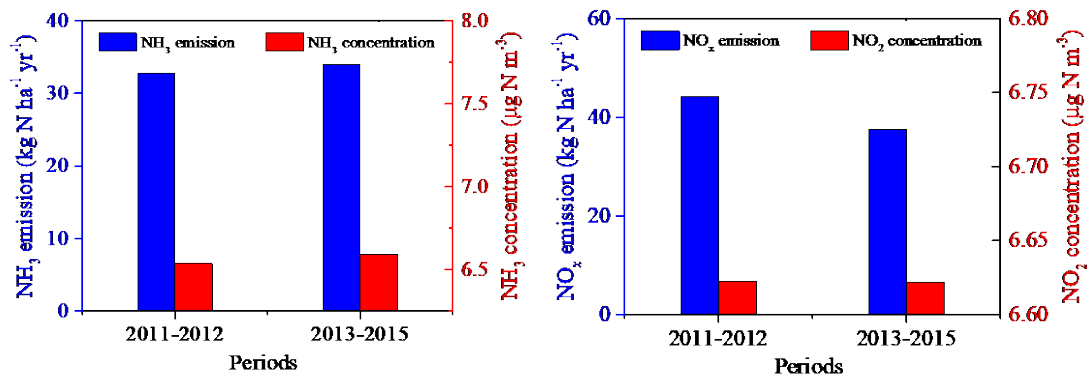


Figure 1. Comparisons of NH₃ emissions and NH₃ concentrations, and NO_x emissions and NO₂ concentrations between the periods 2011-2012 and 2013-2015.

Lines 411-416: Any relationships between precipitation concentration and air concentration trends?

Response: Based on analysis of annual averages at the sixteen sites with continuous and simultaneous measurements of dry and wet/bulk N deposition during 2011-2015 (site names are given in Fig. S6 and Table S1), a positive relationship ($r=0.62$, $p=0.27$) was found between NH₄⁺-N concentrations in precipitation and air concentrations of reduced N_r (the sum of NH₃ and particulate NH₄⁺), whereas a negative relationship ($r= -0.85$, $p=0.07$) was found between NO₃⁻-N concentration in precipitation and air concentration of oxidized N_r (the sum of NO₂, HNO₃, and particulate NO₃⁻). We think that those findings are acceptable. This is because that NH₃ is locally deposited and relatively high NH₃ concentration generally distributed near emission sources. In contrast, local oxidized N_r concentration can be affected by atmospheric transport from nearby regions. No significant correlations between precipitation concentration and air concentration are mainly due to relatively small changes in NH₃ and NO_x emissions (Fig. 12) and annual mean precipitation amount (from 800 to 951 mm, Fig. S14) during 2011-2015.

Lines 422-436: What is the reason for the seasonal trends? E.g. changes in emissions, meteorology, and/or air mass patterns? I think these other factors need to be analyzed in order to understand what is influencing the seasonal trends.

Response: Thank you for pointing it out, and we have analyzed the seasonal trends of N_r concentrations integrated with changes air mass trajectory (please see added context in Section 4.2). As for N_r emissions, it is well known that NH₃ emissions in China typically peaked in summer due to the summertime application of fertilizer for double cropping in together with higher temperature, and the lowest values occurred in winter (Paulot et al., 2014; Kang et al., 2016; Zhang et al., 2018). In contrast, the highest NO₂ emissions generally occur in winter because of domestic heating needs, and minimum values generally occur in spring (Zhang et al., 2007). Thus, we directly used previous literature reported to explain corresponding results in the present study.

References:

- Paulot, F., Jacob, D.J., Pinder, R.W., Bash, J.O., Travis, K., and Henze, D.K.: Ammonia emissions in the United States, European Union, and China derived by high-resolution inversion of ammonium wet deposition data: Interpretation with a new agricultural emissions inventory (MASAGE_NH₃), *J. Geophys. Res. Atmos.*, 119, 4343–4364, <https://doi:10.1002/2013JD021130>, 2014.
- Kang, Y. N., Liu, M. X., Song, Y., Huang, X., Yao, H., Cai, X. H., Zhang, H. S., Kang, L., Liu, X. J., Yan, X. Y., He, H., Zhang, Q., Shao, M., and Zhu, T.: High-resolution ammonia emissions inventories in China from 1980 to 2012, *Atmos. Chem. Phys.*, 16, 2043–2058, 2016.
- Zhang, Q., Streets, D. G., He, K., Wang, Y., Richter, A., Burrows, J. P., Uno, I., Jang, C. J., Chen, D., Yao, Z., and Lei, Y.: NO_x emission trends for China, 1995-2004: The view from the ground and the view from space, *J. Geophys. Res.*, 112, D22306, 2007.
- Zhang, L., Chen, Y. F., Zhao, Y. H., Henze, D. K., Zhu, L. Y., Song, Y., Paulot, F., Liu, X. J., Pan, Y. P., and Huang, B. X.: Agricultural ammonia emissions in China: reconciling bottom-up and top-down estimates, *Atmos. Chem. Phys.*, 18, 339–355, 2018.

Line 478: Instead of presenting bulk deposition, is it possible to estimate wet deposition fluxes by subtracting the dry deposition fluxes from bulk deposition? This allows a comparison between wet and dry deposition.

Response: Our previous work (Liu et al., 2006; Zhang et al., 2008) showed the ratios of wet-only and bulk deposition of inorganic N being 0.68-0.93 in North China Plain. Therefore it seems not possible to estimate wet deposition fluxes by multiplying a coefficient or subtracting the dry deposition fluxes from bulk deposition, since fraction of dry deposited N in bulk deposition is variable and not fixed across monitoring years. Anyway, we mentioned this in the revision.

References:

- Liu X.J., Ju X.T., Zhang Y., He C.E., Kopsch J., and Zhang F.S.: Nitrogen deposition in agroecosystems in the Beijing area. *Agriculture, Ecosystems & Environment* 113,

370-377, 2006.

Zhang Y., Liu X.J., Fangmeier A., Goulding K.T.W., and Zhang F.S.: Nitrogen inputs and isotopes in precipitation in the North China Plain. *Atmospheric Environment* 42, 1436-1448, 2008.

Lines 462-481: How do these deposition fluxes compare to other parts of the world over this recent time period? I also recommend plotting the spatial distribution of the deposition fluxes on a map because it is difficult to get a sense of the spatial patterns from the text and numbers in this paragraph.

Response: On the basis of 2001 ensemble-mean modeling results from 21 global chemical transport models (Vet et al., 2014), three global N deposition hotspots were western Europe (with levels from 20.0 to 28.1 kg N ha⁻¹ yr⁻¹, South Asia (Pakistan, India, and Bangladesh) from 20.0 to 30.6 kg N ha⁻¹ yr⁻¹ and East Asia from 20 to 38.6 kg N ha⁻¹ yr⁻¹ in eastern China (the global maximum). Extensive areas of high deposition from 10 to 20 kg N ha⁻¹ yr⁻¹ appear in the eastern United States and southeastern Canada as well as most of central Europe. Obviously, our estimated total N deposition fluxes (dry plus wet/bulk deposition, averaging from 34.2 kg N ha⁻¹ yr⁻¹ at background sites to 59.7 kg N ha⁻¹ yr⁻¹ at urban sites, Table 1) showed a much higher values. Relevant comparisons have been reported in our previous work (Xu et al., 2015).

As for data presentation, we think that the use of Table is reasonable and useful due to following two reasons. First, our analysis was based on land use types rather than single sampling site, and thus it is impractical to plot the spatial distribution of the deposition fluxes on a map. Second, using Tables can directly provide basic data for scientific communities for carrying out other relevant research. Therefore, we keep the Table as it is.

References:

Xu, W., Luo, X.S., Pan, Y.P., Zhang, L., Tang, A.H., Shen, J.L., Zhang, Y., Li, K.H., Wu, Q.H., Yang, D.W., Zhang, Y.Y., Xue, J., Li, W.Q., Li, Q.Q., Tang, L., Lu, S.H., Liang, T., Tong, Y.A., Liu, P., Zhang, Q., Xiong, Z.Q., Shi, X.J., Wu, L.H., Shi, W.Q., Tian, K., Zhong, X.H., Shi, K., Tang, Q.Y., Zhang, L.J., Huang, J.L., He,

C.E., Kuang, F.H., Zhu, B., Liu, H., Jin, X., Xin, Y.J., Shi, X.K., Du, E.Z., Dore, A.J., Tang, S., Collett, J.L., Goulding, K., Sun, Y.X., Ren, J., Zhang, F.S., and Liu, X.J.: Quantifying atmospheric nitrogen deposition through a nationwide monitoring network across China. *Atmos. Chem. Phys.* 15 (13), 12345–12360, 2015.

Vet, R., Artz, R. S., Carou, S., Shaw, M., Ro, C.-U., Aas, W., Baker, A., Bowersox, V. C., Dentener, F., Galy-Lacaux, C., Hou, A., Pienaar, J. J., Gillett, R., Forti, M. C., Gromov, S., Hara, H., Khodzher, T., Mahowald, N. M., Nickovic, S., Rao, P. S. P., and Reid, N. W.: A global assessment of precipitation chemistry and deposition of sulfur, nitrogen, sea salt, base cations, organic acids, acidity and pH, and phosphorus, *Atmos. Environ.*, 93, 3–100, 2014.

Line 572: If you sum dry and wet/bulk deposition fluxes, the total deposition will be overestimated because the bulk deposition already includes dry deposition.

Response: This concern was answered in our previous response to "Lines 220-221". In fact, our wet/bulk (including wet plus sedimentary deposition) + dry deposition (gases plus fine particles (non-sedimentary) deposition) denote a complete total N deposition. This means the wet/bulk deposition is not pure 'wet' deposition while the dry deposition is not complete 'dry' deposition. According to our previous studies (Liu et al., 2006; Zhang et al., 2008), annual difference between bulk and wet deposition was 1.3-9.6 kg N ha⁻¹ in northern Chinese agroecosystems. Therefore, to avoid misunderstanding, we defined the total N deposition as the sum of dry and bulk deposition in this study, although it is in principle defined as the sum of dry and wet deposition.

References:

Liu, X.J., Ju, X.T., Zhang, Y., He, C.E., Kopsch, J., and Zhang, F.S.: Nitrogen deposition in agroecosystems in the Beijing area, *Agr. Ecosyst. Environ.* 113(1), 370–377, doi:10.1016/j.agee.2005.11.002, 2006.

Zhang, Y., Liu, X. J., Fangmeier, A., Goulding, K. T. W., and Zhang, F. S.: Nitrogen inputs and isotopes in precipitation in the North China Plain, *Atmos. Environ.*, 42, 1436–1448, 2008.

Figure 8: Could you discuss the results in Fig. 8b? All of the previous trends were

urban > rural > background. I find it interesting that the trend for the ratio of reduced to oxidized N is reversed. Also, why is this ratio important?

Response: The opposite trend for the ratio of reduced to oxidized N is reasonable, as it depends on proportion of reduced and oxidized N deposition in the total deposition. This ratio can be used to indicate the relative contribution of N_r from agricultural and industrial activities to N deposition (Xu et al., 2015) because the major anthropogenic source of reduced N (NH_3 and particulate NH_4^+) is mainly affected by NH_3 volatilized from animal excrement and the application of nitrogenous fertilizers in agriculture, while anthropogenic sources of oxidized N (NO_2 , HNO_3 and particulate NO_3^-) is primarily dominated by NO_x emitted from fossil fuel combustion in transportation, power plant, and factories.

As shown in Fig. 8b, the averaged ratios at three land use types were slightly higher in the 2013-2015 period than in the 2011-2012 period, indicating agricultural NH_3 emission played a more and more important role in N deposition. This result, in turn, supports our conclusion from sensitivity tests by the GEOS-Chem model that mitigation of agricultural NH_3 emissions should be a priority to tackle serious N deposition in eastern China.

As suggested by the referee, we added the following discussion in the revision (in the Section 4.4):

“This conclusion to some extent is supported by increased ratios of the ratio of reduced to oxidized N in the total deposition at three land use types (Fig. 8b), as the major anthropogenic source of reduced N is mainly affected by NH_3 volatilized from animal excrement and the application of nitrogenous fertilizers in agriculture. Absence of NH_3 emission controls may be the main reason for a small and non-significant change in the total N deposition between 2011-12 and 2013-15 (Fig. S6, Supplement), despite enforcement of stringent emission controls on NO_x and SO_2 .”

Reference:

Xu, W., Luo, X.S., Pan, Y.P., Zhang, L., Tang, A.H., Shen, J.L., Zhang, Y., Li, K.H., Wu, Q.H., Yang, D.W., Zhang, Y.Y., Xue, J., Li, W.Q., Li, Q.Q., Tang, L., Lu, S.H.,

Liang, T., Tong, Y.A., Liu, P., Zhang, Q., Xiong, Z.Q., Shi, X.J., Wu, L.H., Shi, W.Q., Tian, K., Zhong, X.H., Shi, K., Tang, Q.Y., Zhang, L.J., Huang, J.L., He, C.E., Kuang, F.H., Zhu, B., Liu, H., Jin, X., Xin, Y.J., Shi, X.K., Du, E.Z., Dore, A.J., Tang, S., Collett, J.L., Goulding, K., Sun, Y.X., Ren, J., Zhang, F.S., and Liu, X.J.: Quantifying atmospheric nitrogen deposition through a nationwide monitoring network across China, *Atmos. Chem. Phys.* 15 (13), 12345–12360, 2015.

Section 4.1 and Figure 9: The correlation results show there is good agreement between satellite and ground-based observations. Can you quantify the differences using metrics? E.g., what are the percent differences for each month and annually? The correlation may be good, but the actual concentrations can still be different. Given the good relationship between satellite and surface measurements, are long term satellite data available for conducting temporal trend analysis?

Response: It is difficult to quantify the differences between satellite and ground-based observations using a uniform unit. Since ground and satellite measurements give the mixing ratios of N_r species (NH_3 and NO_2) in the surface layer and tropospheric integrated column densities of the species, respectively, estimating the satellite-derived ground concentrations of N_r species required their corresponding vertical profiles. Unfortunately, measurements of vertical profiles of concentrations above the surface are rare. On this point, in earlier version we stated in the text “To make a more accurate comparison, the vertical profile is recommended to convert the columns to the ground concentrations in future work”. Alternatively, we analyzed the correlations between satellite and ground-based observations to detect whether there is a consistency in spatial and temporal distributions.

As for temporal analysis, the following paragraph in the Section 4.1 can answer whether long term satellite data are available for conducting temporal trend analysis.

“...the OMI_ NO_2 retrieval can well capture the temporal variations of surface NO_2 concentrations over eastern China, whereas the IASI_ NH_3 retrievals better capture temporal variability in surface concentrations for the northern region. The weak correlations observed between IASI_ NH_3 observations and surface measurements at ten of the fourteen sites in the southern region (Fig. S7, Supplement) suggest that the

IASI_NH₃ observations need to be improved for investigating temporal variability in NH₃ concentration, despite that the satellite observation is at a specific time of day while the surface concentrations integrate across the diurnal cycle of emissions and mixing layer evolution.”

Section 4.2: There is too much speculation on the causes of the seasonal trends. Most of the discussion is based on what previous literature reported. I think you need to analyze other datasets to examine the factors affecting the N_r trends.

Response: In the revision, we analyzed datasets of air mass trajectory to examine influence of potential atmospheric transport on the resulting seasonal N_r trends. The following paragraphs were added as follows:

“In order to identify potential transport of NO₂, pNH₄⁺ and pNO₃⁻ from northern region, we calculated three-day backward trajectories arriving at five southern sites (Nanjing, Baiyun, Taojing, Ziyang and Huinong) during January, April, July and October using the TrajStat. The TrajStat analysis generally showed that the high proportions (overall 10-36%) of air masses from the north to the south of eastern China occurred in the autumn/winter, suggesting that the transport of NO₂, pNH₄⁺ and pNO₃⁻ from northern China would result in increases in their respective concentrations in autumn/winter south of the Qinling Mountains-Huaihe River line, except at Ziyang site (Fig. S14, Supplement).

Line 725: Could you provide the actual emissions amount from x tonnes in 2010 to y tonnes in 2014? Even though the emissions declined by a certain percentage, the actual emissions amount in 2014 might still be very large. If this is the case, then you will likely not observe a significant decrease in N_r concentrations.

Response: In the revised paper, we added the actual emission amount for the years 2010 and 2014. We now state that “...total annual emissions of SO₂ and NO_x were reduced by 12.9% and 8.6% in 2014 (approximately 9.9 Tg S yr⁻¹ and 6.3 Tg N yr⁻¹, respectively), respectively, compared with those in 2010 (approximately 11.3 Tg S yr⁻¹ and 6.9 Tg N yr⁻¹, respectively)”.

Yes, since NO_x emissions were still at high level in 2014. We did not find a significant

decrease in NO₂ concentrations in the current study. For total N_r, persistent high concentrations is likely due to the absence of NH₃ regulations, as NH₃ emission reduction had a larger influence on N_r concentration (for details, please see our response to next comment to Lines 733-734)

Lines 733-734: How much ammonia is emitted relative to NO_x and SO₂? I would think NO_x and SO₂ emissions are higher than those of ammonia. If this is the case, wouldn't NO_x and SO₂ emissions reductions have larger effects on N_r?

Response: Yes, total annual emissions of NO_x and SO₂ (average over 2011-2015, approximately 7.0 Tg N yr⁻¹ and 9.8 Tg S yr⁻¹) were higher than those of NH₃ emission (10.0 Tg N yr⁻¹) during the period of 2011-2015 in eastern China (details of emission data are given in Section 4.5). In addition, the annual molar ratios of (2SO₂+NO_x)/NH₃ were greater than 1 (ranging from 1.3 to 1.8) during the period. These results suggest that NH₃ emissions presented the limiting factor to the formation of secondary inorganic ions (e.g., particulate NH₄⁺ and NO₃⁻), and its emission reductions have large effects on N_r (e.g., gaseous NH₃ and particulate NH₄⁺ and NO₃⁻). This is also true at the national scale, as the molar amount of (2SO₂+NO_x) still substantially exceeded that of NH₃ at least until 2015 (Zhang et al., 2017).

Reference:

Zhang, X. M., Wu, Y. Y., Liu, X. J., Reis, S., Jin, J. X., Dragosits, U., Damme, Van M., Clarisse, L., Whitburn, S., and Coheur, P. F.: Ammonia emissions may be substantially underestimated in China, *Environ. Sci. Technol.*, 51, 12089-12096, 2017.

Lines 757-773: I don't think you can really say that ammonia emissions reductions are more important than NO_x and SO₂ emissions reductions. If ammonia emissions have been increasing, why is the N_r concentration in air and precipitation not increasing (many of the trends were not significant in sect. 3.2)? Also, is it possible that the NO_x and SO₂ emissions reductions are not large enough? See earlier comment about the actual emissions amount for NO_x and SO₂ could be very large despite 9-13% decrease in emissions. Is it appropriate to make this conclusion given that five years of data were analyzed? You also discussed how ammonia neutralizes

acidic gases and plays a role in limiting N_r . However, it does not mean that this process is more effective than reducing NO_x and SO_2 emissions which decrease the formation of acidic gases in the first place.

Response: Based on the discussions in Lines 757-773, we did not give the viewpoint that NH_3 emissions reductions are more important than NO_x and SO_2 emissions reductions. We concluded that implementation of NH_3 control strategies, relative to current NO_x and SO_2 emission controls, should be considered to mitigate atmospheric N_r pollution. Between the periods 2013-2015 and 2011-2012, the mean concentrations of NH_3 and pNH_4^+ overall showed non-significant increases (10-38%) at all land use types, whereas small changes in remaining N_r species occurred. As a result, annual total N_r concentration in air showed increases to varying extent at three land use types. This also highlights the importance of NH_3 emission reduction in controlling N_r pollution. Indeed, for individual species small changes in air concentrations of NO_2 , HNO_3 and pNO_3^- may be due to that the NO_x and SO_2 emissions reductions are not large enough.

To avoid misunderstanding, we now state that “implementation of NH_3 control strategies, together with more stringent NO_x and SO_2 emission controls, should be considered to mitigate atmospheric N_r pollution.”

Lines 775-783: This paragraph needs to mention the NO_x and SO_2 emissions in the northern region especially given the increased emissions for winter heating? How does they compare with ammonia emissions over an annual basis? A map of the spatial distribution of the ammonia emissions and agriculture activity levels would easily demonstrate that these are higher in the northern region.

Response: Thank you for this suggestion. We added the following discussions in Section 4.4 in the revision.

“In addition, higher NH_3 concentration is also likely due to the higher NH_3 volatilization in calcareous soils than that in the acidic red soil, as mentioned in Section 2.1. Total annual NH_3 emissions in northern region increased from 4.3 Tg N yr^{-1} in 2011 to 4.7 Tg N yr^{-1} at an annual rate of 1.8%. In contrast, the emissions of NO_x and SO_2 averaged 2.8 Tg N yr^{-1} and 3.7 Tg S yr^{-1} during 2011-2015, and

decreased at annual rates of 6.8 and 5.7%, respectively (details of the emissions will be illustrated in Section 4.5). Such reductions may enhance free NH₃ in the atmosphere. However, according to a modeling study by Han et al. (2017), the influence of removing anthropogenic SO₂ emissions on dry N deposition fluxes during 2010-2014 was quite weak, with the change within -0.5~0.5 (kg N ha⁻¹ yr⁻¹) over most regions in China.”

We think that current discussion is sufficient to explain why total dry N deposition fluxes at three land use types were higher in the northern region of eastern China than in the southern region. Given that the article is already relatively lengthy and this part of discussion is not the core, we did not compare the spatial distribution of the ammonia emissions and agriculture activity levels in eastern China in the revision.

Reference:

Han, X., Zhang, M. G., Skorokhod, A., and Kou, X. X.: Modeling dry deposition of reactive nitrogen in China with RAMS-CMAQ, *Atmos. Environ.*, 166, 47–61, 2017.

Line 801: This should be Fig. S12

Response: Corrected.

Line 803: This should be Sect. S2

Response: Corrected.

Lines 799-811: I think the model simulation and results require further analysis and discussion. The model apportions the contributions of various sources to ammonium and nitrate deposition and suggests agricultural activity is the main contributor. There needs to be more details on the model scenario (e.g. NH₃ and NO_x emissions estimated from the various sources). Is the larger contribution from agriculture due to larger emissions relative to other sources or is it because area sources have larger impact than point sources in the model? Also, to support the idea that NH₃ emissions reductions are important in reducing Nr deposition, you could perform a sensitivity analysis using different scenarios of NH₃ emissions reductions for future years.

Response: Thank you for this suggestion. The larger contribution from agriculture is due to larger emissions relative to other sources. In the revised paper, we now state

that “The total NH₃ and NO_x emissions from each source over eastern China and its contribution to total emissions in China are presented in Table S13 in the Supplement. The NH₃ and NO_x emissions over eastern China are 11.6 Tg N yr⁻¹ and 8.5 Tg N yr⁻¹ in 2010, which, respectively, account for 90% and 89% of their total emissions over China. Agricultural sources, including fertilizer use and livestock, comprise most of the NH₃ emissions while fuel combustion activities, including industry, power plant, and transportation contribute most of the NO_x emissions and small amounts of NH₃ emissions. Both NH₃ and NO_x have natural sources (including lightning, biomass burning and soil emissions), but are negligible compared to anthropogenic emissions over eastern China.”

Based on outputs from the model simulation, it is obvious that controlling agricultural NH₃ emission can undoubtedly lower N deposition. Thanks for the suggestion on performance of scenarios analysis of NH₃ emission reduction, we conducted a separate model simulation which reduce emissions from fertilizer use by 20%. We add the following sentences in the text:

“To test the importance of future ammonia emission control strategies, we conducted separate model simulations which reduced NH₃ emissions from fertilizer use by 20%. The results showed that a 20% reduction in fertilizer NH₃ emissions can lead to a 7.4% decrease in total N deposition over Eastern China”

In future study, we will attempt to use improved NH₃ emission (e.g., Zhang et al., 2018) inventories to detail the relative contribution of emissions sources to N deposition and further scenarios analysis of NH₃ emissions.

Reference:

Zhang, L., Chen, Y. F., Zhao, Y. H., Henze, D. K., Zhu, L. Y., Song, Y., Paulot, F., Liu, X. J., Pan, Y. P., and Huang, B. X.: Agricultural ammonia emissions in China: reconciling bottom-up and top-down estimates, *Atmos. Chem. Phys.*, 18, 339–355, 2018.

Line 809: What do you mean by improper fertilizer application? Do you mean too excessive? How much fertilizer is applied annually and is this amount much higher than normal? More background on this issue would be useful.

Response: “improper fertilizer application” means N fertilizers were not applied in appropriate fertilization pattern (e.g., fertilizing with a suitable choice of chemical, at the correct application level, selecting the best of the year and location). To make it clear, we now state that “These results indicate that reducing NH₃ emissions by use of appropriate fertilization patterns (e.g., 4 R technologies (Right amount, Right time, Right form and Right application technique), Ju et al., 2009) should be a priority in curbing N deposition in eastern China”.

Reference:

Ju, X.T., Xing, G.X., Chen, X.P., Zhang, S.L., Zhang, L.J., Liu, X.J., Cui, Z.L., Yin, B., Christie, P., Zhu, Z.L., and Zhang, F.S.: Reducing environmental risk by improving N management in intensive Chinese agricultural systems, Proc. Natl. Acad. Sci. U. S. A. 106, 3041-3046, 2009.

Line 884: Do you have annual precipitation amounts from weather stations, which can show whether interannual variability in precipitation amounts affect wet deposition?

Response: We measured precipitation amounts at 27 study sites during 2011-2015. According to suggestion by the referee, we selected 16 sites with continuous 5-year measurements, and our results demonstrated an obvious interannual variability in precipitation amounts. Thus, wet deposition to some extent can be affected by the change in precipitation amounts.

In the revised paper, we added Figure S14 in the Supplement, and stated in the text that “For example, a large inter-annual variation in precipitation amount was observed at the selected 16 sites during 2011-2015, which partially lead to inter-annual changes in wet/bulk N deposition.

Anonymous Referee #2

This paper presents a statistical summary and discussion of measurements of components of reactive nitrogen (Nr) in the air and in bulk deposition from the 27 sites of a national network that are located in the eastern part of China. The measurement dataset spans the 5-year period from 2011-2015 inclusive. Measurements are also converted into estimates of wet and dry deposition. The authors analyse various spatiotemporal aspects of the concentrations and deposition dataset including seasonality, trends over the 5-year period, and a comparison between sites in the northern half and the southern half of eastern China. The authors supplement the analysis of measurement data with some GEOS-Chem model runs to explore source contributions to Nr in this region. Discussion includes implication for policymakers concerning the different trends in emissions of Nr versus concentrations and deposition of Nr and of the need to include emissions of NH₃ in emissions reductions planning. The dataset is comprehensive. The presentation of the results is thorough and the text and figures and tables are very clearly presented. There is an extensive discussion. The data are of importance for understanding Nr in eastern China.

Response: Thanks for the recognition of our contribution. Below we provide a point-by-point response to the species comments, together with proposed changes in the revised manuscript (in blue).

Specific comments:

Five years is not a long time period to attempt to discern ‘true’ long-term trends in concentrations of atmospheric species. The authors recognise that their time period is short in respect of this aspect of their analysis but they could phrase relevant parts of their text to be more cautious about conclusions on long-term trends.

Response: The suggestion has been implemented in the revision.

L124: Replace “subsequence” with “subsequent”

Response: Agree and done.

L207: It is not clear what is meant by the phrase “where field sampling was carried

out after the year 2010”. Is this intended to mean that at some sites the measurements did not begin until after 2010?

Response: We are sorry for confusing the referee. It means that at eleven sites the measurements begin after the year 2011. We now state that “...where field sampling was carried out after the year 2011 (i.e., the years between 2012 and 2015) and/or interrupted during the period due to instrument failure (details in Table S1, Supplement)”.

L271-2: There is a contradiction between a sentence that states that IASI data up until 31 December 2015 was used and the following sentence that states that data only up until 30 September 2014 was used.

Response: There was a wrong expression in this sentence. Actually, we used the daily IASI-NH₃ data from 1 January 2011 to 31 December 2015 for the spatial analysis, and from January 2011 to 30 September 2014 for temporal analysis.

We now state that “The daily IASI-NH₃ data (provided by the Atmospheric Spectroscopy Group at Université Libre De Bruxelles, data available at <http://iasi.aeris-data.fr/NH3/>) from 1 January 2011 to 31 December 2015 was used for the spatial analysis in the present study. For the temporal analysis, we used the IASI_NH₃ from 1 January 2011 to 30 September 2014 because an update of the input meteorological data on 30 September 2014 had caused a substantial increase in the retrieved atmospheric NH₃ columns.”

Table 1: (1) State in the caption or footnote what the significance test is testing, i.e. that it is testing for significant difference in mean concentration of a pollutant at a given site type between the northern region and the southern region. (2) The footnote should read LUY not LSY to be consistent with column heading.

Response: We now state in the footnote that “* and ** denote significance at the 0.05 and 0.01 probability levels for difference in annual mean N_r concentrations at a given site type between northern and southern regions, respectively.”

Also, we uniformly used “LUT” as an abbreviation of land use types in the footnote and column heading.

Figure 2: The reader is referred to Table S1 in the supplement for the number of sites

for each land use type in each region, but cannot the reader be directed more easily to Table 1 in the main paper for these numbers?

Response: The reader cannot be directly referred to Table 1. For comparison between the periods 2011-2012 and 2013-2015, the sampling sites for land use types shown in Figure 2 have continuous 5-year (2011-2015) measurements (in total 21 sites for dry measurements, and 16 sites for wet/bulk measurements). For spatial comparisons in Table 1, the annual mean concentrations of N_r species in air and precipitation for land use types were calculated based on measurements at all 27 sites.

Figure 3: (1) I assume the data shown are the means for the 5-year period, in which case it may be helpful to make this explicit in the opening sentence thus: “Seasonal mean concentrations averaged over 2011-2015 of: : :.” (2) As for Figure 2 (**should be 3?**), can the text “in Table S1 in the supplement” be replaced more directly with “in Table 1”. (3) The last part of the caption should refer to significant differences between “seasons” not “sites”.

Response: In the revised paper, we rephrased the start of caption of Figure 2 to “Seasonal mean concentrations averaged over 2011-2015 of...”.

We replaced “Table S1 in the supplement” by “Table 1”, as seasonal averages were calculated based on measurements at all 27 sites. Also, we changed “sites” to “seasons”.

Figure 4: The same 3 comments as made above in connection with Figure 3.

Response: In the revised paper, we have made corresponding corrections on Figure 4 according to the referee’s comments on Figure 3.

Table 2: Same comments as for Table 1.

Response: In the revision we made corresponding corrections on Table 2 according to the referee’s comments on Table 1.

Figure 5: Can the reader be directed to Table 2, rather than to Table S1 in the supplement, for the number of sites of each type in each region.

Response: The reader cannot be referred to Table 2. For details, please see our response to similar comments on Figure 2.

Figure 7: Same comments as for Figure 3 (but with substitution of reference to Table 22

2 rather than to Table 1).

Response: In the revised paper, we made corresponding corrections on the caption of Figure 7 according to the referee's comments on Figure 3.

Figure 8: Same comments as for Figure 7.

Response: The reader cannot be directly referred to Table 1. Please see our response to the referee's comment on Figure 2.

L598: Rephrase start of sentence to "Eastern China is a highly industrialized: : .:"

Response: Agree and done.

L 761: In comparing ion balance, presumably the (molar) concentration of NH_4^+ was compared against the sum of the molar concentrations of NO_3^- and TWICE the molar concentration of SO_4^{2-} ? The factor 2 is missing from the text and from the axis title of Figure 10f.

Response: Thank you for pointing it out. In the revised paper, we analyzed the correlation of NH_4^+ with the sum of $\text{NO}_3^- + 2\text{SO}_4^{2-}$. Also, Figure 10f was redrawn and the corresponding sentences were changed, now read as: "At urban and rural sites, monthly mean $p\text{NH}_4^+$ concentrations significantly positively correlated with the sum of $p2\text{SO}_4^{2-}$ and $p\text{NO}_3^-$ concentrations (Fig. 10f). However, the slopes of regression equations between them were both smaller than unity (0.35 and 0.46 at urban and rural sites, respectively)...". In addition, we changed "Table S1" to "Table 1" in the caption of Figure 10.

1 | [MS No.: acp-2018-424](#)

2 | **Spatial-temporal patterns of inorganic nitrogen air concentrations**
3 | **and deposition in eastern China**

4 | Wen Xu^{1,2}, Lei Liu³, Miaomiao Cheng⁴, Yuanhong Zhao⁵, Lin Zhang⁵, Yuepeng Pan⁶,
5 | Xiuming Zhang⁷, Baojing Gu⁷, Yi Li⁸, Xiuying Zhang³, Jianlin Shen⁹, Li Lu¹⁰,
6 | Xiaosheng Luo¹¹, Yu Zhao¹², Zhaozhong Feng^{2*}, Jeffrey L. Collett, Jr.¹³, Fusuo
7 | Zhang¹, Xuejun Liu^{1*}

8 | ¹College of Resources and Environmental Sciences, Key Laboratory of Plant-Soil Interactions of
9 | MOE, Beijing Key Laboratory of Cropland Pollution Control and Remediation, China
10 | Agricultural University, Beijing 100193, China

11 | ²State Key Laboratory of Urban and Regional Ecology, Research Center for Eco-Environmental
12 | Sciences, Chinese Academy of Sciences, Shuangqing Road 18, Haidian District, Beijing, 100085,
13 | China

14 | ³Jiangsu Provincial Key Laboratory of Geographic Information Science and Technology,
15 | International Institute for Earth System Science, Nanjing University, Nanjing, 210023, China

16 | ⁴State Key Laboratory of Environmental Criteria and Risk Assessment, Chinese Research
17 | Academy of Environmental Sciences, Beijing 100012, China

18 | ⁵Laboratory for Climate and Ocean-Atmosphere Sciences, Department of Atmospheric and
19 | Oceanic Sciences, School of Physics, Peking University, Beijing 100871, China

20 | ⁶State Key Laboratory of Atmospheric Boundary Layer Physics and Atmospheric Chemistry
21 | (LAPC), Institute of Atmospheric Physics, Chinese Academy of Sciences, Beijing, 100029, China

22 | ⁷Department of Land Management, Zhejiang University, Hangzhou 310058, People's Republic of
23 | China

24 | ⁸Arizona Department of Environmental Quality, Phoenix, AZ 85007, USA

25 | ⁹Institute of Subtropical Agriculture, Chinese Academy of Sciences, Changsha 4410125, China

26 | ¹⁰Institute of Surface-Earth System Science, Tianjin University, Tianjin, 300072, China

27 | ¹¹Institute of Plant Nutrition, Resources and Environmental Sciences, Henan Academy of
28 | Agricultural Sciences, Henan Key Laboratory of Agricultural Eco-environment, Zhengzhou,
29 | 450002, China

30 | ¹²State Key Laboratory of Pollution Control & Resource Reuse, School of the Environment,
31 | Nanjing University, 163 Xianlin Ave., Nanjing, Jiangsu 210023, China

32 | ¹³Department of Atmospheric Science, Colorado State University, Fort Collins, Colorado, 80523
33 | USA

34 | *Correspondence to: X. J. Liu (liu310@cau.edu.cn) and Z.Z. Feng (fzz@rcees.ac.cn)

35

36

37

38

39

40 **Abstract:**

41 Five-year (2011-2015) measurements of gaseous NH_3 , NO_2 and HNO_3 and
42 particulate NH_4^+ and NO_3^- in air and/or precipitation were conducted at twenty-seven
43 sites in a Nationwide Nitrogen Deposition Monitoring Network (NNDMN) to better
44 understand spatial and temporal (seasonal and annual) characteristics of reactive
45 nitrogen (N_r) concentrations and deposition in eastern China. Our observations reveal
46 annual average concentrations ($16.4\text{-}32.6 \mu\text{g N m}^{-3}$), dry deposition fluxes ($15.8\text{-}31.7$
47 $\text{kg N ha}^{-1} \text{ yr}^{-1}$) and wet/bulk deposition fluxes ($18.4\text{-}28.0 \text{ kg N ha}^{-1} \text{ yr}^{-1}$) based on land
48 use were ranked as urban > rural > background sites. Annual concentrations and dry
49 deposition fluxes of each N_r species in air were comparable at urban and background
50 sites in northern and southern regions, but were significantly higher at northern rural
51 sites. These results, together with good agreement between spatial distributions of
52 NH_3 and NO_2 concentrations determined from ground measurements and satellite
53 observations, demonstrate that atmospheric N_r pollution is heavier in the northern
54 region than in the southern region. No significant inter-annual trends were found in
55 the annual N_r dry and wet/bulk N deposition at almost all of the selected sites. A lack
56 of significant changes in annual averages between the 2013-2015 and 2011-2012
57 periods for all land use types, suggests that any effects of current emission controls
58 are not yet apparent in N_r pollution and deposition in the region. Ambient
59 concentrations of total N_r exhibited a non-significant seasonal variation at all land use
60 types, although significant seasonal variations were found for individual N_r species
61 (e.g., NH_3 , NO_2 and $p\text{NO}_3^-$) in most cases. In contrast, dry deposition of total N_r
62 exhibited a consistent and significant seasonal variation at all land use types, with the
63 highest fluxes in summer and the lowest in winter. Based on sensitivity tests by the
64 GEOS-Chem model, we found that NH_3 emissions from fertilizer use (including
65 chemical and organic fertilizers) were the largest contributor (36%) to total inorganic
66 N_r deposition over eastern China. Our results not only improve the understanding of
67 spatial-temporal variations of N_r concentrations and deposition in this pollution
68 hotspot, but also provide useful information for policy-makers that mitigation of NH_3

69 emissions should be a priority to tackle serious N deposition in eastern China.

70 **1. Introduction**

71 In China, and globally, human activities have dramatically increased emissions
72 of nitrogen oxides ($\text{NO}_x = \text{NO} + \text{NO}_2$) and ammonia (NH_3) into the atmosphere since
73 the beginning of the industrial revolution (Galloway et al., 2008; Liu et al., 2013).
74 NO_x and NH_3 emitted to the atmosphere are transformed to nitrogen-containing
75 particles (e.g., particulate NH_4^+ and NO_3^- , and organic nitrogen) (Ianniello et al., 2010;
76 Zhang et al., 2015), which are major chemical constituents of airborne $\text{PM}_{2.5}$
77 (particulate matter with a diameter of 2.5 μm or less) and have implications for air
78 quality and climate (Fuzzi et al., 2015). As a result of elevated **reactive nitrogen (N_r)**
79 emissions, nitrogen (N) deposition through dry and wet processes has also
80 substantially increased over China (Liu et al., 2013; Lu et al., 2007, 2014; Jia et al.,
81 2014, 2016), and excessive deposition of N has resulted in detrimental impacts
82 including decreased biological diversity (Bobbink et al., 2010), nutrient imbalance (Li
83 et al., 2016), increased soil acidification (Yang et al., 2015), **and** eutrophication of
84 water bodies (Fenn et al., 2003), ~~and increased greenhouse gas emissions (Gruber and~~
85 ~~Galloway, 2008)~~. Furthermore, N_r -associated haze pollution episodes, characterized
86 by high concentrations of $\text{PM}_{2.5}$, occur frequently in China, as evidenced in particular
87 in 2013 (Guo et al., 2014; Huang et al., 2014; Tian et al., 2014).

88 In order to control its notorious air pollution, China has reduced national
89 emissions of SO_2 and particulate matter by 14% and 30%, respectively, from 2005 to
90 2010 (MEPC, 2011). Additionally, stringent measures (e.g., using selective
91 catalytic/non-catalytic reduction systems, and implementing tighter vehicle emission
92 standards) were implemented during the 12th Five Year Plan (FYP) period
93 (2011-2015), with aims to reduce 2015 annual emissions of SO_2 and NO_x by 8% and
94 10%, respectively, relative to 2010 levels (Xia et al., 2016). However, there is as yet
95 no regulation or legislation that deals with national NH_3 emissions and thus emission
96 reductions of SO_2 and NO_x to achieve desired air-quality improvement goals will be
97 compromised (Gu et al., 2014). Significant increases in $\text{PM}_{2.5}$ concentrations have
98 been observed in the years 2013 and 2014 as compared to 2012, excluding the

99 influence of meteorological conditions on inter-annual variations (Liang et al., 2015).
100 Other studies with more conclusive evidence have likewise suggested that NH₃ plays
101 a vital role in sulfate formation and exacerbates severe haze pollution development in
102 urban regions of China (Wang et al., 2016), even acting as the key limiting factor for
103 the formation of secondary inorganic aerosol (Wu et al., 2016). In addition, due to
104 higher local and regional concentrations of NH₃ in the atmosphere, nitrate-driven
105 haze pollution occurred during summertime in urban environment in the North China
106 Plain (Li et al., 2018). The absolute and relative concentrations of particulate nitrate in
107 urban Beijing increased with haze development (Pan et al., 2016). Also, nitrate
108 contributed to a large fraction of the elevated PM_{2.5} concentrations at a rural site in
109 the North China Plain and high NH₃ in the early morning accelerated the formation of
110 fine nitrates (Wen et al., 2015).

111 High rates of N deposition have also been observed during 2011-2014 across
112 China (Xu et al., 2015). However, to date no study, based on long-term ground-based
113 observations, has provided any information on the effectiveness of SO₂ and NO_x
114 emission controls on N deposition in China. Non-linearities have been identified
115 between reductions in emission and deposition in Europe over the last 3 decades
116 (Aguillaume et al., 2016; Fowler et al., 2007). Due to the tightly coupled yet complex
117 relationship between emissions, concentrations and deposition, long-term monitoring
118 networks can provide a test of the effectiveness of emission controls (Erisman et al.,
119 2003). Currently two national N deposition networks are operational in China, i.e. the
120 Nationwide Nitrogen Deposition Monitoring Network (NNDMN, Liu et al., 2011; Xu
121 et al., 2015) and the Chinese Ecosystem Research Network (CERS, Zhu et al., 2015).
122 The NNDMN containing 43 *in situ* monitoring sites has been operational since 2010
123 to measure wet N deposition and ambient concentrations of five major N_r species (i.e.,
124 gaseous NH₃, NO₂ and HNO₃, and particulate NH₄⁺ and NO₃⁻), the latter for
125 ~~subsequence~~-~~subsequent~~ estimation of dry deposition. The CERS was established in
126 1988 and mainly focused on wet N deposition at 41 field stations. In addition to
127 ground-based measurements, satellite observations enable retrieval of atmospheric
128 NH₃ and NO₂ with high temporal and spatial resolutions (Dammer et al., 2016;

129 Russell et al., 2012), providing a means to reveal spatial distributions and long-term
130 trends of ambient NH₃ and NO₂ levels at regional to global scales, and also to
131 evaluate the effectiveness of emission controls (Krotkov et al., 2016). However, to
132 effectively use the vast satellite data sets for environmental monitoring, it is critical to
133 validate these remote sensing observations using *in situ* surface observations (Pinder
134 et al., 2011; Van Damme et al., 2015).

135 Eastern China is a developed region with the largest densities of population,
136 economic activity and resource consumption in the country (He et al., 2015). Recent
137 satellite observations indicate that tropospheric NH₃ and NO₂ levels in eastern China
138 were both much greater than other regions of the world from 2005-2015 (Demmer et
139 al., 2016; Krotkov et al., 2016). Accordingly, this region received the highest levels of
140 dry N deposition in the world (Vet et al., 2014), and was regarded as a primary export
141 region of N deposition for neighboring countries (Ge et al., 2014). Based on
142 meta-analysis of published observations, some studies have provided information on
143 the magnitudes, spatial distributions, and decadal variations of wet/bulk N deposition
144 in China (Liu et al., 2013; Jia et al., 2014), but the analyzed data were limited to time
145 periods between 1980 and 2010. Although a recent study (Jia et al., 2016) has
146 reported a clear increasing trend of dry N deposition in eastern China between 2005
147 and 2014, considerable uncertainty may exist due to estimates of gaseous HNO₃ and
148 particulate NH₄⁺ and NO₃⁻ (*p*NH₄⁺ and *p*NO₃⁻) concentrations using NO₂ satellite
149 data, which is in part manifested by Liu et al. (2017a). Furthermore, seasonal patterns
150 of N_r concentrations and deposition have not yet been systematically investigated at a
151 large spatial scale in this region, although spatial patterns of dry N_r deposition for
152 representative months of four seasons (i.e., January for winter, April for spring, July
153 for summer, October for autumn) in 2010 have been mapped with the RAMS-CMAQ
154 model (Han et al., 2017). Thus, the spatial and temporal (annual and seasonal)
155 variations of N_r concentrations, and dry and wet deposition in eastern China require
156 further exploration using ground-based measurements, especially for time periods
157 after 2010. Our previous work (Xu et al., 2015) used multiyear measurements (mainly
158 from Jan. 2010 to Sep. 2014) at the 43 sites in the NNDMN, aiming to provide the

159 first quantitative information on atmospheric N_r concentrations and pollution status
160 across China, and to analyze overall fluxes and spatial variations of N deposition in
161 relation to anthropogenic N_r emissions from six regions.

162 The present study aims to examine spatial-temporal (annual and seasonal)
163 characteristics of N_r concentrations in air (NH_3 , NO_2 , HNO_3 , pNH_4^+ and pNO_3^-) and
164 precipitation (NH_4^+ -N and NO_3^- -N) and their corresponding dry and wet/bulk N
165 deposition, through a 5-year (2011-2015) monitoring period at 27 NNDMN sites in
166 eastern China. In addition, we compare spatial-temporal variability of measured NH_3
167 and NO_2 concentrations with variations of the corresponding satellite retrieval
168 columns, as well as inter-annual trends in N_r deposition and emissions. Finally,
169 emission sources contributing to total N deposition over eastern China are examined.

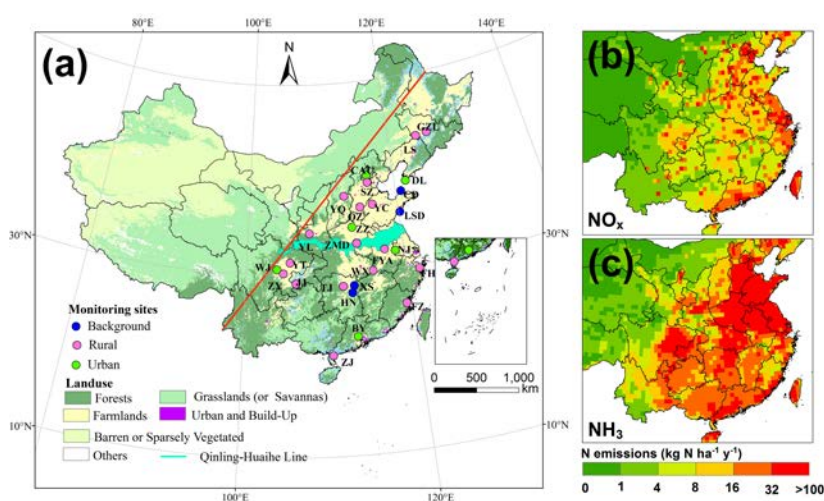
170 **2. Materials and methods**

171 **2.1 Study area and site descriptions**

172 The present study was conducted in eastern China, which is distinguished by the
173 “Hu Line” (She, 1998). This region has spatial heterogeneity in levels of economic
174 development, ~~and resulting in~~ significant spatial differences in NH_3 and NO_x
175 emissions (Fig. 1b and c). Thus, to better analyze spatial and temporal variabilities in
176 measured N_r concentrations and deposition, we divided eastern China into northern
177 and southern regions using the Qinling Mountains-Huaihe River line (Fig. 1a), of
178 which the division basin was based on the differences in natural conditions,
179 agricultural production, geographical features and living customs. As for specific
180 differentiations, for example, the northern region adopted a centralized domestic
181 heating policy for late autumn and winter seasons but the south has not; annual
182 average precipitation amounts were generally greater than 800 mm in the south but
183 were less than 800 mm in the north. In addition, the north is dominated by calcareous
184 soils, which could result in higher soil NH_3 volatilization (Huang et al., 2015), vs. the
185 acidic red soil in the south.

186 The NNDMN was operated in line with international standards by China
187 Agricultural University (CAU); 35 NNDMN sites were located in eastern China (Xu
188 et al., 2015). For our analysis, we considered twenty-seven sites in total, with 5-year

189 continuous data: 13 sites were located in north of the Qinling Mountains-Huaihe
 190 River line (China Agricultural University-CAU, Zhengzhou-ZZ, Dalian-DL,
 191 Shuangzhuang-SZ, Quzhou-QZ, Yangqu-YQ, Zhumadian-ZMD, Yanglin-YL,
 192 Yucheng-YC, Gongzhulin-GZL, Lishu-LS, Lingshandao-LSD, Changdao-CD), and
 193 14 sites were located in south of the line (Nanjing-NJ, Baiyun-BY, Wenjiang-WJ,
 194 Wuxue-WX, Taojing-TJ, Fengyang-FY, Zhanjiang-ZJ, Fuzhou-FZ, Fenghua-FH,
 195 Ziyang-ZY, Yangting-YT, Jiangjin-JJ, Huinong-HN, Xishan-XS).



196
 197 **Figure 1.** Spatial distributions of the 27 monitoring sites (a), NO_x emissions (b)
 198 and NH_3 emissions (c) in Eastern China (NH_3 and NO_x emission data were for the
 199 year 2010 and obtained from Liu et al. (2017b)).

200 All the sites are located as far away as possible and practical from local direct
 201 emission sources to increase regional representativeness. They can be divided into
 202 three categories according to their geopolitical location and their proximity to the
 203 main emission sources: urban sites (abbreviated as U), rural sites (cropland areas, R),
 204 and background sites (coastal and forest areas, B). Information on the monitoring sites,
 205 such as land use types, coordinates, and measurement periods are listed in Table S1 of
 206 the Supplement. Detailed descriptions of all the sites including the surrounding
 207 environment and nearby emission sources can be found in Xu et al. (2015).

208 2.2 Field sampling and chemical analysis

209 Continuous measurements were performed during the period from January 2011
210 to December 2015 at the 27 study sites, except for eleven sites (ZZ, ZMD, YC, LSD,
211 NJ, WX, FYA, ZJ, YT, JJ, and HN), where field sampling was carried out after the
212 year ~~2010–2011~~ (i.e., the years between 2012 and 2015) and/or interrupted during the
213 period due to instrument failure (details in Table S1, Supplement). Ambient N_r
214 concentrations of gaseous NH_3 and HNO_3 , and pNH_4^+ and pNO_3^- (for which the
215 empirically determined effective size cut-off for aerosol sampling is of the order of
216 $4.5 \mu m$) were measured using an active DELTA (DENuder for Long-Term
217 Atmospheric sampling; Tang et al., 2009) system; gaseous NO_2 was sampled in three
218 replicates with passive diffusion tubes (Gradko International Limited, UK). The air
219 intakes of the DELTA system and the NO_2 tubes were mounted 2 m above the ground
220 at most sites and protected from precipitation and direct sunlight with a rigid plastic
221 box and a PVC shelter, respectively. All measurements of N_r concentration were
222 based on monthly sampling (one sample per month for each N_r species). Detailed
223 information on measuring methods and collection are given in Sect. S1 of the
224 Supplement.

225 To collect precipitation (here termed as wet/bulk deposition, which contains wet
226 and some dry deposition due to the use of an open sampler) samples, a standard
227 precipitation gauge (SDM6, Tianjin Weather Equipment Inc., China) was
228 continuously exposed beside the DELTA system (ca. 2 m). Immediately after each
229 precipitation event (08:00–08:00 next day, Greenwich Mean Time +8), samples
230 (including rain and melted snow) were collected and stored in clean polyethylene
231 bottles (50 mL) at $-18^\circ C$ until sent to the CAU laboratory for analysis. Each collector
232 was rinsed three times with high-purity water after each collection.

233 In the analytical laboratory, acid-coated denuders and aerosol filters were
234 extracted with 6 and 10 mL of high-purity water ($18.2 M\Omega$), respectively, and
235 analyzed for NH_4^+-N with an AA3 continuous-flow analyzer (CFA) (BranC Luebbe
236 GmbH, Norderstedt, Germany). Carbonate-coated denuders and filters were both
237 extracted with 10 mL 0.05% H_2O_2 solution followed by analysis of $NO_3^- -N$ using the
238 same CFA. NO_2 samples, extracted with a solution containing sulfanilamide, H_3PO_4 ,

239 and N-1-naphthylethylene-diamine, were determined using a colorimetric method by
240 absorption at a wavelength of 542 nm (Xu et al., 2016). Precipitation samples were
241 filtered through a syringe filter (0.45 mm, Tengda Inc., Tianjin, China) and analyzed
242 for $\text{NH}_4^+\text{-N}$ and $\text{NO}_3^-\text{-N}$ using the CFA as mentioned above. Quality assurance and
243 quality control procedures adopted in the analytical laboratory are described by Xu et
244 al. (2017). Further details of precipitation measurement, samples handling, and
245 chemical analysis are reported in Xu et al. (2015).

246 **2.3 Deposition estimate**

247 Wet/bulk deposition of $\text{NH}_4^+\text{-N}$ and $\text{NO}_3^-\text{-N}$ were calculated per month and year
248 by multiplying the precipitation amount by their respective volume-weighted mean
249 (VWM) concentrations. The dry deposition flux of gaseous and particulate N_r species
250 was calculated as the product of measured concentrations by modeled deposition
251 velocities (V_d). The dry deposition velocities of five N_r species were calculated by the
252 GEOS (Goddard Earth Observing System)-Chem chemical transport model (CTM)
253 (Bey et al., 2001; <http://geos-chem.org>), and have been reported in a companion paper
254 (Xu et al., 2015). In brief, the model calculation of dry deposition of N_r species
255 follows a standard big-leaf resistance-in-series model as described by Wesely (1989)
256 for gases and Zhang et al. (2001) for aerosol. We used archived hourly V_d from
257 January 2011 to May 2013 and filled the gap for the period (from June 2013 to
258 December 2015) when GEOS meteorological data are unavailable using the mean
259 values calculated from all the available simulations. The monthly V_d at each site was
260 averaged from the hourly dataset.

261 **2.4 Satellite retrievals of NH_3 and NO_2**

262 Comparisons between satellite observations and ground-based measurements
263 were evaluated at the twenty-seven sites in order to accurately examine the
264 spatial-temporal pattern of NH_3 and NO_2 concentrations. For NH_3 , we used the
265 products retrieved from the Infrared Atmospheric Sounding Interferometer (IASI)
266 instrument (aboard the MetOp-A platform), which crosses the equator at a mean local
267 solar time of 9:30 a.m. and 9:30 p.m. The IASI- NH_3 product is based on the
268 calculation of a spectral hyperspectral range index and subsequent conversion to NH_3

269 total columns via a neural network. The details of the IASI-NH₃ retrieval method are
270 described in Whitburn et al. (2016). We only considered the observations from the
271 morning overpass as they are generally more sensitive to NH₃ because of higher
272 thermal contrast at this time of day (Van Damme et al., 2015; Dammers et al., 2016).
273 The daily IASI-NH₃ data (provided by the Atmospheric Spectroscopy Group at
274 Université Libre De Bruxelles, data available at [http://iasi.aeris-data.fr/NH₃/](http://iasi.aeris-data.fr/NH3/)) from 1
275 January 2011 to 31 December 2015 was used for the spatial analysis in the present
276 study. For the temporal analysis, We-we did-not used the IASI_NH₃ after 30
277 September 2014 for the temporal analysis from 1 January 2011 to 30 September 2014
278 because an update of the input meteorological data on 30 September 2014 had caused
279 a substantial increase in the retrieved atmospheric NH₃ columns. Only observations
280 with a cloud coverage lower than 25%, and relative error lower than 100% or absolute
281 error smaller than 5×10^{15} molecules cm⁻² were processed. The methodology is
282 provided in detail in Liu et al. (2017b). In brief, all observations were gridded to a 0.5°
283 latitude × 0.5° longitude grid, and then we calculated the monthly arithmetic mean by
284 averaging the daily values with observations points within each grid cell. Similarly,
285 we calculated the annual arithmetic mean by averaging the daily values with
286 observations points within the grid cell over the whole year.

287 For NO₂ we used the products from the Ozone Monitoring Instrument (OMI)
288 resided on NASA's EOS-Aura satellite, which was launched in July 2004 into a
289 sun-synchronous orbit with a local equator crossing time at approximately 1:45 p.m.
290 OMI detects the backscattered solar radiation from the Earth's atmosphere within the
291 UV-vis spectral window between 270-500 nm, to achieve nearly global coverage daily,
292 with a spatial resolution ranging from 13 km × 24 km at nadir to 24 km × 128 km at
293 the edge of the swath (Russell et al., 2012). We used tropospheric NO₂ retrievals from
294 the DOMINO (Dutch Finnish Ozone Monitoring Instrument) algorithm version 2. The
295 retrieval algorithm is described in detail in Boersma et al. (2007). The tropospheric
296 NO₂ columns used in this study are monthly means from 1 January 2011 to 30
297 December 2015 with a spatial resolution of 0.125° latitude × 0.125° longitude (data
298 available at <http://www.temis.nl/airpollution/no2.html>).

299 2.5 Statistical analysis

300 One-way analysis of variance (ANOVA) and two-independent-samples *t* tests
301 were applied to detect significant differences in seasonal mean concentrations and
302 deposition fluxes of measured N_r species as well as their annual mean deposition
303 fluxes for three land use types (rural, urban and background). As there was large
304 site-to-site variability in annual N_r concentrations and deposition fluxes at monitoring
305 sites within the same land use types, averaging data into annual values for land use
306 types is unlikely to be truly representative of actual trends. Thus, annual trends of the
307 variables were evaluated at a single site scale rather than by land use type. Trend
308 analysis was conducted using Theil regression (Theil, 1992) and the Mann-Kendall
309 test (Gilbert, 1987; Marchetto et al., 2013). We defined an increasing (decreasing)
310 trend as a positive (negative) slope of the Theil regression, while a statistical
311 significance level ($p < 0.01$) of a trend was evaluated by the non-parametric
312 Mann-Kendall test (p value). Non-parametric methods usually have the advantage of
313 being insensitive to outliers, and allow missing data and non-normal distribution of
314 data (Gilbert, 1987; Salmi et al., 2002), appropriate for the analyzed data set. The
315 Mann-Kendall method is appropriate for detection of monotonic trends in data series
316 that have no seasonal variation or autocorrelation. Atmospheric concentrations and
317 deposition fluxes of N_r species, however, generally have distinct seasonal variability
318 (Pan et al., 2012) and the Mann-Kendall test is thus applied to annual values.

319 Satellite observations during 2005-2015 indicate that tropospheric NO_2 levels
320 peaked in 2011 over China (Krotkov et al., 2016; Duncan et al., 2016) and NO_x
321 emissions peaked in 2011/2012 (Miyazaki et al., 2017; van der A et al., 2017; Souri et
322 al., 2017). To assess the impact of emission control measures on measured N_r
323 concentrations and deposition fluxes at different land use types, we compared
324 arithmetic mean values averaged from the last 3-year period (2013-2015) with those
325 averaged from the first 2-year period (2011-2012) for monitoring sites with
326 continuous 5-year measurements (twenty-one sites for dry, and seventeen sites for
327 wet/bulk). Seasonal concentrations and deposition fluxes of measured N_r species were
328 calculated using the arithmetic average of matched seasons during the sampling

329 periods; spring refers to March-May, summer covers June-August, autumn refers to
 330 September-November, and winter covers December-February.

331

332 3. Results

333 3.1 Spatial variability in concentrations of N_r species in air and precipitation

334 Summary statistics of monthly mean concentrations of NH_3 , NO_2 , HNO_3 ,
 335 pNH_4^+ , and pNO_3^- at the twenty-seven monitoring sites during 2011-2015 are listed
 336 in Table S2 of the Supplement. Monthly mean concentrations of NH_3 , NO_2 , HNO_3 ,
 337 pNH_4^+ , and pNO_3^- ranged from 0.16 (TJ)-39.57 (WJ), 0.55 (LS)-29.06 (WJ), 0.04
 338 (YQ)-4.93 (CAU), 0.11 (ZY)-57.20 (QZ), and 0.01 (DL)-32.06 (ZZ) $\mu g N m^{-3}$,
 339 respectively. On the basis of geographical location and classification of each site, the
 340 annual mean concentrations of each N_r species were calculated for three land use
 341 types in eastern China and its northern and southern regions (Table 1).

342 **Table 1.** Annual average (standard error) concentrations of various N_r compounds in
 343 air and precipitation at different land use types in eastern China and its northern and
 344 southern regions for the 5-year period 2011-2015.

Region ^a	LUT ^b	Ambient conc. $\mu g N m^{-3}$					Rainwater conc. $mg N L^{-1}$			
		NH_3	NO_2	HNO_3	pNH_4^+	pNO_3^-	Total N_r	NH_4^+	NO_3^-	TIN
EC	Urban	8.5	10.2	1.6	8.2	4.0	32.6	1.6	1.9	3.5
	(n=6)	(1.4)	(1.0)	(0.2)	(1.8)	(0.8)	(4.1)	(0.3)	(0.2)	(0.5)
	Rural	7.2	6.0	1.2	6.7	2.8	23.9	1.7	1.4	3.1
	(n=17)	(0.9)	(0.5)	(0.1)	(1.1)	(0.3)	(2.7)	(0.2)	(0.2)	(0.4)
	BKD ^c	3.9	5.2	0.9	4.5	1.9	16.4	1.4	1.2	2.6
	(n=4)	(0.6)	(0.3)	(0.1)	(0.4)	(0.3)	(1.4)	(0.3)	(0.4)	(0.6)
NREC	Urban	8.1	11.7	1.6	8.6	5.1	35.1	2.2	2.4	4.6
	(n=3)	(2.4)	(1.6)	(0.3)	(2.3)	(1.4)	(7.7)	(0.4)	(0.2)	(0.4)
	Rural	9.9	7.4	1.4	9.2	3.7	31.6	2.4	2.0	4.4
	(n=8)	(1.2)**	(0.7)*	(0.1)*	(1.9)*	(0.5)*	(3.8)**	(0.3)**	(0.2)**	(0.4)**
	BKD	4.7	5.7	1.0	5.1	2.4	18.8	1.8	1.5	3.3
	(n=2)	(0.6)	(0.3)	(0.1)	(0.2)	(0.3)	(0.1)	(0.2)	(0.3)	(0.1)
SREC	Urban	8.9	8.7	1.6	7.9	2.9	30.1	1.1	1.5	2.6
	(n=3)	(1.8)	(0.6)	(0.1)	(3.1)	(0.2)	(4.5)	(0.3)	(0.3)	(0.6)
	Rural	4.9	4.6	1.0	4.5	1.9	17.0	1.1	0.9	2.0

(n=9)	(0.6)	(0.6)	(0.1)	(0.6)	(0.2)	(1.7)	(0.2)	(0.1)	(0.3)
BKD	3.1	4.7	0.8	4.0	1.4	14.0	1.0	0.6	1.6
(n=2)	(0.7)	(0.4)	(0.1)	(0.2)	(0.2)	(0.6)	(0.0)	(0.0)	(0.0)

345 ^aEC: eastern China; NREC: northern region of eastern China; SREC: southern region
346 of eastern China. ^bLUTLSY: land use type; n denotes number of monitoring sites. ^c
347 BKD: Background. * and ** denote significance at the 0.05 and 0.01 probability levels
348 for difference in annual mean N_r concentrations at a given site type between northern
349 and southern regions, respectively. ~~—*Significant at the 0.05 probability~~
350 ~~level. **Significant at the 0.01 probability level.~~

351 In eastern China, annual mean concentrations of NH₃, NO₂, HNO₃, pNH₄⁺, and
352 pNO₃⁻ at the urban sites (averages for the 5-year, 1.6 ± 0.2 (for HNO₃) to 10.2 ± 1.0
353 (for NO₂) μg N m⁻³) were increased by 18, 70, 33, 23, and 43%, respectively,
354 compared with their corresponding concentrations at the rural sites (1.2 ± 1.0 (for
355 HNO₃) to 7.2 ± 0.9 (for NH₃) μg N m⁻³); they also increased by 78-118% compared
356 with the concentrations at the background sites (0.9 ± 0.1 (for HNO₃) to 5.2 ± 0.3 (for
357 NO₂) μg N m⁻³), 18-44% and 78-120% higher than their corresponding concentrations
358 at the rural (1.2 ± 1.0 to 7.2 ± 0.9 μg N m⁻³) and background (0.9 ± 0.1 to 5.2 ± 0.3 μg
359 N m⁻³) sites, respectively (Table 1). Analogous patterns also occurred for all measured
360 N_r in each region, except for NH₃ and pNH₄⁺ in the northern region, for which the
361 mean concentrations were 18% and 7% lower at the urban sites than at the rural sites,
362 respectively.

363 Comparing northern vs. southern regions (Table 1), at urban sites the annual
364 mean concentrations of NH₃, HNO₃, and pNH₄⁺ showed smaller non-significant
365 differences (-1~9%), whereas NO₂ and pNO₃⁻ showed larger non-significant increases
366 (34 and 76%, respectively) in the north. By contrast, the mean concentrations of all
367 measured N_r species were significantly (p<0.05) higher (by 40-104%) at rural sites in
368 northern region. Similarly, individual concentrations at background sites were 21-71%
369 higher in the northern than southern region. Averaged across three land use types, the
370 annual mean N_r concentrations of five N_r species in the north increased to varying
371 extent (by 84% for pNO₃⁻, 63% for pNH₄⁺, 57% for NH₃, 47% for NO₂, and 28% for

372 | HNO₃) compared with those in the south. The annual concentrations of total N_r (i.e.,
373 the sum of five N_r species) decreased in the order urban > rural > background in
374 eastern China as a whole and in the north and south regions; further, the annual total
375 N_r concentrations at urban and background sites were 17 and 34% higher ($p > 0.05$) in
376 the north than in the south, respectively, whereas those at northern rural sites ($31.6 \pm$
377 $3.8 \mu\text{g N m}^{-3}$) were significantly ($p < 0.05$) higher than the means at southern rural sites
378 ($17.0 \pm 1.7 \mu\text{g N m}^{-3}$).

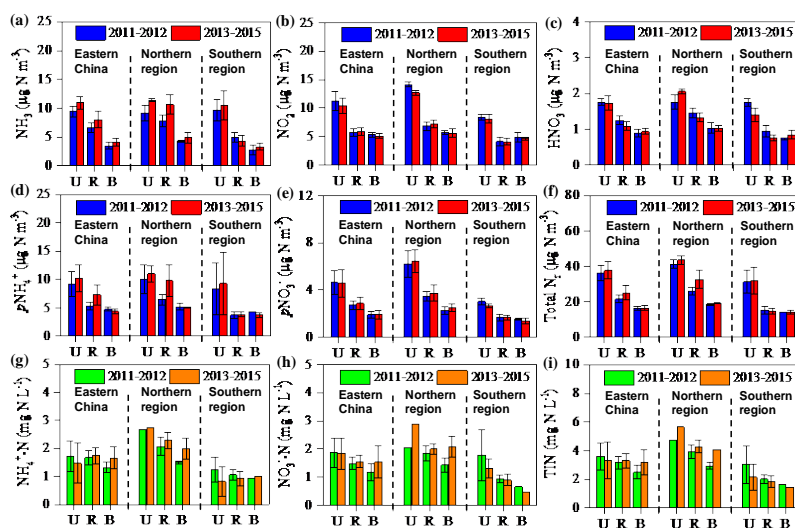
379 The monthly VWM concentrations of NH₄⁺-N, NO₃⁻-N, and TIN (the sum of
380 NH₄⁺-N and NO₃⁻-N) were in the ranges 0.01 (BY)-26.77 (YC), 0.06 (XS)-28.92
381 (WJ), and 0.09 (XS)-50.29 (YC) mg N L⁻¹, respectively (Table S3, Supplement). In
382 eastern China and in each region, the annual VWM concentrations of NO₃⁻-N and
383 TIN showed a declining trend of urban > rural > background, whereas those of
384 NH₄⁺-N followed the order rural \geq urban > background (Table 1). Comparing
385 northern and southern regions, the annual concentrations of NH₄⁺-N, NO₃⁻-N, and
386 TIN were comparable at urban and background sites, and were significantly ($p < 0.05$)
387 higher at northern rural sites.

388 **3.2 Annual variability in concentrations of N_r species in air and precipitation**

389 During the 2011-2015 period the annual mean concentrations of measured N_r
390 species in air exhibited no significant trends at the twenty-two selected sites except
391 for NH₃ at four sites (ZZ, DL, ZMD, YL), HNO₃ at three sites (DL, LSD, BY),
392 $p\text{NH}_4^+$ at one site (XS), and total N_r at three sites (ZMD, YL, WJ) (Fig. S1a-f,
393 Supplement). Similarly, no significant trends were found for the annual VWM
394 concentrations of NH₄⁺-N, NO₃⁻-N, and TIN in precipitation at the seventeen selected
395 sites, with the exception of NO₃⁻-N at one site (SZ) (Fig. S2a-c, Supplement).

396 Fig. 2 compares annual average concentrations of all measured N_r species
397 between the periods 2013-2015 and 2011-2012 for three land use types. In eastern
398 China the mean concentrations of NH₃ and $p\text{NH}_4^+$ showed non-significant increases
399 (10-38%) at all land use types except $p\text{NH}_4^+$ at background sites, which showed a
400 small reduction (8%) (Fig. 2a, d). By contrast, the mean concentrations of remaining
401 N_r species at three land use types showed smaller and non-significant changes: -8~3%

402 for NO_2 (Fig. 2b), -13~5% for HNO_3 (Fig. 2c), and -1~5% for pNO_3^- (Fig. 2e). The
 403 relative changes in the annual total N_r concentration were also not significant, with
 404 the largest increase at rural sites (16%) and smaller increases at urban (4%) and
 405 background (1%) sites (Fig. 2f). Separated by regions, annual mean concentrations of
 406 five N_r species at three land use types mostly showed increases (4-57%) in the north,
 407 and reductions (0.3-21%) in the south (Fig. 2a-f). The relative changes in individual
 408 concentrations at northern rural sites (9% reduction for HNO_3 , and 9-52% increases
 409 for the other species) and southern rural sites (4% increase for pNH_4^+ , and 0.3-21%
 410 reductions for other species) were not significant. The annual total N_r concentrations
 411 showed small relative changes (from -1% to 5%) across all land use types in the two
 412 regions, except at northern rural sites, which exhibited a larger but non-significant
 413 increase (25%) (Fig. 2f). Due to significant interannual variability, longer records are
 414 needed to better assess the significance of any concentration changes.



415
 416 **Figure 2.** Comparison of annual mean concentrations of (a) NH_3 ; (b) NO_2 ; (c) HNO_3 ;
 417 (d) pNH_4^+ ; (e) pNO_3^- ; and (f) total N_r ; sum of all measured N_r in air and
 418 volume-weighted concentrations of NH_4^+ (g); NO_3^- (h) and total inorganic N (TIN):
 419 sum of NH_4^+ and NO_3^- (i) in precipitation between the 2011-2012 period and the
 420 2013-2015 period for different land use types in eastern China and its northern and
 421 southern regions. U, R, and B denote urban, rural, and background sites, respectively.

422 The number of sites for each land use type in each region can be found in Table S1 in
423 the Supplement. The error bars are the standard errors of means.

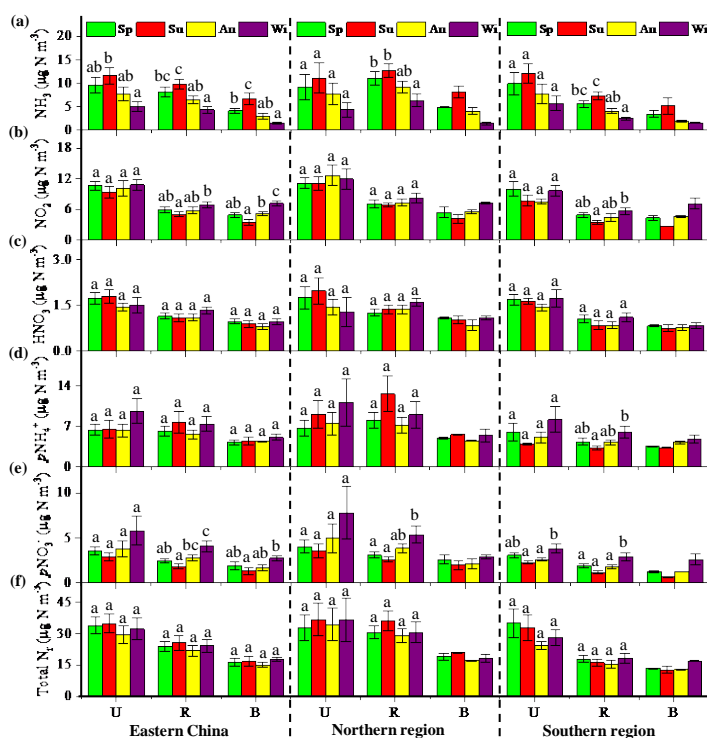
424

425 In eastern China, the annual VWM concentrations of $\text{NH}_4^+\text{-N}$, $\text{NO}_3^-\text{-N}$ and TIN
426 showed the largest increase of 26-31% at background sites, a smaller increase of 4-5%
427 at rural sites, and a decrease of 2-14% at urban sites; however, those changes were not
428 significant (Fig. 2g-i). Regionally, their respective concentrations showed increases
429 (3-45%) in the north and reductions (5-33%) in the south, except for a small increase
430 (4%) in $\text{NH}_4^+\text{-N}$ at background sites.

431 3.3 Seasonal variability in concentrations of N_r species in air and precipitation

432 Fig. 3 shows seasonal patterns of NH_3 , NO_2 , HNO_3 , $p\text{NH}_4^+$, $p\text{NO}_3^-$ and total N_r
433 concentrations for three land use types in eastern China and its northern and southern
434 regions, averaged from corresponding measurements at the twenty-seven study sites
435 (details for each site are given in Tables S4-S9 of the Supplement). Average NH_3
436 concentrations at all land use types decreased in the order summer > spring > autumn >
437 winter, and significant seasonal differences generally occurred between summer and
438 winter (Fig. 3a). Conversely, the average NO_2 concentration generally showed the
439 highest value in winter and the lowest in summer; differences between seasonal
440 concentrations were sometimes significant at rural sites in the south and background
441 sites, but not at urban sites (Fig. 3b). The seasonal changes in the HNO_3 concentration
442 were generally small and not significant for all land use types (Fig. 3c).

443 The average $p\text{NH}_4^+$ concentration exhibited a non-significant seasonal variation
444 across all land use types, except for southern rural sites which showed significantly
445 higher values in winter than in summer (Fig. 3d). The highest $p\text{NH}_4^+$ concentrations
446 mostly occurred in winter. The average $p\text{NO}_3^-$ concentrations at all land use types
447 followed the order winter > spring, ~ autumn > summer; the seasonal changes are
448 sometimes significant, except for urban sites in eastern China and its northern region
449 (Fig. 3e). The average concentration of total N_r usually showed small and
450 non-significant seasonal differences for all land use types (Fig. 3f).



451

452

Figure 3. Seasonal mean concentrations averaged over 2011-2015 of (a) NH_3 ; (b)

453

NO_2 ; (c) HNO_3 ; (d) $p\text{NH}_4^+$; (e) $p\text{NO}_3^-$; and (f) total N_r : sum of all measured N_r in air

454

at different land use types in eastern China and its northern and southern regions. Sp,

455

Su, Au, and Wi represent spring, summer, autumn, and winter, respectively. U, R, and

456

B denote urban, rural, and background sites, respectively. The number of sites for

457

each land use type in each region can be found in Table S1 in the Supplement Table 1.

458

The error bars are the standard errors of means, and values without same letters on the

459

bars denote significant differences between the sites-seasons ($p < 0.05$).

460

461

In eastern China and its two regions, the seasonal VWM concentrations of

462

$\text{NH}_4^+\text{-N}$, $\text{NO}_3^-\text{-N}$ and TIN in precipitation at three land use types (averaged from the

463

twenty-seven sites, details in Tables S10-S12 of the Supplement) showed a similar

464

seasonal pattern, with the highest values in winter and the lowest in summer or

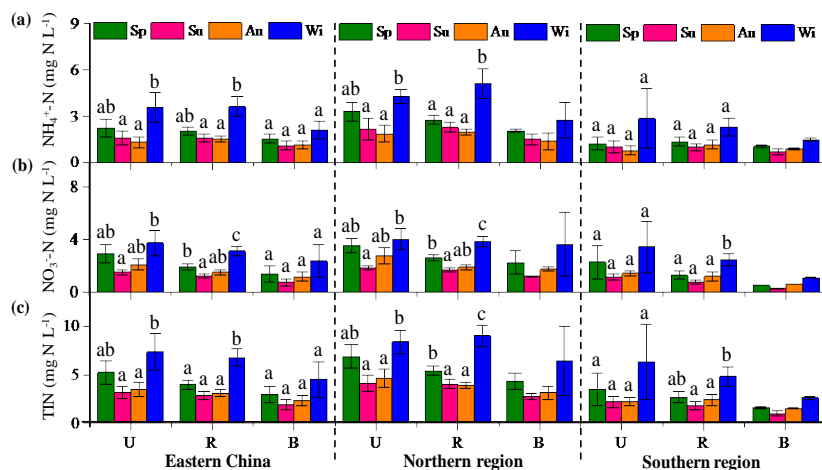
465

autumn (Fig. 4a-c). Significant seasonal differences usually occurred between winter

466

and the other three seasons at all land use types, except background sites and southern

467 urban sites.



468

469 **Figure 4.** Seasonal mean concentrations averaged over 2011-2015 of NH_4^+ (a); NO_3^-
 470 (b) and total inorganic N (TIN): sum of NH_4^+ and NO_3^- (c) in precipitation at
 471 different land use types in eastern China and its northern and southern regions. Sp, Su,
 472 Au, and Wi represent spring, summer, autumn, and winter, respectively. U, R, and B
 473 denote urban, rural, and background sites, respectively. The number of sites for each
 474 land use type in each region can be found in Table S1 in the Supplement Table 1. The
 475 error bars are the standard errors of means, and values without same letters on the bars
 476 denote significant differences between the sites-seasons ($p < 0.05$).

477 3.4 Spatial variability in dry and wet/bulk N deposition of N_r species

478 Dry deposition fluxes of NH_3 , HNO_3 , NO_2 , $p\text{NH}_4^+$, and $p\text{NO}_3^-$ ranked in the
 479 order urban > rural > background in eastern China and in both southern and northern
 480 regions (except for $p\text{NH}_4^+$ in the north) (Table 2). Comparing northern and southern
 481 regions, at urban sites the mean dry $p\text{NH}_4^+$ deposition was slightly higher (2%) in the
 482 north, whereas larger enhancements (24-69%) in the mean fluxes were found in the
 483 north for the remaining N_r species. By contrast, individual fluxes were significantly
 484 higher (by 64-138%) at northern rural sites, except for HNO_3 which showed a large
 485 non-significant increase (58%). At northern background sites, the mean dry deposition
 486 fluxes of NH_3 and NO_2 were much higher (159%) and lower (68%), respectively;
 487 however, only small differences in the means were found for HNO_3 (6% lower in the

488 north), $p\text{NH}_4^+$ (5% lower), and $p\text{NO}_3^-$ (14% higher). The spatial pattern of total N dry
 489 deposition flux (the sum of the fluxes of the five N_r species) by land use types ranked
 490 in the same order as individual N_r species in eastern China. Compared with the
 491 southern region, mean total N fluxes in the north region were significantly higher (by
 492 85%) at rural sites, but showed non-significant increases at urban and background
 493 sites (33 and 38%, respectively).

494 The wet/bulk deposition fluxes of $\text{NH}_4^+\text{-N}$, $\text{NO}_3^-\text{-N}$, and TIN ranked in the order
 495 urban > rural > background in eastern China and in each region (except for $\text{NH}_4^+\text{-N}$ in
 496 the south) (Table 2). In addition, their respective fluxes were generally comparable in
 497 northern and southern regions.

498
 499 **Table 2.** Annual average (standard error) dry and wet/bulk deposition fluxes (kg N
 500 $\text{ha}^{-1} \text{yr}^{-1}$) of various N_r compounds at different land use types in eastern China and its
 501 northern and southern regions for the 5-year period 2011-2015.

Region ^a	LUX ^b	LUT ^b	Dry deposition					Wet/bulk deposition			
			NH_3	NO_2	HNO_3	$p\text{NH}_4^+$	$p\text{NO}_3^-$	Total N_r	NH_4^+	NO_3^-	TIN
EC	Urban		12.6	4.4	7.7	4.8	2.1	31.7	12.6	15.4	28.0
	(n=6)		(1.4)	(1.2)	(1.6)	(1.4)	(0.5)	(4.6)	(1.9)	(0.7)	(2.2)
	Rural		9.1	2.9	4.6	4.0	1.5	22.1	11.9	10.2	22.1
	(n=17)		(0.9)	(0.3)	(0.6)	(0.7)	(0.2)	(2.3)	(1.0)	(0.5)	(1.4)
	BKD ^c		7.9	1.8	3.5	1.9	0.8	15.8	10.7	7.7	18.4
	(n=4)		(2.1)	(0.6)	(0.2)	(0.3)	(0.1)	(1.5)	(1.8)	(0.3)	(1.8)
NREC	Urban		13.9	5.2	9.4	4.9	2.7	36.2	13.9	14.1	28.0
	(n=3)		(1.9)	(2.5)	(3.0)	(1.9)	(1.0)	(8.2)	(3.5)	(1.0)	(4.4)
	Rural		12.1 ^{**}	3.6 [*]	5.7	5.7 [*]	2.1 ^{**}	29.3 ^{**}	12.3	10.3	22.6
	(n=8)		(1.3)	(0.4)	(1.0)	(1.2)	(0.3)	(3.2)	(1.3)	(0.7)	(1.8)
	BKD		11.4	0.9	3.4	1.9	0.8	18.4	7.8	7.6	15.4
	(n=2)		(0.6)	(0.7)	(0.3)	(0.7)	(0.2)	(0.7)	(1.4)	(0.8)	(0.6)
SREC	Urban		11.2	3.6	5.9	4.8	1.6	27.2	11.4	16.6	28.0
	(n=3)		(2.0)	(0.3)	(0.6)	(2.6)	(0.2)	(4.0)	(2.0)	(0.4)	(2.1)
	Rural		6.5	2.2	3.6	2.4	1.0	15.8	11.6	10.2	21.8
	(n=9)		(0.5)	(0.4)	(0.6)	(0.4)	(0.2)	(1.4)	(1.5)	(0.9)	(2.2)

BKD	4.4	2.7	3.6	2.0	0.7	13.3	13.6	7.9	21.5
(n=2)	(1.0)	(0.2)	(0.3)	(0.1)	(0.1)	(0.7)	(0.1)	(0.1)	(0.1)

502 ^aEC: eastern China; NREC: northern region of eastern China; SREC: southern region
503 of eastern China. ^bLUTLSY: land use type; n denotes number of monitoring sites. ^c
504 BKD: Background. * and ** denote significance at the 0.05 and 0.01 probability levels
505 for difference in annual mean N_r concentrations at a given site type between northern
506 and southern regions, respectively. ~~* Significant at the 0.05 probability~~
507 ~~level. ** Significant at the 0.01 probability level.~~

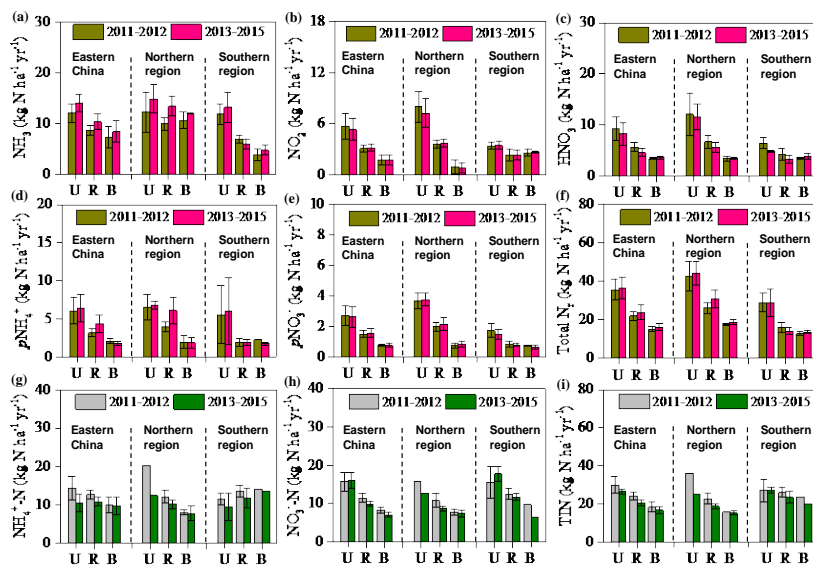
508 3.5 Annual variability in dry and wet/bulk N deposition

509 The annual trends of dry deposition fluxes of individual N_r species at the
510 twenty-one selected sites are consistent with trends in their respective ambient
511 concentrations, except for HNO₃ at three sites (SZ, LSD, and ZY) (Figs. S3a-e and
512 S1a-e, Supplement). A consistent picture is also seen for the total dry N deposition
513 fluxes at all but two sites (DL and WJ) (Figs. S3f and S1f, Supplement). Similarly, the
514 annual trends of wet/bulk deposition fluxes of NH₄⁺-N, NO₃⁻-N and TIN at seventeen
515 selected sites are similar to their respective concentrations in precipitation (Fig. S4a-c,
516 Supplement).

517 In eastern China the annual average dry deposition fluxes of NH₃, NO₂, HNO₃,
518 pNH₄⁺ and pNO₃⁻ showed non-significant increases (2-39%) or reductions (1-19%)
519 between the periods 2011-2012 and 2013-2015 at the three land use types (Fig. 5a-e),
520 similar in sign and magnitude to their respective concentrations described earlier. The
521 annual average total N dry deposition fluxes showed small and non-significant
522 increases across the study periods: 2% at urban sites, 9% at rural sites, and 7% at
523 background sites (Fig. 5f). The sign and magnitude of period-to-period changes in dry
524 deposition and ambient concentrations of all measured N_r species were generally
525 similar between the southern and northern regions.

526 Wet/bulk deposition fluxes of NH₄⁺-N, NO₃⁻-N, and TIN generally decreased
527 (4-29%) between 2011-2012 and 2013-2015 periods at all land use types in eastern
528 China; one exception was NO₃⁻-N, which exhibited a small increase (3%) at urban
529 sites (Fig. 5g-i). Similar tendencies were also observed in both northern and southern

530 regions.



531

532 **Figure 5.** Comparison of dry deposition of (a) NH_3 ; (b) NO_2 ; (c) HNO_3 ; (d) $p\text{NH}_4^+$;

533 (e) $p\text{NO}_3^-$; and (f) total N_r : sum of all measured N_r in air and wet/bulk deposition of

534 NH_4^+ (g); NO_3^- (h) and total inorganic N (TIN): sum of NH_4^+ and NO_3^- (i) in

535 precipitation between the 2011-2012 period and the 2013-2015 period for different

536 land use types in eastern China and its northern and southern regions. U, R, and B

537 denote urban, rural, and background sites, respectively. The number of sites for each

538 land use type in each region can be found in Table S1 in the Supplement. The error

539 bars are the standard errors of means.

540

541 3.6 Seasonal variability in dry and wet/bulk deposition of N_r species

542 Seasonal variations of dry deposition of individual N_r species at each site are

543 shown in Tables S4-S9 in the Supplement. In eastern China and in each region, dry

544 NH_3 deposition fluxes at all land use types followed the order summer > spring >

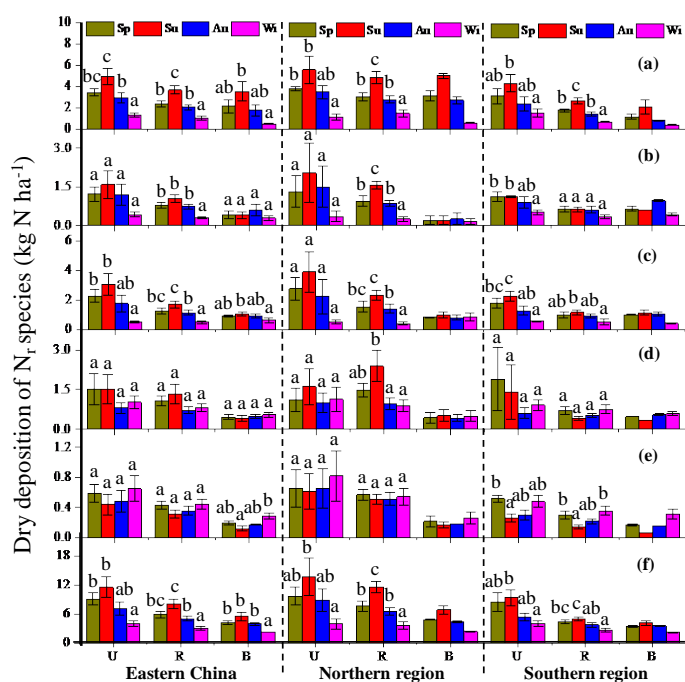
545 autumn > winter, with the seasonal changes usually significantly different (Fig. 6a).

546 Similarly, dry the NO_2 deposition flux was also at its minimum in winter, but its

547 maximum was found in summer at urban and rural sites and in autumn at background

548 site; seasonal differences in most cases were not significant (Fig. 6b). Seasonal

549 patterns of dry HNO_3 deposition flux at all land use types were similar to those for
 550 dry NH_3 deposition fluxes, and the resulting seasonal changes were sometimes
 551 significant, except at northern urban sites (Fig. 6c).



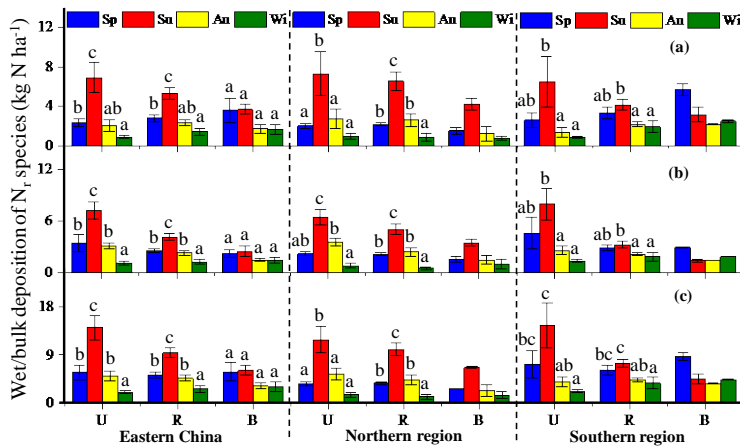
552

553 **Figure 6.** Seasonal mean dry deposition averaged over 2011-2015 of (a) NH_3 ; (b)
 554 NO_2 ; (c) HNO_3 ; (d) $p\text{NH}_4^+$; (e) $p\text{NO}_3^-$; and (f) total N_r : sum of all measured N_r in air
 555 at different land use types in eastern China and its northern and southern regions. Sp,
 556 Su, Au, and Wi represent spring, summer, autumn, and winter, respectively. U, R, and
 557 B denote urban, rural, and background sites, respectively. The number of sites for
 558 each land use type in each region can be found in Table S1 in the Supplement Table 2.
 559 The error bars are the standard errors of means, and values without same letters on the
 560 bars denote significant differences between the sites-seasons ($p < 0.05$).
 561

562 Dry $p\text{NH}_4^+$ deposition fluxes peaked in spring or summer at urban and rural sites,
 563 but remained at similar levels across the four seasons at background sites; however,
 564 no significant seasonal variations were found at any land use types except for rural
 565 sites in the north (Fig. 6d). Dry $p\text{NO}_3^-$ deposition fluxes were higher in spring and

566 winter than in summer and autumn at all land use types, and the seasonal changes
 567 were sometimes significant at background sites and at southern urban and rural sites
 568 (Fig. 6e). Total dry N deposition fluxes at all land use types showed similar seasonal
 569 variations to dry NH₃ deposition, with the highest values in summer and the lowest in
 570 winter; significant seasonal differences generally were observed between winter and
 571 the other three seasons (Fig. 6f).

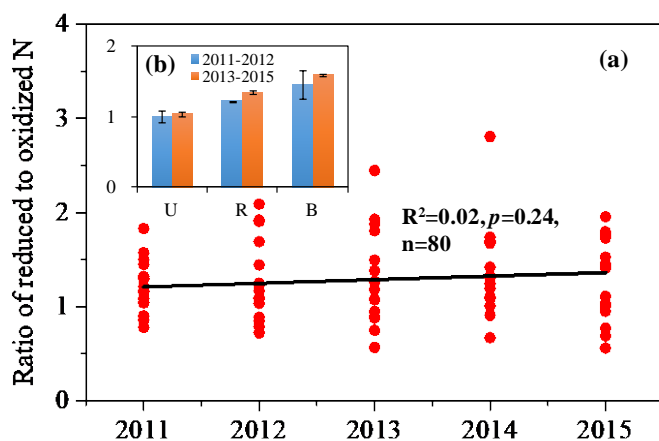
572 Wet/bulk deposition fluxes of NH₄⁺-N, NO₃⁻-N, and TIN all showed significant
 573 seasonal variation at urban and rural sites, but not at background sites, with the
 574 highest values in summer and the lowest in winter (Fig. 7a-c).



575 **Figure 7.** Seasonal mean wet/bulk deposition averaged over 2011-2015 of NH₄⁺ (a);
 576 NO₃⁻ (b) and total inorganic N (TIN): the sum of NH₄⁺ and NO₃⁻ (c) in precipitation
 577 at different land use types in eastern China and its northern and southern regions. Sp,
 578 Su, Au, and Wi represent spring, summer, autumn, and winter, respectively. U, R, and
 579 B denote urban, rural, and background sites, respectively. The number of sites for
 580 each land use type in each region can be found in Table S1 in the Supplement2. The
 581 error bars are the standard errors of means, and values without same letters on the bars
 582 denote significant differences between the sites-seasons ($p < 0.05$).
 583

584
 585 **3.7 Spatial-temporal variability in total annual dry and wet/bulk deposition of N_r**
 586 **species**

587 In eastern China total annual mean N deposition (dry plus wet/bulk) fluxes at
 588 rural and background sites were comparable (on average, 44.3 ± 3.0 and 34.3 ± 0.7 kg
 589 $\text{N ha}^{-1} \text{ yr}^{-1}$, respectively), but significantly lower than those at urban sites (59.7 ± 6.1
 590 $\text{kg N ha}^{-1} \text{ yr}^{-1}$) (Tables 1 and 2, and Fig. S5, Supplement). Similar tendencies for total
 591 N deposition fluxes were observed in the southern region, while in the north a
 592 significant difference was only found between urban and background sites (Fig. S5,
 593 Supplement). From 2011 to 2015, no significant annual trend was found in the total N
 594 deposition at sixteen selected sites (Fig. S6a, Supplement). The total annual mean N
 595 deposition fluxes at three land use types showed small and non-significant reductions
 596 (1-5%) between 2011-12 and 2013-15 (Fig. S6b, Supplement). Regionally, the total
 597 fluxes at each land use type were of similar magnitude in the two periods. Also, the
 598 NH_x (wet/bulk NH_4^+ -N deposition plus dry deposition of NH_3 and particulate
 599 NH_4^+)/ NO_y (wet/bulk NO_3^- -N deposition plus dry deposition of NO_2 , HNO_3 and
 600 particulate NO_3^-) ratio showed a non-significant annual trend across all sites (Fig. 8a).
 601 At all land use types, the averaged ratios were slightly higher in the 2013-2015 period
 602 than in the 2011-2012 period (Fig. 8b).



603
 604 **Figure 8.** Annual trend of the ratio of NH_x (wet/bulk NH_4^+ -N deposition plus
 605 dry deposition of NH_3 and particulate NH_4^+) to NO_y (wet/bulk NO_3^- -N deposition
 606 plus dry deposition of NO_2 , HNO_3 and particulate NO_3^-) across sixteen selected sites
 607 (a), with a comparison between the 2011-2012 period and the 2013-2015 period for

608 different land use types in eastern China (**b**). U, R, and B denote urban, rural, and
609 background sites, respectively. The number of sites with the same land use type can
610 be found in Fig. S6 in the Supplement.

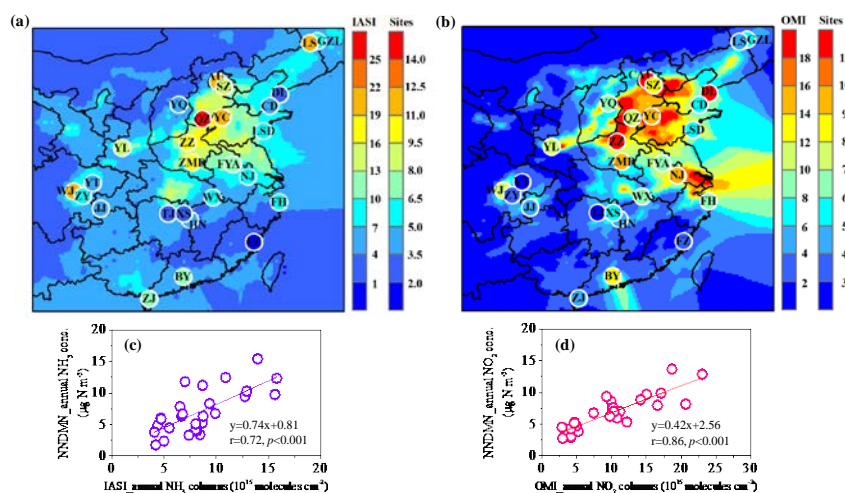
612 4. Discussion

613 4.1 Comparisons of NH₃ and NO₂ measurements with satellite data

614 Eastern China ~~as~~ is a highly industrialized and polluted region, and has been
615 proven to be a hot-spot of N_r (NH₃ and NO_x) emission and deposition globally (Vet et
616 al., 2014; Kanakidou et al., 2016). The results presented above showed that, in eastern
617 China, annual mean concentrations of measured N_r species in air and precipitation
618 were generally higher in the north than in the south (Table 1). This is likely due to
619 higher consumption of energy and application of N-fertilizers, along with lower
620 precipitation amounts in the north, previously identified as key factors affecting
621 spatial patterns of N deposition in China (Liu et al., 2013; Jia et al., 2014; Zhu et al.,
622 2015). Because only 27 sites covering a range of land use types were included in the
623 present study, additional information would be valuable in determining whether the
624 observed spatial patterns adequately represent conditions in eastern China. To address
625 this issue, we use measured NH₃ and NO₂ concentrations to evaluate remote sensing
626 techniques for retrieving NH₃ and NO₂ concentrations. If accurate, those remote
627 sensing techniques are well suited to ascertain regional species distributions. NH₃ and
628 NO_x are primary emissions with important anthropogenic emissions (Fowler et al.,
629 2013). NO, the main component of emitted NO_x, is oxidized in the atmosphere to
630 NO₂. NO₂ is further oxidized via daytime or nighttime chemistry to HNO₃ (Khoder,
631 2002). NH₃ and HNO₃ can react to form fine particle ammonium nitrate (Seinfeld and
632 Pandis, 2006). Thus, spatial patterns of NH₃ and NO₂ observed from space can be
633 useful indicators of reduced and oxidized N_r pollution over eastern China.

634 From satellite observations (Fig. 9a, b), it can be seen that both IASI_NH₃ and
635 OMI_NO₂ columns show clearly higher values over the northern region of eastern
636 China. Overall, satellite observations and surface measurements for NH₃ and NO₂
637 (plotted on the maps of Fig. 9a, b) show a similar spatial pattern. Significant positive

638 correlations were found between IASI_NH₃ column observations and NNDMN_NH₃
 639 measurements ($r=0.72$, $p<0.001$) (Fig. 9c) and between OMI_NO₂ observations and
 640 NNDMN_NO₂ measurements ($r=0.86$, $p<0.001$) (Fig. 9d) at the 27 surface
 641 measurement locations, suggesting that satellite measurements of NH₃ and NO₂ can
 642 be used to capture regional differences in NH₃ and NO₂ pollution. Looking beyond
 643 the surface measurement location, the satellite observations further confirm the
 644 existence of greater N_r pollution in the northern region of eastern China than in the
 645 southern region.



646

647

648

649

650

651

Figure 9. Spatial variation of atmospheric N_r in eastern China: (a) NNDMN_NH₃ concentrations vs. IASI_NH₃ columns; (b) NNDMN_NO₂ concentrations vs. OMI_NO₂ columns; (c) relationship of NNDMN_NH₃ concentrations vs. IASI_NH₃ columns; (d) relationship of NNDMN_NO₂ concentrations vs. OMI_NO₂ columns.

652

653

654

655

656

657

658

To further explore temporal concentration variability, monthly mean satellite NH₃ and NO₂ columns are compared with monthly mean ground concentrations of NH₃ and NO₂ (Figs. S7 and S8, Supplement). The linear correlation between satellite columns and surface NH₃ concentrations is significant ($p<0.05$) at the ten sites ($r=0.32-0.87$) in the northern region and at four sites ($r=0.46-0.84$) in the southern region (Fig. S7, Supplement), while the linear correlation between satellite columns and surface NO₂ concentrations is significant at the ten sites ($r=0.28-0.68$) in the

659 northern region and nine sites ($r=0.36-0.66$) in the southern region (Fig. S8,
660 Supplement). These results indicate that the OMI_NO₂ retrieval can well capture the
661 temporal variations of surface NO₂ concentrations over eastern China, whereas the
662 IASI_NH₃ retrievals better capture temporal variability in surface concentrations for
663 the northern region. The weak correlations observed between IASI_NH₃ observations
664 and surface measurements at ten of the fourteen sites in the southern region (Fig. S7,
665 Supplement) suggest that the IASI_NH₃ observations need to be improved for
666 investigating temporal variability in NH₃ concentration, despite that the satellite
667 observation is at a specific time of day while the surface concentrations integrate
668 across the diurnal cycle of emissions and mixing layer evolution. It should be noted
669 that a direct comparison between surface concentration and satellite column
670 measurements is inevitably affected by many factors, such as changes in boundary
671 layer height, vertical profiles of species, and interferences from cloud and aerosol
672 (Van Damme et al., 2015). Nevertheless, the ratio of satellite column to surface
673 concentration measurements is meaningful as it can provide insight into sensitivity of
674 a satellite retrieval to variation in the concentration of a gas in the surface layer (Meng
675 et al., 2008). To make a more accurate comparison, the vertical profile is
676 recommended to convert the columns to the ground concentrations in future work.

677 **4.2 Seasonal variations of N_r concentration and deposition**

678 The seasonal concentrations of N_r species in air and precipitation are dependent
679 on their sources and meteorological conditions. The highest concentrations of NH₃ in
680 summer at all land use types (Fig. 3a) are most likely due to enhanced NH₃ emission
681 from natural and fertilized soils, and biological sources such as humans, sewage
682 systems and organic waste in garbage containers (Chang et al., 2016). Zhang et al.
683 (2018) showed that NH₃ emissions in China show a strong summer peak, with
684 emissions about 50% higher in summer than spring and autumn. The lowest
685 concentrations of NH₃ in winter (Fig. 3a) can be ascribed to ~~low the reduced~~ NH₃
686 volatilization ~~under cold condition at low air temperature~~, high snow coverage, and
687 ~~lowless~~ agricultural activities (Cao et al., 2009) ~~with large as well as~~ consumption of
688 NH₃ to form NH₄NO₃ ~~(Fig. 3a, d and e)~~ and/or (NH₄)₂SO₄. The lower NO₂

689 concentration in summer (Fig. 3b) might result from ~~greater~~higher atmospheric
690 mixing in a deeper boundary layer and a higher rate of oxidation of NO₂ to HNO₃ by
691 reaction with OH (Atkins and Lee, 1995), which is more abundant in summer due to
692 greater photochemical activity. Increased NO₂ emissions from greater coal
693 combustion for domestic heating (from middle November to middle March) in
694 ~~Northern~~northern China may also enhance NO_x emissions and subsequent NO₂
695 concentrations in autumn/winter (Zhao et al., 2011).

696 Particulate NH₄⁺ and NO₃⁻ are mainly generated via chemical reactions between
697 NH₃ and inorganic acids (e.g., HNO₃, H₂SO₄). We found that concentrations of
698 *p*NH₄⁺ and *p*NO₃⁻ at all land use types usually peaked in winter because low
699 temperature and high emissions of NO_x and SO₂ are favorable for formation of
700 NH₄NO₃ and (NH₄)₂SO₄ aerosols (Xu et al., 2016), consistent with higher
701 concentrations of *p*NH₄⁺ and *p*NO₃⁻. In addition, in winter temperature inversions in
702 combination with stable meteorological conditions (e.g., low wind speed) limit
703 horizontal and vertical exchange of pollutants, and further elevated atmospheric
704 *p*NH₄⁺ and *p*NO₃⁻ levels (Liu et al., 2017). In order to identify potential transport of
705 NO₂, *p*NH₄⁺ and *p*NO₃⁻ from northern region, we calculated three-day backward
706 trajectories arriving at five southern sites (Nanjing, Baiyun, Taojing, Ziyang and
707 Huinong) during January, April, July and October using the TrajStat. The TrajStat
708 analysis generally showed that the high proportions (overall 10-36%) of air masses
709 from the north to the south of eastern China occurred in the autumn/winter, suggesting
710 that the transport of NO₂, *p*NH₄⁺ and *p*NO₃⁻ from northern China would result in
711 increases in their respective concentrations in autumn/winter south of the Qinling
712 Mountains-Huaihe River line, except at Ziyang site (Fig. S13, Supplement).

713 Nitric acid is a secondary pollutant, formed through gas phase reaction of NO₂
714 with the OH radical, reaction of NO₃ with aldehydes or hydrocarbons or hydrolysis of
715 N₂O₅ (Khoder, 2002). Nitric acid concentrations are expected to be further influenced
716 by air temperature, relative humidity and ambient NH₃ concentrations (Allen et al.,
717 1989); fine particle NH₄NO₃ formation is favored at low temperatures and high
718 relative humidities. Due to a lack of information regarding primary formation

719 pathways and influencing factors at our study sites, we cannot offer a definitive
720 explanation for small and differing seasonal patterns of HNO_3 concentrations
721 observed at the three land use types (Fig. 3c).

722 Ammonium-N and nitrate-N in precipitation mainly originate from
723 corresponding reduced (e.g., NH_3 , $p\text{NH}_4^+$) and oxidized (e.g., HNO_3 , NO_2 , $p\text{NO}_3^-$) N
724 in air, scavenged respectively, by rain and/or snow events (Seinfeld and Pandis, 2006).
725 At all land use types, the seasonal variation of NH_4^+ -N concentration in precipitation
726 was opposite to that of reduced N (the sum of NH_3 and $p\text{NH}_4^+$) concentrations (Figs.
727 4a and S9a in the Supplement), whereas a similar seasonal pattern was found between
728 NO_3^- -N and oxidized N (the sum of HNO_3 , NO_2 and $p\text{NO}_3^-$) concentrations (Figs. 4b
729 and S9b in the Supplement). Higher precipitation amounts in summer could account
730 for lower NH_4^+ -N concentrations in summer (Figs. 4a and S10 in the Supplement)
731 due to a dilution effect (Xu et al., 2015). In contrast, seasonal variations of rainwater
732 NO_3^- -N concentrations were more likely dominated by seasonal changes in oxidized
733 N concentrations rather than precipitation amount.

734 The seasonal variation of NH_3 dry deposition is generally similar to that of NH_3
735 concentration (Figs. 3a and 6a). Given comparable seasonal mean V_d for NH_3 across
736 the four seasons in most cases (Fig. S11a-c, Supplement), the seasonality of NH_3
737 deposition is mainly dominated by changes in ambient NH_3 concentrations. Seasonal
738 deposition fluxes of NO_2 and HNO_3 both differ appreciably (Fig. 6b, c), showing
739 similar variation to seasonality of their respective V_d values (Fig. S11d-i, Supplement).
740 Given weaker seasonal fluctuations of NO_2 and HNO_3 concentrations, the seasonality
741 of NO_2 and HNO_3 dry deposition are primarily functions of changes in V_d . Similar
742 analyses suggest that seasonal variation of $p\text{NO}_3^-$ dry deposition was mainly caused
743 by differences in seasonal $p\text{NO}_3^-$ concentrations (Figs. 3e and 6e), whereas that of
744 $p\text{NH}_4^+$ dry deposition was primarily driven by seasonal changes in V_d (Figs. 6c and
745 S11j-l, Supplement).

746 **4.3 The role of NH_3 in mitigation of N_r air pollution**

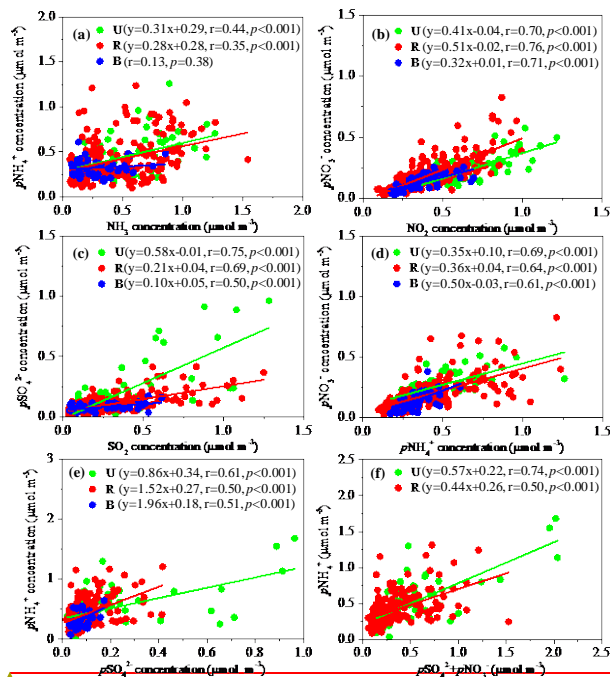
747 The latest pollutant emissions statistics from the Chinese Ministry of
748 Environmental Protection

749 (http://www.zhb.gov.cn/gkml/hbb/qt/201507/t20150722_307020.htm) showed that
750 total annual emissions of SO₂ and NO_x were reduced by 12.9% and 8.6% in 2014
751 (approximately 9.9 Tg S yr⁻¹ and 6.3 Tg N yr⁻¹, respectively), respectively, compared
752 with those in 2010 (approximately 11.3 Tg S yr⁻¹ and 6.9 Tg N yr⁻¹, respectively). This
753 suggests that the goal set for the 12th FYP period was fulfilled ahead of time. Our field
754 measurements demonstrate that annual mean concentrations of each N_r species and
755 total N_r did not show significant decreasing trends at most sites during the 2011-2015
756 period (Fig. S1a-f, Supplement). Furthermore, annual mean total N_r concentrations
757 showed non-significant increases (1-16%) at three land use types during the
758 2013-2015 period compared with 2011-2012 (Fig. 2f). These results together suggest
759 that N_r pollution may be not effectively mitigated in eastern China during the 12th
760 FYP, likely due to the absence of NH₃ regulations, despite enforcement of a “Zero
761 Increase Action Plan” by the Ministry of Agriculture for national fertilizer use (X. J.
762 Liu et al., 2016).

763 Ammonia is the primary alkaline gas in the atmosphere. It plays an important
764 role in formation of (NH₄)₂SO₄ and NH₄NO₃ aerosols (Seinfeld and Pandis, 2006).
765 These secondary inorganic aerosols account for 40–57 % of the PM_{2.5} concentrations
766 in eastern China (Yang et al., 2011; Huang et al., 2014). Based on monthly mean
767 molar concentrations, there were significant positive linear correlations between NH₃
768 and pNH₄⁺, NO₂ and pNO₃⁻, SO₂ and pSO₄²⁻, pNH₄⁺ and pNO₃⁻, and pNH₄⁺ and
769 pSO₄²⁻ at all land use land types except for a non-significant relationship of NH₃ with
770 pNH₄⁺ at background sites (Fig. 10a-e). These results suggest that the precursor gases
771 are responsible for the formation of secondary inorganic ions (i.e., pNH₄⁺, pNO₃⁻, and
772 pSO₄²⁻) locally at urban and rural sites, while secondary inorganic ions at background
773 sites likely originated from long-distance transport. The ratio of NH₃ to NH_x (NH₃
774 plus pNH₄⁺) concentrations at urban (0.53 ± 0.15) and rural (0.52 ± 0.16) sites
775 exceeded values at background (0.43 ± 0.16) sites. According to Walker et al. (2004),
776 a value greater than 0.5 indicates that NH_x is more likely to be from local sources as
777 opposed to long-range transport.

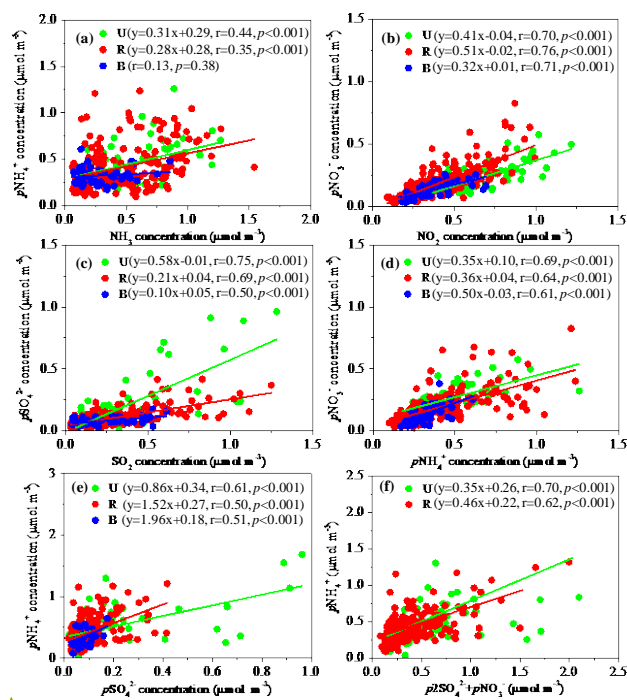
带格式的: 字体: (默认) Times New Roman, 小四, 字体颜色: 自动设置

带格式的: 缩进: 首行缩进: 2 字符



带格式的: 字体: +西文正文, 五号, 字体颜色: 自动设置

带格式的: 缩进: 首行缩进: 2 字符



778

779

780 **Figure 10.** Correlations of monthly mean molar concentrations of (a) $p\text{NH}_4^+$ vs. NH_3 ;
781 (b) $p\text{NO}_3^-$ vs. NO_2 ; (c) $p\text{SO}_4^{2-}$ vs. SO_2 ; (d) $p\text{NO}_3^-$ vs. $p\text{NH}_4^+$; (e) $p\text{NH}_4^+$ vs. $p\text{SO}_4^{2-}$;

782 (f) $p\text{NH}_4^+$ vs. ($p\text{SO}_4^{2-} + p\text{NO}_3^-$) at three land use types in eastern China. The number
783 of sites with the same land use type in each region can be found in Table ~~1S1 in the~~
784 ~~Supplement.~~

785 It is known that NH_3 in the atmosphere is preferentially neutralized by H_2SO_4 to
786 form $(\text{NH}_4)_2\text{SO}_4$ and/or NH_4HSO_4 , with any remainder available for potential
787 reaction with HNO_3 to form NH_4NO_3 . At urban and rural sites, monthly mean $p\text{NH}_4^+$
788 concentrations significantly positively correlated with the sum of $p\text{SO}_4^{2-}$ and $p\text{NO}_3^-$
789 concentrations (Fig. 10f). However, the slopes of regression equations between them
790 were both smaller than unity (~~0.57–35~~ and ~~0.44–46~~ at urban and rural sites,
791 respectively), indicating an incomplete neutralization of acidic species (HNO_3 and
792 H_2SO_4) by NH_3 at urban and rural sites. In other words, NH_3 is a factor limiting the
793 formation of secondary inorganic ions. A model simulation by Wang et al. (2011)
794 found that, without NH_3 emission controls, NO_3^- in $\text{PM}_{2.5}$ will be enhanced by 10%
795 in 2030 compared with 2005 in China, despite improved NO_x emissions controls. As
796 reported by Zhang et al. (2017), total NH_3 emissions in China increased from 12.1 Tg
797 N yr^{-1} in 2000 to 15.6 Tg N yr^{-1} in 2015 at an annual rate of 1.9%. In contrast, total
798 emissions of NO_x and SO_2 have decreased or stabilized in recent years, and were
799 estimated to be 8.4 Tg N yr^{-1} and 12.5 Tg S yr^{-1} in 2014, respectively (Xia et al.,
800 2016). Based on these factors, implementation of NH_3 control strategies, ~~relative~~
801 ~~together with more stringent~~ ~~current~~ NO_x and SO_2 emission controls, should be
802 considered to mitigate atmospheric N_r pollution.

803 4.4 The role of NH_3 emission in control of N deposition

804 The present results showed that total dry N deposition fluxes at three land use
805 types were higher in the northern region of eastern China than in the southern region
806 (Table 1), mainly due to higher NH_3 dry deposition resulting from higher NH_3
807 concentrations in the north. This is especially true for northern rural sites (Table 1),
808 mostly located in the North China Plain (NCP) (see details in Xu et al. (2015)). The
809 NCP (that is, the plain areas in Beijing, Tianjin, Hebei, Henan, and Shandong
810 provinces), a highly populated region with intensive agricultural production,
811 contributes 30-40% of the total annual NH_3 emissions in China (Huang et al., 2012).

812 In addition, higher NH₃ concentration is also likely due to the higher NH₃
813 volatilization in calcareous soils than that in the acidic red soil, as mentioned in
814 Section 2.1. Total annual NH₃ emissions in northern region increased from 4.3 Tg N
815 yr⁻¹ in 2011 to 4.7 Tg N yr⁻¹ at an annual rate of 1.8%. In contrast, the emissions of
816 NO_x and SO₂ averaged 2.8 Tg N yr⁻¹ and 3.7 Tg S yr⁻¹ during 2011-2015, and
817 decreased at annual rates of 6.8 and 5.7%, respectively (details of the emissions will
818 be illustrated in Section 4.5). Such reductions may enhance free NH₃ in the
819 atmosphere. However, according to a modeling study by Han et al. (2017), the
820 influence of removing anthropogenic SO₂ emissions on dry N deposition fluxes
821 during 2010-2014 was quite weak, with the change within -0.5~0.5 (kg N ha⁻¹ yr⁻¹)
822 over most regions in China. Thus, we anticipate that reducing NH₃ emissions can
823 effectively control N deposition.

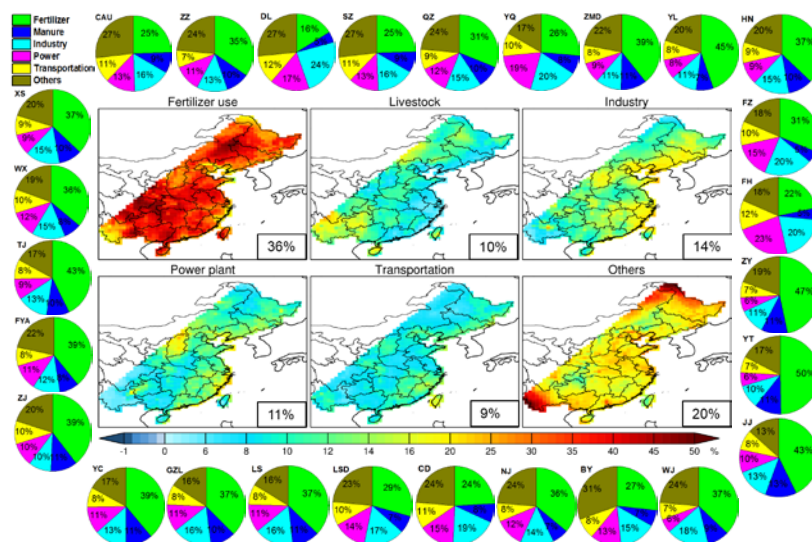
824 To further examine contributions of NH₃ emissions to total (wet plus dry) N
825 deposition at each site and over eastern China, we conducted model sensitivity tests
826 using the nested GEOS-Chem atmospheric chemistry model driven by the GEOS-5
827 assimilated meteorological fields at a horizontal resolution of 1/2° × 2/3°. The model
828 used anthropogenic emissions from the Multi-Resolution Emission Inventory of
829 China (MEIC, <http://meicmodel.org>) for the year 2010, except for NH₃ emissions that
830 are taken from the Regional Emission in Asia (REAS-v2) inventory (Kurokawa et al.,
831 2013), with an improved seasonality derived by Zhao et al. (2015). The total NH₃ and
832 NO_x emissions from each source over eastern China and its contribution to total
833 emissions in China are presented in Table S13 in the Supplement. The NH₃ and NO_x
834 emissions over eastern China are 11.6 Tg N yr⁻¹ and 8.5 Tg N yr⁻¹ in 2010, which,
835 respectively, account for 90% and 89% of their total emissions over China.
836 Agricultural sources including fertilizer use and livestock, comprise most of the NH₃
837 emissions while fuel combustion activities, including industry, power plant, and
838 transportation contribute most of the NO_x emissions and small amounts of NH₃
839 emissions. Both NH₃ and NO_x have natural sources (including lightning, biomass
840 burning and soil emissions), but are negligible compared to anthropogenic emissions
841 over eastern China. Details of the model emissions and mechanisms have been

842 described elsewhere (Zhao et al., 2017, Xu et al., 2018).

843 ~~In brief, anthropogenic sources of NH₃ emissions include fertilizer use,~~
844 ~~livestock, human waste, and fuel combustion (that in power plant, industry,~~
845 ~~transportation and residential), whereas NO_x emission sources include industry, power,~~
846 ~~transportation, and residential. Both NH₃ and NO_x have natural sources (including~~
847 ~~lighting, biomass burning and soil emissions). It should be pointed out that fertilizer~~
848 ~~NH₃ emissions include both chemical fertilizer and manure fertilizer.~~

849 We evaluate the model simulations by comparing with measured bulk (both
850 NH₄⁺-N and NO₃⁻-N) fluxes. The model biases for bulk NH₄⁺-N and NO₃⁻-N
851 deposition were 23 and -23%, respectively (Fig. S8S12, Supplement). These biases
852 are reasonable, given uncertainties in N_r emissions and predictions of meteorology.
853 Given that model evaluation is not central to this work, we presented the details in
854 Sect. S1-S2 in the Supplement. As shown in Fig. 11, fertilizer use is the dominant
855 source of total N deposition at all sites, with contributions between 16-50%. Also,
856 over eastern China the largest contribution was from fertilizer use (36%) relative to
857 livestock (10%), industry (14%), power plant (11%), transportation (9%), and other
858 sources (20%, the sum of contributions from human waste, residential activities, soil,
859 lighting and biomass burning). These results indicate that reducing NH₃ emissions
860 ~~from improper by use of appropriate fertilization patterns (e.g., 4 R technologies~~
861 ~~(Right amount, Right time, Right form and Right application technique). Ju et al.,~~
862 ~~2009) fertilizer (including chemical and organic fertilizer) application~~ should be a
863 priority in curbing N deposition in eastern China.—, This conclusion to some extent is
864 supported by increased ratios of reduced to oxidized N in the total deposition at three
865 land use types (Fig. 8b), as the major anthropogenic source of reduced N is mainly
866 affected by NH₃ volatilized from animal excrement and the application of nitrogenous
867 fertilizers in agriculture. Absence of NH₃ emission controls may be the main reason
868 for a small and non-significant change in the total N deposition between 2011-12 and
869 2013-15 (Fig. S6, Supplement), despite enforcement of stringent emission controls on
870 NO_x and SO₂. To test the importance of future NH₃ emission control strategies, we
871 conducted separate model simulations which reduced NH₃ emissions from fertilizer

872 use by 20%. The results show that a 20% reduction in fertilizer NH₃ emissions can
 873 lead to 7.4% decrease in total N deposition over Eastern China.



874 **Figure 11.** Fractional contributions to total N deposition from emission sectors (i.e.
 875 fertilizer use, livestock, industry, power plant, transportation, and others including
 876 emissions from human waste, residential activities, soil, lighting and biomass burning)
 877 at the twenty-seven sites and over eastern China.
 878

880 4.5 Deposition response to emission change

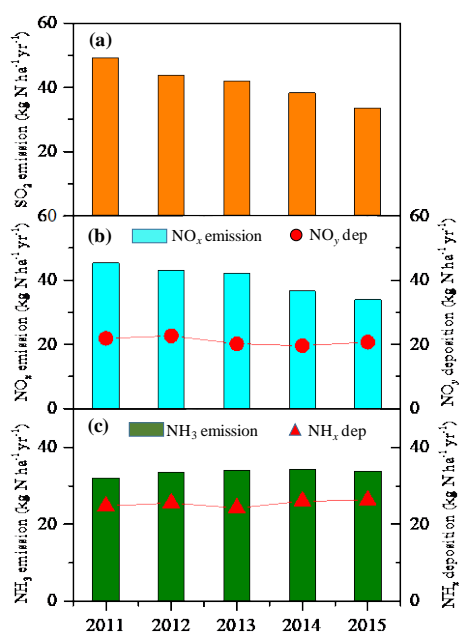
881 Similar to N_r concentrations, there were no significant decreasing trends in dry
 882 and bulk deposition of total N or of individual N_r species at almost all study sites
 883 (Figs. S3 and S4, Supplement). In addition, we found that changes in annual mean
 884 deposition fluxes of various N_r species are fairly small between the 2013-2015 and
 885 2011-2012 periods (Fig. 5). These results suggest that current emission controls did
 886 not effectively reduce N deposition in eastern China.

887 To further assess the relationship between emission and deposition change, we
 888 considered the emissions of SO₂, NO_x and NH₃ affecting the sixteen study sites with
 889 continuous and simultaneous dry and bulk deposition measurements (Fig. S6 and
 890 Table S1, Supplement). The regional NH₃ emission data for 2011-2015 were derived
 891 from Zhang et al. (2017), while SO₂ and NO_x emission data for 2011-2014 were

892 derived from Xia et al. (2016) (emission data for the year 2015 were provided by Prof.
 893 Yu Zhao, and were unpublished). We compared these annual data with annual mean
 894 deposition values from the 16 sites. It should be noted that such assessment is subject
 895 to some uncertainty, as emission data was estimated based on the areas belonging to
 896 eastern China.

897 A clear decreasing trend in SO_2 and NO_x emissions was observed, with
 898 reductions of 32% and 25% in 2015 compared to 2011, respectively (Fig. 12a, b). This
 899 reduction is directly related to the widespread use of selective catalytic reduction and
 900 flue gas de-sulfurization on power plants and industries (Van der A et al., 2017), and
 901 to a lesser extent to the introduction of new emission standards for cars (F. Liu et al.,
 902 2016). In contrast, NH_3 emissions generally showed a gradual increasing trend
 903 between 2011 and 2015 (Fig. 12c), as control strategies have not yet been enacted and
 904 implemented for NH_3 emissions in China.

905



906

907 **Figure 12.** Emissions of SO_2 (a), NO_x (b) and NH_3 (c) obtained as average data from
 908 the areas belonging to eastern China, compared with deposition values in the same
 909 periods (mean values from the sixteen sites showing in Fig. S6 and Table S1 in the

910 Supplement , 5-year averages).

911 Regarding N deposition, a non-significant increasing trend was found for NH_x
912 (slope= $0.36 \text{ kg N ha}^{-1} \text{ yr}^{-1}$) between the 2011 and 2015 period, whereas NO_y
913 deposition exhibited a non-significant decreasing trend (slope= $0.54 \text{ kg N ha}^{-1} \text{ yr}^{-1}$).
914 Also, there were non-significant linear correlations between NH_x deposition and NH_3
915 emission and between NO_y deposition and NO_x emission. This is not surprising given
916 that atmospheric chemistry is complex and often behaves non-linearly (Fowler et al.,
917 2007; Fagerli and Aas, 2008). Interactions between the different pollutants,
918 precipitation variability, changes in the relative amounts and lifetimes of the chemical
919 species and in gas-particle partitioning all may contribute to the lack of correlation
920 between emission and deposition trends. Non-linearities between emission and
921 deposition change have been described also elsewhere (Aguillaume et al., 2016;
922 Karlsson et al., 2011). Deposition in eastern China is also influenced by emissions
923 from outside the region, further degrading any expected correlation with local
924 emissions.

925 **4.6 Uncertainties and limitations**

926 The present study examined annual trends of concentrations of N_r species in air
927 and precipitation as well as dry and bulk N deposition based on Kendall tests and only
928 five annual data values (2011-2015). Although the test can use as few as 4 data points,
929 indications of statistically significant trends for datasets are unlikely to be truly
930 representative of the trends that are actually occurring due to in the short duration of
931 the measurement dataset. Longer time series (e.g., more than 10-year) will likely
932 allow detection of more significant time trends in future work. Another uncertainty
933 may arise from the fact that we used fixed monthly mean dry deposition velocities of
934 gaseous and particulate N_r species for the same months from June 2013 to December
935 2015. Nevertheless, the uncertainty in the V_d value did not largely affect the
936 deposition trend, as the annual trend in dry deposition of N_r species is more likely
937 driven by changes in ambient N_r concentrations than to changing deposition velocities,
938 as evident from fairly low standard deviations of annual mean V_d of N_r species at our
939 selected 27 sites between 2008 and 2012 (~ 0.029 for NH_3 , ~ 0.005 for NO_2 , ~ 0.054

940 for HNO_3 , and ~ 0.019 for both $p\text{NH}_4^+$ and $p\text{NO}_3^-$, data were extracted from Zhao et
941 al. (2017)).

942 In addition, we did not account for inter-annual changes in meteorology, which
943 also strongly influences atmospheric N_r levels and N deposition (Xu et al., 2015,
944 2017). For example, air concentrations of NO_2 , NH_3 , and $p\text{NH}_4^+$ and $p\text{NO}_3^-$ trend to
945 increase under the relatively stagnant conditions prior to a cold front's arrival and
946 decrease substantially after the cold front brings precipitation and strong winds into
947 the region (Xu et al., 2017). On the inter-annual time scale, the frequency of cold front
948 passages may be affected by large-scale circulation patterns such as the position of the
949 Siberian high for eastern China (Jia et al., 2015). For example, a large inter-annual
950 variation in precipitation amount was observed at the selected 16 sites during
951 2011-2015 (Fig. S14, Supplement), which partially lead to inter-annual changes in
952 wet/bulk N deposition. However, Given-given that *in-situ* measurements of other
953 meteorological variables (e.g., air temperature, relative humidity, air pressure, wind
954 speed and direction) are not available, and that GEOS-5 assimilated meteorological
955 fields were updated after May 2013, an evaluation of the effect of meteorology on N_r
956 concentration and deposition is recommended for future work.

957 Uncertainties also exist in the source attribution calculated with the GEOS-Chem
958 simulations, since results largely depend on the emission inventories fed to the model.
959 Zhao et al. (2017) pointed out that uncertainties in current NH_3 emissions inventories
960 (e.g. large range of the emission value in current studies and absence of inclusion of
961 bi-directional NH_3 exchange between the land and atmosphere) may influence
962 nitrogen deposition simulation in China. Future work based on improved NH_3
963 emission inventories (e.g., Zhang et al., 2018) and including bidirectional ammonia
964 exchange with the surface is essential to better examine source attribution of N
965 deposition in China.

966 **5. Conclusion**

967 We have characterized spatial and temporal (annual and seasonal) variations in
968 concentrations and deposition of major N_r species in air (NH_3 , NO_2 , HNO_3 , $p\text{NH}_4^+$,
969 and $p\text{NO}_3^-$) and precipitation ($\text{NH}_4^+\text{-N}$ and $\text{NO}_3^-\text{-N}$) for three land use types (e.g.,

970 urban, rural and background) in eastern China by examining five-year (2011-2015) *in*
971 *situ* measurements at twenty-seven sites. We further examined regional features of N_r
972 pollution by comparison of satellite and surface measurements of NH_3 and NO_2 and
973 examined the sources of total N deposition over the whole region for the year 2010
974 using the GEOS-Chem model at horizontal resolution of $1/2^\circ \times 2/3^\circ$. Our major
975 results and conclusions are as follows:

976 In eastern China, annual mean concentrations and dry and bulk deposition fluxes
977 of measured N_r species in air and precipitation generally ranked in the order urban >
978 rural > background. The air concentrations and dry deposition were usually higher at
979 all land use types in the northern region of eastern China than in the southern region,
980 especially (except HNO_3) at rural sites, for which the differences reached statistically
981 significant levels. This is also true for the annual VWM concentrations of NH_4^+-N ,
982 NO_3^--N , and TIN in precipitation, whereas bulk deposition fluxes of these species
983 were comparable for matched land use types between the northern and southern
984 regions.

985 No significant trends in the annual mean concentrations and dry and bulk
986 deposition fluxes of measured N_r species in air and precipitation were observed at
987 almost all sites during the 2011-2015 period. Also, annual averages of these values
988 showed non-significant changes between the 2011-2012 and 2013-2015 periods for all
989 land use types. Ambient total concentrations of measured N_r species showed a
990 non-significant seasonal variation at all land use types, whereas individual N_r species
991 exhibited a significant seasonal variation in most cases, except for NO_2 and pNH_4^+ at
992 urban sites, and HNO_3 at all land use types. Unlike air concentrations, dry deposition
993 of total N_r showed a consistent and significant seasonal variation for each land use
994 type, with the highest values in summer and the lowest values in winter. The V_d was a
995 dominant factor influencing seasonal variations of NO_2 , HNO_3 , and pNH_4^+
996 concentrations, while seasonal variations of NH_3 and pNO_3^- are mainly influenced by
997 their respective air concentrations. The concentrations of NH_4^+-N , NO_3^--N , and TIN
998 in precipitation showed significant seasonal variations, ranking in a consistent order
999 of winter > spring > autumn ~ summer. Also, significant seasonal variations in bulk

1000 deposition were also found, following in a consistent order of summer > spring ~
1001 autumn > winter.

1002 Both IASI satellite-retrieved NH₃ columns and OMI satellite-retrieved NO₂
1003 columns over eastern China showed higher values in the north than in the south. In
1004 addition, significant positive correlations were found between measured NH₃
1005 concentrations and retrieved NH₃ columns, and between measured NO₂
1006 concentrations and columns. These results together reveal that atmospheric N_r
1007 pollution is more serious in the northern region, and also suggest that satellite
1008 retrievals of NH₃ and NO₂ columns can provide useful information on spatial
1009 concentration variability of these two key N_r species at a regional or national scale.
1010 Weak correlations between IASI_NH₃ observations and surface NH₃ measurements
1011 were found at most selected sites, suggesting that IASI_NH₃ observations in their
1012 current state are not as readily used to accurately track temporal variability in surface
1013 NH₃ concentrations.

1014 Ammonia is currently not included in China's emission control policies of air
1015 pollution precursors, although the necessity of mitigation has been the subject of
1016 discussion during recent years. Across all urban and rural sites, the slopes of the
1017 regression relation between $p\text{NH}_4^+$ and the sum of $p\text{SO}_4^{2-}$ and $p\text{NO}_3^-$ were both
1018 smaller than unity, indicating control of NH₃ emission not only can directly reduce
1019 ambient NH₃ concentrations, but also lower the formation of $p\text{NH}_4^+$ and $p\text{NO}_3^-$.
1020 Fertilizer use contributed 36% of the total N deposition over eastern China,
1021 suggesting reducing NH₃ emissions from fertilizer application would be an effective
1022 strategy for reducing N deposition. Overall, our findings reveal persistent serious N_r
1023 pollution during the 12th FYP period despite implementation of current emission
1024 controls, and highlight the importance of NH₃ emission control on mitigating future
1025 atmospheric N_r concentrations and deposition in eastern China.

1026

1027 **Acknowledgments**

1028 This study was supported by the National Key R&D Program of China
1029 (2017YFC0210101 & 2017YFC0210106, 2014BC954202), the National Natural

1030 Science Foundation of China (41705130, 41425007, 31421092) as well as the
1031 National Ten-thousand Talents Program of China (X.J. Liu).

1032

1033

1034

1035

1036 **References**

1037 | Aguilhaume, L., Rodrigo, A., and Avila, A.: Long-term effects of changing
1038 atmospheric pollution on throughfall, bulk deposition and streamwaters in a
1039 Mediterranean forest, *Sci. Total Environ.* 544,
1040 919–928, <https://doi.org/10.1016/j.scitotenv.2015.12.017>, 2016.

1041 Allen, A. G., Harrison, R. M., and Erisman, J. W.: Field measurements of the
1042 dissociation of ammonium nitrate and ammonium chloride aerosols, *Atmos.*
1043 *Environ.*, 23, 1591–1599, 1989.

1044 Atkins, D. H. F., and Lee, D. S.: Spatial and temporal variation of rural nitrogen
1045 dioxide concentrations across the United Kingdom, *Atmos. Environ.*, 29, 223–239,
1046 1995.

1047 Bobbink, R., Hicks, K., Galloway, J., Spranger, T., Alkemade, R., Ashmore, M.,
1048 Bustamante, M., Cinderby, S., Davidson, E., and Dentener, F.: Global assessment
1049 of nitrogen deposition effects on terrestrial plant diversity: a synthesis, *Ecol. Appl.*
1050 20, 30–59, 2010.

1051 Boersma, K. F., Eskes, H. J., Veefkind, J. P., Brinksma, E. J., van der A, R. J., Sneep,
1052 M., van den Oord, G. H. J., Levelt, P. F., Stammes, P., Gleason, J. F., and Bucsela,
1053 E. J.: Near-real time retrieval of tropospheric NO₂ from OMI, *Atmos. Chem.*
1054 *Phys.*, 7, 2103–2118, <https://doi.org/10.5194/acp-7-2103-2007>, 2007.

1055 Cao, J. J., Zhang, T., Chow, J. C., Watson, J. G., Wu, F., and Li, H.: Characterization
1056 of atmospheric ammonia over Xi'an, China, *Aerosol Air Qual. Res.*, 9, 277–289,
1057 2009.

1058 Chang, Y. H., Liu, X. J., Deng, C. R., Dore, A. J., and Zhuang, G. S.: Source
1059 apportionment of atmospheric ammonia before, during, and after the 2014 APEC

1060 summit in Beijing using stable nitrogen isotope signatures, *Atmos. Chem. Phys.*, 16,
1061 11635–11647, <https://doi.org/10.5194/acp-16-11635-2016>, 2016.

1062 Dammers, E., Palm, M., Van Damme, M., Vigouroux, C., Smale, D., Conway, S.,
1063 Toon, G. C., Jones, N., Nussbaumer, E., Warneke, T., Petri, C., Clarisse, L.,
1064 Clerbaux, C., Hermans, C., Lutsch, E., Strong, K., Hannigan, J. W., Nakajima, H.,
1065 Morino, I., Herrera, B., Stremme, W., Grutter, M., Schaap, M., Wichink Kruit, R. J.,
1066 Notholt, J., Coheur, P. F., and Erismann, J. W.: An evaluation of IASI-NH₃ with
1067 ground-based Fourier transform infrared spectroscopy measurements, *Atmos.*
1068 *Chem. Phys.*, 16, 10351–10368, <https://doi.org/10.5194/acp-16-10351-2016>, 2016.

1069 Erismann, J.W., Grennfelt, P., and Sutton, M.: The European perspective on nitrogen
1070 emission and deposition. *Environ. Int.*, 29,
1071 311–325, [https://doi.org/10.1016/S0160-4120\(02\)00162-9](https://doi.org/10.1016/S0160-4120(02)00162-9), 2003.

1072 Fagerli, H., and Aas, W.: Trends of nitrogen in air and precipitation: model results
1073 and observations at EMEP sites in Europe, 1980-2003, *Environ. Pollut.* 154,
1074 448–461, <https://doi.org/10.1016/j.envpol.2008.01.024>, 2008.

1075 Fenn, M. E., Baron, J. S., Allen, E. B., Rueth, H. M., Nydick, K. R., Geiser, L.,
1076 Bowman, W. D., Sickman, J. O., Meixner, T., Johnson, D. W., and Neitlich, P.:
1077 Ecological Effects of Nitrogen Deposition in the Western United States,
1078 *BioScience*, 53,
1079 404–420, [https://doi.org/10.1641/0006-3568\(2003\)053\[0404:EEONDI\]2.0.CO;2](https://doi.org/10.1641/0006-3568(2003)053[0404:EEONDI]2.0.CO;2),
1080 2003.

1081 | Fowler, D., Smith, R., Muller, J., Cape, J. N., Sutton, M., Erismann, J. W., **and** Fagerli,
1082 H.: 2007. Long term trends in sulphur and nitrogen deposition in Europe and the
1083 cause of non-linearities, *Water Air Soil Pollut.*, 7,
1084 41–47, <https://doi.org/10.1007/s11267-006-9102-x>, 2007.

1085 Fowler, D., Coyle, M., Skiba, U., Sutton, M. A., Cape, J. N., Reis, S., Sheppard, L. J.,
1086 Jenkins, A., Grizzetti, B., Galloway, J. N., Vitousek, P., Leach, A., Bouwman, A. F.,
1087 Butterbach-Bahl, K., Dentener, F., Stevenson, D., Amann, M., and Voss, M.: The
1088 global nitrogen cycle in the twenty-first century, *Philos. T. R. Soc. B*, 368,
1089 20130164, <https://doi.org/10.1098/rstb.2013.0164>, 2013.

1090 Fuzzi, S., Baltensperger, U., Carslaw, K., Decesari, S., van Der Gon, H. D., Facchini,
1091 M. C., Fowler, D., Koren, I., Langford, B., Lohmann, U., Nemitz, E., Pandis, S.,
1092 Riipinen, I., Rudich, Y., Schaap, M., Slowik, J. G., Spracklen, D. V., Vignati, E.,
1093 Wild, M., Williams, M., and Gilardoni, S.: Particulate matter, air quality and
1094 climate: lessons learned and future needs, *Atmos. Chem. Phys.*, 15,
1095 8217–8299, <https://doi.org/10.5194/acp-15-8217-2015>, 2015.

1096 Galloway, J. N., Townsend, A. R., Erisman, J. W., Bekunda, M., Cai, Z., Freney, J. R.,
1097 Martinelli, L. A., Seitzinger, S. P., and Sutton, M. A.: Transformation of the
1098 Nitrogen Cycle: Recent trends, questions, and potential solutions, *Science*, 320,
1099 889–892, <https://doi.org/10.1126/science.1136674>, 2008.

1100 Ge, B. Z., Wang, Z. F., Xu, X. B., Wu, J. B., Yu, X. L., and Li, J.: Wet deposition of
1101 acidifying substances in different regions of China and the rest of East Asia:
1102 modeling with updated NAQPMS, *Environ. Pollut.*, 187,
1103 10–21, <https://doi.org/10.1016/j.envpol.2013.12.014>, 2014.

1104 Gilbert, R. O.: *Statistical methods for environmental pollution monitoring*, John
1105 Wiley & Sons, 1987.

1106 Gruber, N. and Galloway, J. N.: An Earth-system perspective of the global nitrogen
1107 cycle, *Nature*, 451, 293–296, <https://doi.org/10.1038/nature06592>, 2008.

1108 Gu, B. J., Sutton, M. A., Chang, S. X., Ge, Y., and Jie, C.: Agricultural ammonia
1109 emissions contribute to China’s urban air pollution, *Front. Ecol. Environ.*, 12,
1110 265–266, <https://doi.org/10.1890/14.WB.007>, 2014.

1111 Guo, S., Hu, M., Zamora, M. L., Peng, J. F., Shang, D. J., Zheng, J., Du, Z. F., Wu, Z.
1112 J., Shao, M., and Zeng, L. M.: Elucidating severe urban haze formation in China,
1113 *Proc. Natl. Acad. Sci. U.S.A.*, 111,
1114 17373, <https://doi.org/10.1073/pnas.1419604111>, 2014.

1115 Han, X., Zhang, M. G., Skorokhod, A., and Kou, X. X.: Modeling dry deposition of
1116 reactive nitrogen in China with RAMS-CMAQ, *Atmos. Environ.*, 166,
1117 47–61, <https://doi.org/10.1016/j.atmosenv.2017.07.015>, 2017.

1118 He, N. P., Zhu, J. X., and Wang, Q. F.: Uncertainty and perspectives in studies of
1119 atmospheric nitrogen deposition in China: A response to Liu et al. (2015), *Sci.*

1120 Total Environ., 520, 302–304, <https://doi.org/10.1016/j.scitotenv.2015.03.063>,
1121 2015.

1122 Huang, P., Zhang, J. B., Xin, X. L., Zhu, A. N., Zhang, C. Z., Ma, D. H., Zhu, Q. G.,
1123 Yang, S., and Wu, S. J.: Proton accumulation accelerated by heavy chemical
1124 nitrogen fertilization and its long-term impact on acidifying rate in a typical arable
1125 soil in the Huang-Huai-Hai Plain, *J. Integr. Agric.* 14, 148–157, 2015.

1126 Huang, R. J., Zhang, Y., Bozzetti, C., Ho, K. F., Cao, J. J., Han, Y., Daellenbach, K.
1127 R., Slowik, J. G., Platt, S. M., Canonaco, F., Zotter, P., Wolf, R., Pieber, S. M.,
1128 Bruns, E. A., Crippa, M., Ciarelli, G., Piazzalunga, A., Schwikowski, M.,
1129 Abbaszade, G., Schnelle-Kreis, J., Zimmermann, R., An, Z., Szidat, S.,
1130 Baltensperger, U., El Haddad, I., and Prevot, A. S.: High secondary aerosol
1131 contribution to particulate pollution during haze events in China, *Nature*, 514,
1132 218–222, <https://doi.org/10.1038/nature13774>, 2014.

1133 Huang, X., Song, Y., Li, M. M., Li, J. F., Huo, Q., Cai, X. H., Zhu, T., Hu, M., and
1134 Zhang, H. S.: A high-resolution ammonia emission inventory in China, *Global*
1135 *Biogeochem. Cycles* 26, GB1030, <https://doi.org/10.1029/2011GB004161>, 2012.

1136 Ianniello, A., Spataro, F., Esposito, G., Allegrini, I., Rantica, E., Ancora, M. P., Hu,
1137 M., and Zhu, T.: Occurrence of gas phase ammonia in the area of Beijing (China),
1138 *Atmos. Chem. Phys.*, 10, 9487–9503, <https://doi.org/10.5194/acp-10-9487-2010>,
1139 2010.

1140 Jia, B., Wang, Y., Yao, Y., and Xie, Y.: A new indicator on the impact of large-scale
1141 circulation on wintertime particulate matter pollution over China, *Atmos. Chem.*
1142 *Phys.*, 15, 11919–11929, <https://doi.org/10.5194/acp-15-11919-2015>, 2015.

1143 Jia, Y. L., Yu, G. R., He, N. P., Zhan, X. Y., Fang, H. J., Sheng, W. P., Zuo, Y.,
1144 Zhang, D. Y., and Wang, Q. F.: Spatial and decadal variations in inorganic nitrogen
1145 wet deposition in China induced by human activity, *Sci. Rep.*, 4,
1146 3763, <https://doi.org/10.1038/srep03763>, 2014.

1147 Jia, Y. L.; Yu, G. R.; Gao, Y. N.; He, N. P.; Wang, Q. F.; Jiao, C. C.; and Zuo, Y.:
1148 Global inorganic nitrogen dry deposition inferred from ground and space-based
1149 measurements, *Sci. Rep.*, 6, 19810, <https://doi.org/10.1038/srep19810>, 2016.

1150 [Ju, X. T., Xing, G. X., Chen, X. P., Zhang, S. L., Zhang, L. J., Liu, X. J., Cui, Z. L.,](#)
1151 [Yin, B., Christie, P., Zhu, Z. L., and Zhang, F. S.: Reducing environmental risk by](#)
1152 [improving N management in intensive Chinese agricultural systems, Proc. Natl.](#)
1153 [Acad. Sci. U. S. A. 106, 3041-3046, <https://doi/10.1073/pnas.0902655106>, 2009.](#)

1154 Kanakidou, M., Myriokefalitakis, S., Daskalakis, N., and Fanourgakis, G.: Past,
1155 present, and future atmospheric nitrogen deposition, *J. Atmos. Sci.*, 73,
1156 160303130433005, <https://doi.org/10.1175/JAS-D-15-0278.s1>, 2016.

1157 Karlsson, G. P., Akselsson, C., Hellsten, S., [and](#) Karlsson, P. E.: Reduced European
1158 emissions of S and N effects on air concentrations, deposition and soil water
1159 chemistry in Swedish forests, *Environ. Pollut.* 159,
1160 3571–3582. <https://doi.org/10.1016/j.envpol.2011.08.007>, 2011.

1161 Khoder, M. I.: Atmospheric conversion of sulfur dioxide to particulate sulfate and
1162 nitrogen dioxide to particulate nitrate and gaseous nitric acid in an urban area,
1163 *Chemosphere*, 49, 675–684, 2002.

1164 Krotkov, N. A., Mclinden, C. A., Li, C., Lamsal, L. N., Celarier, E. A., Marchenko, S.
1165 V., Swartz, W. H., Bucsela, E. J., Joiner, J., Duncan, B. N., Boersma, K. F.,
1166 Veeffkind, J. P., Levelt, P. F., Fioletov, V. E., Dickerson, R. R., He, H., Lu, Z. F.,
1167 and Streets, D. G.: Aura OMI observations of regional SO₂ and NO₂ pollution
1168 changes from 2005 to 2015, *Atmos. Chem. Phys.*, 16,
1169 4605–4629, <https://doi.org/10.5194/acp-16-4605-2016>, 2016.

1170 Kurokawa, J., Ohara, T., Morikawa, T., Hanayama, S., JanssensMaenhout, G., Fukui,
1171 T., Kawashima, K., and Akimoto, H.: Emissions of air pollutants and greenhouse
1172 gases over Asian regions during 2000–2008: Regional Emission inventory in Asia
1173 (REAS) version 2, *Atmos. Chem. Phys.*, 13,
1174 11019–11058, <https://doi.org/10.5194/acp-13-11019-2013>, 2013.

1175 Li, H., Zhang, Q., Zheng, B., Chen, C., Wu, N., Guo, H., Zhang, Y., Zheng, Y., Li, X.,
1176 and He, K.: Nitrate-driven urban haze pollution during summertime over the North
1177 China Plain, *Atmos. Chem. Phys.*, 18,
1178 5293-5306, <https://doi.org/10.5194/acp-18-5293-2018>, 2018.

1179 Li, Y., Niu, S., and Yu, G.: Aggravated phosphorus limitation on biomass production

1180 under increasing nitrogen loading: a meta-analysis, *Global Change Biol.*, 22,
1181 934–943, <https://doi.org/10.1111/gcb.13125>, 2016.

1182 | Liang, X., Zou, T., Guo, B., Li, S., Zhang, H. Z., Zhang, S. Y., Huang, H., **and** Chen,
1183 S. X.: Assessing Beijing's PM_{2.5} pollution: severity, weather impact, APEC and
1184 winter heating, *Proc. R. Soc. A.*, 471,
1185 20150257, <https://doi.org/10.1098/rspa.2015.0257>, 2015.

1186 Liu, F., Beirle, S., Zhang, Q., van der A, R. J., Zheng, B., Tong, D., and He, K.: NO_x
1187 emission trends over Chinese cities estimated from OMI observations during 2005
1188 to 2015, *Atmos. Chem. Phys.*, 17,
1189 9261–9275, <https://doi.org/10.5194/acp-17-9261-2017>, 2017.

1190 Liu, L., Zhang, X. Y., Zhang, Y., Xu, W., Liu, X. J., Zhang, X. M., Feng, J. L., Chen,
1191 X. R., Zhang, Y. H., Lu, X. H., Wang, S. Q., Zhang, W. T., and Zhao, L. M.: Dry
1192 particulate nitrate deposition in China, *Environ. Sci. Technol.*, 51,
1193 5572, <https://doi.org/10.1021/acs.est.7b00898>, 2017a.

1194 | Liu, L., Zhang, X., Xu, W., Liu, X., Li, Y., Lu, X., Zhang, Y., **and** Zhang, W.:
1195 Temporal characteristics of atmospheric ammonia and nitrogen dioxide over China
1196 based on emission data, satellite observations and atmospheric transport modeling
1197 since 1980, *Atmos. Chem. Phys.*, 17,
1198 9365–9378, <https://doi.org/10.5194/acp-17-9365-2017>, 2017b.

1199 | Liu, X. J., Duan, L., Mo, J. M., Du, E. Z., Shen, J. L., Lu, X. K., Zhang, Y., Zhou, X.
1200 B., He, C. E., **and** Zhang, F. S.: Nitrogen deposition and its ecological impact in
1201 China: An overview, *Environ. Pollut.*, 159,
1202 2251–2264, <https://doi.org/10.1016/j.envpol.2010.08.002>, 2011.

1203 Liu, X. J., Zhang, Y., Han, W. X., Tang, A., Shen, J. L., Cui, Z. L., Vitousek, P.,
1204 Erisman, J. W., Goulding, K., Christie, P., Fangmeier, A., and Zhang, F. S.:
1205 Enhanced nitrogen deposition over China, *Nature*, 494,
1206 459–462, <https://doi.org/10.1038/nature11917>, 2013.

1207 Liu, X. J., Vitousek, P., Chang, Y. H., Zhang, W. F., Matson, P., and Zhang, F. S.:
1208 Evidence for a historic change occurring in China, *Environ. Sci. Technol.*, 50,
1209 505–506, <https://doi.org/10.1021/acs.est.5b05972>, 2016.

1210 Lu, C. Q. and Tian, H. Q.: Spatial and temporal patterns of nitrogen deposition in
1211 China: Synthesis of observational data, *J. Geophys. Res.*, 112,
1212 D22S05, <https://doi.org/10.1029/2006JD007990>, 2007.

1213 Lu, C. Q. and Tian, H. Q.: Half-century nitrogen deposition increase across China: A
1214 gridded time-series data set for regional environmental assessments, *Atmos.*
1215 *Environ.*, 97, 68–74, <https://doi.org/10.1016/j.atmosenv.2014.07.061>, 2014.

1216 Marchetto, A., Rogora, M., and Arisci, S.: Trend analysis of atmospheric deposition
1217 data: A comparison of statistical approaches, *Atmos. Environ.*, 64, 95–102, 2013.

1218 Meng, Z. Y., Xu, X. B., Wang, T., Zhang, X. Y., Yu, X. L., Wang, S. F., Lin, W. L.,
1219 Chen, Y. Z., Jiang, Y. A., and An, X. Q.: Ambient sulfur dioxide, nitrogen dioxide,
1220 and ammonia at ten background and rural sites in China during 2007-2008, *Atmos.*
1221 *Environ.*, 44, 2625–2631.

1222 Meng, Z. Y., Xu, X. B., Lin, W. L., Ge, B. Z., Xie, Y. L., Song, B., Jia, S. H., Zhang,
1223 R., Peng, W., Wang, Y., Cheng, H. B., Yang, W., and Zhao, H.: Role of ambient
1224 ammonia in particulate ammonium formation at a rural site in the North China
1225 Plain, *Atmos. Chem. Phys.*, 18, 167–184, <https://doi.org/10.5194/acp-18-167-2018>,
1226 2018.

1227 MEPC (Ministry of Environmental Protection of the People’s Republic of China):
1228 Report on Environmental Quality in China, 2010. Available online
1229 at: http://jcs.mep.gov.cn/hjzl/zkgb/2010zkgb/201106/t20110602_211579.htm,
1230 2011.

1231 Miyazaki, K., Eskes, H., Sudo, K., Boersma, K. F., Bowman, K., and Kanaya, Y.:
1232 Decadal changes in global surface NO_x emissions from multi-constituent satellite
1233 data assimilation, *Atmos. Chem. Phys.*, 17,
1234 807–837, <https://doi.org/10.5194/acp-17-807-2017>, 2017.

1235 Pan, Y. P., Wang, Y. S., Tang, G. Q., and Wu, D.: Wet and dry deposition of
1236 atmospheric nitrogen at ten sites in Northern China, *Atmos. Chem. Phys.*, 12,
1237 6515–6535, <https://doi.org/10.5194/acp-12-6515-2012>, 2012.

1238 Pan, Y. P., Wang, Y. S., Zhang, J. K., Liu, Z. R., Wang, L. L., Tian, S. L., Tang, G.
1239 Q., Gao, W. K., Ji, D. S., and Song, T.: Redefining the importance of nitrate during

1240 haze pollution to help optimize an emission control strategy, *Atmos. Environ.*, 141,
1241 197–202, <http://dx.doi.org/10.1016/j.atmosenv.2016.06.035>, 2016.

1242 Pinder, R. W., Walker, J. T., Bash, J. O., Cady-Pereira, K. E., Henze, D. K., Luo, M.
1243 Z., Osterman, G. B., and Shephard, M. W.: Quantifying spatial and seasonal
1244 variability in atmospheric ammonia with in situ and space-based observations,
1245 *Geophys. Res. Lett.*, 38, L04802, <https://doi.org/10.1029/2010GL046146>, 2011.

1246 Russell, A. R., Valin, L. C., and Cohen, R. C.: Trends in OMI NO₂ observations over
1247 the United States: effects of emission control technology and the economic
1248 recession, *Atmos. Chem. Phys.*, 12,
1249 12197–12209, <https://doi.org/10.5194/acp-12-12197-2012>, 2012.

1250 Salmi, T., Maatta, A., Anttila, P., Ruoho-Airola, T., and Amnell, T.: Detecting trends
1251 of annual values of atmospheric pollutants by the Mann–Kendall test and Sen's
1252 slope estimates—the Excel template application MAKESENS. Publications on Air
1253 Quality No. 31, Finnish Meteorological Institute, Helsinki, Finland, 2002.

1254 Seinfeld, J. H. and Pandis, S. N.: Atmospheric chemistry and physics: from air
1255 pollution to climate change, 2nd Edn., Wiley Interscience, New Jersey, 2006.

1256 She, W.: Hu Huanyong: father of China's population geography, *China Popul. Today*
1257 15, 1–20, 1998.

1258 Sourì, A. H., Choi, Y., Jeon, W., Woo, J.-H., Zhang, Q., and Kurokawa, J.-i.: Remote
1259 sensing evidence of decadal changes in major tropospheric ozone precursors over
1260 East Asia, *J. Geophys. Res.*, 122,
1261 2474–2492, <https://doi.org/10.1002/2016JD025663>, 2017.

1262 Tang, Y. S., Simmons, I., van Dijk, N., Di Marco, C., Nemitz, E., Dammgén, U.,
1263 Gilke, K., Djuricic, V., Vidic, S., and Gliha, Z.: European scale application of
1264 atmospheric reactive nitrogen measurements in a low-cost approach to infer dry
1265 deposition fluxes, *Agr. Ecosyst. Environ.*, 133, 183–195, <https://doi.org/10.1016/j.agee.2009.04.027>, 2009.

1267 Theil, H.: A Rank-Invariant Method of Linear and Polynomial Regression Analysis,
1268 in: Henri Theil's Contributions to Economics and Econometrics, edited by: Raj, B.
1269 and Koerts, J., *Advanced Studies in Theoretical and Applied Econometrics*,

1270 Springer Netherlands, 345–381, 1992.

1271 Tian, S. L., Pan, Y. P., Liu, Z. R., Wen, T. X., and Wang, Y. S.: Size-resolved aerosol
1272 chemical analysis of extreme haze pollution events during early 2013 in urban
1273 Beijing, China, *J. Hazard. Mater.*, 279, 452–460, <https://doi.org/10.1016/j.jhazmat.2014.07.023>, 2014.

1275 Van Damme, M., Clarisse, L., Dammers, E., Liu, X., Nowak, J. B., Clerbaux, C.,
1276 Flechard, C. R., Galy-lacaux, C., Xu, W., and Neuman, J. A.: Towards validation of
1277 ammonia (NH₃) measurements from the IASI satellite, *Atmos. Meas. Tech.*, 8,
1278 1575–1591, <https://doi.org/10.5194/amt-8-1575-2015>, 2015.

1279 van der A, R. J., Mijling, B., Ding, J., Koukouli, M. E., Liu, F., Li, Q., Mao, H., and
1280 Theys, N.: Cleaning up the air: effectiveness of air quality policy for SO₂ and NO_x
1281 emissions in China, *Atmos. Chem. Phys.*, 17,
1282 1775–1789, <https://doi.org/10.5194/acp-17-1775-2017>, 2017.

1283 Vet, R., Artz, R. S., Carou, S., Shaw, M., Ro, C.-U., Aas, W., Baker, A., Bowersox, V.
1284 C., Dentener, F., Galy-Lacaux, C., Hou, A., Pienaar, J. J., Gillett, R., Forti, M. C.,
1285 Gromov, S., Hara, H., Khodzher, T., Mahowald, N. M., Nickovic, S., Rao, P. S. P.,
1286 and Reid, N. W.: A global assessment of precipitation chemistry and deposition of
1287 sulfur, nitrogen, sea salt, base cations, organic acids, acidity and pH, and
1288 phosphorus, *Atmos. Environ.*, 93, 3–100, <https://doi.org/10.1016/j.atmosenv.2013.10.060>, 2014.

1290 Walker, J. T., Whittall, D. R., Robarge, W., and Paerl, H. W.: Ambient ammonia and
1291 ammonium aerosol across a region of variable ammonia emission density, *Atmos.*
1292 *Environ.*, 38, 1235–1246, 2004.

1293 Wang, G. H., Zhang, R. Y., Gomez, M. E., Yang, L. X., Zamora, M. L., Hu, M., Lin,
1294 Y., Peng J. F., Guo, S., Meng, J. J., Li, J. J., Cheng, C. L., Hu, T. F., Ren, Y. Q.,
1295 Wang, Y. S., Gao, J., Cao, J. J., An, Z. S., Zhou, W. J., Li, G. H., Wang, J. Y., Tian,
1296 P. F., Marrero-Ortiz, W., Secretst J., Du, Z. F., Zheng, J., Shang, D. J., Zeng, L. M.,
1297 Shao, M., Wang, W. G., Huang, Y., Wang, Y., Zhu, Y. J., Li, Y. X., Hu, J. X., Pan,
1298 B. W., Cai, L., Cheng, Y. T., Ji, Y. M., Zhang, F., Rosenfeld, D., Liss, P. S., Duce,
1299 R. A., Kolb, C. E., and Molina, M. J.: Persistent sulfate formation from London

1300 Fog to Chinese haze, *Proc. Natl. Acad. Sci. U.S.A.*, 113, 13630, <https://doi.org/10.1073/pnas.1616540113>, 2016.

1301

1302 Wang, S. X., Xing, J., Jang, C. R., Zhu, Y., Fu, J. S., and Hao, J. M.: Impact
1303 assessment of ammonia emissions on inorganic aerosols in East China using
1304 response surface modeling technique, *Environ. Sci. Technol.*, 45,
1305 9293–9300, <https://doi.org/10.1021/es2022347>, 2011.

1306 Wen, L., Chen, J. M., Yang, L. X., Wang, X. F., Xu, C. H., Sui, X., Yao, L., Zhu, Y.
1307 H., Zhang, J. M., Zhu, T., and Wang, W. X.: Enhanced formation of fine particulate
1308 nitrate at a rural site on the North China Plain in summer: The important roles of
1309 ammonia and ozone, *Atmos. Environ.*, 101,
1310 294–302, <http://dx.doi.org/10.1016/j.atmosenv.2014.11.037>, 2015.

1311 Wesely, M. L.: Parameterization of surface resistances to gaseous dry deposition in
1312 regional-scale numerical-models, *Atmos. Environ.*, 23, 1293–1304, 1989.

1313 Whitburn, S., Van Damme, M., Clarisse, L., Bauduin, S., Heald, C. L., Hadji-Lazaro,
1314 J., Hurtmans, D., Zondlo, M. A., Clerbaux, C., and Coheur, P. F.: A flexible and
1315 robust neural network IASINH3 retrieval algorithm, *J. Geophys. Res.-Atmos.*, 121,
1316 6581–6599, <https://doi.org/10.1002/2016JD024828>, 2016.

1317 Xia, Y. M., Zhao, Y., and Nielsen, C. P.: Benefits of China's efforts in gaseous
1318 pollutant control indicated by the bottom-up emissions and satellite observations
1319 2000–2014, *Atmos. Environ.*, 136, 43–53, <https://doi.org/10.1016/j.atmosenv.2016.04.013>, 2016.

1320

1321 Xu, W., Luo, X.S., Pan, Y.P., Zhang, L., Tang, A.H., Shen, J.L., Zhang, Y., Li, K.H.,
1322 Wu, Q.H., Yang, D.W., Zhang, Y.Y., Xue, J., Li, W.Q., Li, Q.Q., Tang, L., Lu,
1323 S.H., Liang, T., Tong, Y.A., Liu, P., Zhang, Q., Xiong, Z.Q., Shi, X.J., Wu, L.H.,
1324 Shi, W.Q., Tian, K., Zhong, X.H., Shi, K., Tang, Q.Y., Zhang, L.J., Huang, J.L., He,
1325 C.E., Kuang, F.H., Zhu, B., Liu, H., Jin, X., Xin, Y.J., Shi, X.K., Du, E.Z., Dore,
1326 A.J., Tang, S., Collett, J.L., Goulding, K., Sun, Y.X., Ren, J., Zhang, F.S., and Liu,
1327 X.J.: Quantifying atmospheric nitrogen deposition through a nationwide monitoring
1328 network across China. *Atmos. Chem. Phys.*, 15, 12345–12360, <https://doi.org/10.5194/acp-15-12345-2015>, 2015.

1329

1330 Xu, W., Wu, Q. H., Liu, X. J., Tang, A. H., Dore, A. J., and Heal, M. R.:
1331 Characteristics of ammonia, acid gases, and PM_{2.5} for three typical land-use types
1332 in the North China Plain, *Environ. Sci. Pollut. Res.*, 23, 1158–1172, <https://doi.org/10.1007/s11356-015-5648-3>, 2016.

1334 Xu, W., Song, W., Zhang, Y., Liu, X., Zhang, L., Zhao, Y., Liu, D., Tang, A., Yang,
1335 D., Wang, D., Wen, Z., Pan, Y., Fowler, D., Collett Jr., J. L., Erisman, J. W.,
1336 Goulding, K., Li, Y., and Zhang, F.: Air quality improvement in a megacity:
1337 implications from 2015 Beijing Parade Blue pollution control actions, *Atmos.*
1338 *Chem. Phys.*, 17, 31–46, <https://doi.org/10.5194/acp-17-31-2017>, 2017.

1339 Xu, W., Zhao, Y. H., Liu, X. J., Dore, A. J., Zhang, L., Liu, L., and Cheng, M.:
1340 Atmospheric nitrogen deposition in the Yangtze River basin: Spatial pattern and
1341 source attribution, *Environ. Pollut.*, 232,
1342 546–555, <https://doi.org/10.1016/j.envpol.2017.09.086>, 2018.

1343 Yang, F., Tan, J., Zhao, Q., Du, Z., He, K., Ma, Y., Duan, F., Chen, G., and Zhao, Q.:
1344 Characteristics of PM_{2.5} speciation in representative megacities and across China,
1345 *Atmos. Chem. Phys.*, 11, 5207–5219, <https://doi.org/10.5194/acp-11-5207-2011>,
1346 2011.

1347 Yang, Y. H., Li, P., He, H. L., Zhao, X., Datta, A., Ma, W. H., Zhang, Y., Liu, X. J.,
1348 Han, W. X., Wilson, M. C., and Fang, J. Y.: Long-term changes in soil pH across
1349 major forest ecosystems in China, *Geophys. Res. Lett.*,
1350 42, <https://doi.org/10.1002/2014GL062575>, 2015.

1351 Zhao, Y., Nielsen, C. P., Lei, Y., McElroy, M. B., and Hao, J.: Quantifying the
1352 uncertainties of a bottom-up emission inventory of anthropogenic atmospheric
1353 pollutants in China, *Atmos. Chem. Phys.*, 11,
1354 2295–2308, <https://doi.org/10.5194/acp-11-2295-2011>, 2011.

1355 Zhang, L., Chen, Y. F., Zhao, Y. H., Henze, D. K., Zhu, L. Y., Song, Y., Paulot, F.,
1356 Liu, X. J., Pan, Y. P., and Huang, B. X.: Agricultural ammonia emissions in China:
1357 reconciling bottom-up and top-down estimates, *Atmos. Chem. Phys.*, 18,
1358 339–355, <https://doi.org/10.5194/acp-18-339-2018>, 2018.

1359 Zhang, L. M., Gong, S. L., Padro, J., and Barrie, L.: A size-segregated particle dry

1360 deposition scheme for an atmospheric aerosol module, *Atmos. Environ.*, 35,
1361 549–560, [https://doi.org/10.1016/s1352-2310\(00\)00326-5](https://doi.org/10.1016/s1352-2310(00)00326-5), 2001.

1362 | Zhang, Q., Duan, F. K., He, K. B., Ma, Y. L., Li, H. Y., Kimoto, T., [and](#) Zheng, A. H.:
1363 Organic nitrogen in PM_{2.5} in Beijing, *Front. Env. Sci. Eng.*, 9,
1364 1004–1014, <https://doi.org/10.1007/s11783-015-0799-5>, 2015.

1365 Zhang, X. M., Wu, Y. Y., Liu, X. J., Reis, S., Jin, J. X., Dragosits, U., Damme, Van
1366 M., Clarisse, L., Whitburn, S., and Coheur, P. F.: Ammonia emissions may be
1367 substantially underestimated in China, *Environ. Sci. Technol.*, 51,
1368 12089–12096, <https://doi.org/10.1021/acs.est.7b02171>, 2017.

1369 Zhao, Y., Zhang, L., Pan, Y., Wang, Y., Paulot, F., and Henze, D. K.: Atmospheric
1370 nitrogen deposition to the northwestern Pacific: seasonal variation and source
1371 attribution, *Atmos. Chem. Phys.*, 15,
1372 10905–10924, <https://doi.org/10.5194/acp-15-10905-2015>, 2015.

1373 Zhao, Y., Zhang, L., Chen, Y. F., Liu, X. J., Xu, W., Pan, Y. P., and Duan, L.:
1374 Atmospheric nitrogen deposition to China: a model analysis on nitrogen budget and
1375 critical load exceedance, *Atmos. Environ.*, 153,
1376 32–40, <https://doi.org/10.1016/j.atmosenv.2017.01.018>, 2017.

1377 Zhu, J. X., He, N. P., Wang, Q. F., Yan, G. F., Wen, D., Yu, G. R., and Jia, Y. L.: The
1378 composition, spatial patterns, and influencing factors of atmospheric wet nitrogen
1379 deposition in Chinese terrestrial ecosystems, *Sci. Total Environ.*, 511,
1380 777–785, <https://doi.org/10.1016/j.scitotenv.2014.12.038>, 2015.

Sect. S1. Information on measuring methods, sample replications and collection

The DELTA system comprises contains a sampling train consisted of two potassium carbonate/glycerol-coated denuders in series for trapping acidic trace gases (HNO_3 , SO_2 and HCl), followed by two citric acid-coated borosilicate glass denudes for NH_3 and finally by two sets of cellulose filter papers in a 2-stage filter pack at the end of the sampling train. These filters were impregnated with the same alkaline solution as the denuders to capture NH_4^+ , and with the same acid solution for the collection of NO_3^- , SO_4^{2-} and Cl^- . The empirically determined effective size cut-off for particle sampling is of the order of $4.5 \mu\text{m}$ (E. Nemitz, personal communication). The air was drawn through the sampling train at a rate of $0.2\text{-}0.4 \text{ L min}^{-1}$ and directly into the first denuder with no inlet line to avoid sampling losses. The total sampled air volume of the DELTA system was recorded by the gas meter which was checked every month for data reading, performance and maintenance.

The Gradko passive sampler consists of a $71.0 \text{ mm long} \times 11.0 \text{ mm internal diameter}$ acrylic tube with coloured and white thermoplastic rubber caps. Gaseous NO_2 is absorbed into a 20% triethanolamine/deionised-water solution coated onto two stainless steel wire meshes within the coloured cap. A constant gas diffusion coefficient based on an assumption of $25 \text{ }^\circ\text{C}$ was used for the calculation of NO_2 concentration, in accordance with the Gradko introduction manual and previous studies (Luo et al., 2013; Shen et al., 2013).

The sampling trains and tubes for field measurements were prepared and measured in the analytical laboratory at China Agricultural University (CAU), Beijing. Each batch of new trains and field (travel) blanks was sealed in individual airtight storage bags and sent monthly to monitoring sites to replace the old ones. After sampling, the blank and exposed trains and tubes were sealed in individual airtight storage bags and sent back to the laboratory, being stored at $4 \text{ }^\circ\text{C}$ prior to analysis.

Sect. S2. The information on the evaluation of GEOS-Chem model

To evaluate the model simulations, we compared modeled annual wet deposition fluxes of $\text{NH}_4^+\text{-N}$ and $\text{NO}_3^-\text{-N}$ for the year 2010 with their respective observed fluxes (5-year averages). The comparison results are shown in Fig. S12 in the Supplement. The model can partly capture the spatial variations of measured bulk deposition fluxes of NH_4^+ and NO_3^- with correlation coefficients of 0.6 and 0.4, respectively. Compared with measurements, model results were 23% higher for bulk NH_4^+ deposition, and 23%

lower for bulk NO_3^- -N deposition. The model biases were reasonable since simulated N deposition fluxes were for 2010 whereas the observations cover a period from 2000 to 2015. Both NH_3 and NO_x emissions change over the time periods, resulting in difference in subsequent N deposition. Besides emissions, inter-annual variations of meteorological conditions especially precipitation can also affect wet deposition fluxes. So model simulated wet deposition fluxes show larger biases. In addition, the model biases also reflect the incapability of the coarse model resolution (about 50 km) to distinguish different land use types (e.g., the forest, rural and urban sites) at such regional scale. Future work is needed to conduct high resolution simulation using regional models combined with improved N_r emission inventories.

References

- Luo, X. S., Liu, P., Tang, A. H., Liu, J. Y., Zong, X. Y., Zhang, Q., Kou, C. L., Zhang, L. J., Fowler, D., Fangmeier, A., Christie, P., Zhang, F. S., and Liu, X. J.: An evaluation of atmospheric N_r pollution and deposition in North China after the Beijing Olympics, *Atmos. Environ.*, 74, 209–216, <https://doi.org/10.1016/j.atmosenv.2013.03.054>, 2013.
- Shen, J. L., Li, Y., Liu, X.J., Luo, X. S., Tang, A. H., Zhang, Y. Z., and Wu, J. S.: Atmospheric dry and wet nitrogen deposition on three contrasting land use types of an agricultural catchment in subtropical central China, *Atmos. Environ.*, 67, 415–424, <https://doi.org/10.1016/j.atmosenv.2012.10.068>, 2013.

Figure captions

Figure S1. Annual mean concentrations of (a) NH_3 ; (b) NO_2 ; (c) HNO_3 ; (d) $p\text{NH}_4^+$; (e) $p\text{NO}_3^-$; and (f) total N_r : sum of all measured N_r in air at twenty-seven sites. Trend analysis (annual concentration vs. time) was conducted at each site. The slope of the Theil regression and p value for each site are labeled in black and yellow. U, R, and B denote urban, rural, and background sites, respectively.

Figure S2. Annual volume-weighted mean concentrations of NH_4^+ (a); NO_3^- (b) and total inorganic N (TIN): sum of NH_4^+ and NO_3^- (c) in precipitation at twenty-seven sites. Trend analysis (annual concentration vs. time) was conducted at each site. The slope of the Theil regression and p value for each site are labeled in black and red. U, R, and B denote urban, rural, and background sites, respectively.

Figure S3. Annual dry deposition fluxes of (a) NH_3 ; (b) NO_2 ; (c) HNO_3 ; (d) $p\text{NH}_4^+$; (e) $p\text{NO}_3^-$; and (f) total N_r : sum of all measured N_r in air at twenty-seven sites. Trend analysis (annual concentration vs. time) was conducted at each site. The slope of the Theil regression and p value for each site are labeled in black and green. U, R, and B denote urban, rural, and background sites, respectively.

Figure S4. Annual wet/bulk deposition of NH_4^+ (a); NO_3^- (b) and total inorganic N (TIN): sum of NH_4^+ and NO_3^- (c) in precipitation at twenty-seven sites. Trend analysis (annual concentration vs. time) was conducted at each site. The slope of the Theil regression and p value for each site are labeled in black and red. U, R, and B denote urban, rural, and background sites, respectively.

Figure S5. Total (dry plus wet/bulk) deposition fluxes at the three land use types in eastern China and its northern and southern regions. The number of sixteen selected sites with the same land use type in each region can be found in Figure S6 and Table S1. The error bars are the standard errors of means, and values without same letters different letters on the bars denote significantly difference between the sites land use types at $p < 0.05$.

Figure S6. Annual total (dry plus wet/bulk) deposition fluxes during 2011-2105 period at different observation scales: the annual deposition fluxes at sixteen sites (a), and averaged deposition fluxes during the 2011-2012 and 2013-2015 periods for three land use types (b). The number of sixteen selected sites with the same land use type in each region can be found in Table S1. The error bars are the standard errors of means.

Trend analysis (annual concentration vs. time) was conducted at each site. The slope of the Theil regression and p value for each site are labeled in black and blue. U, R, and B denote urban, rural, and background sites, respectively.

Figure S7. Correlations between NNDMN_NH₃ concentration and IASI_NH₃ columns at twenty-seven sites. Sites with non-significant correlation were marked in red.

Figure S8. Correlations between NNDMN_NO₂ measurements and OMI_NO₂ columns at twenty-seven sites. Sites with non-significant correlation were marked in green.

Figure S9. Seasonal mean concentrations of reduced (the sum of NH₃ and p NH₄⁺) and oxidized (the sum of HNO₃, NO₂ and p NO₃⁻) N in air at different land use types in eastern China and its northern and southern regions. The number of sites with the same land use type in each region can be found in Table S1. The error bars are the standard errors of means, and values without same lettersdifferent letters on the bars denote significantly difference between the sites-seasons at $p < 0.05$. U, R, and B denote urban, rural, and background sites, respectively.

Figure S10. Seasonal mean precipitation amount at different land use types in eastern China and its northern and southern regions. The number of sites with the same land use type in each region can be found in Table S1. The error bars are the standard errors of means, and values without same lettersdifferent letters on the bars denote significantly difference between the sites-seasons at $p < 0.05$. U, R, and B denote urban, rural, and background sites, respectively.

Figure S11. Seasonal ~~mean concentrations~~dry deposition velocities of NH₃, NO₂, HNO₃, p NH₄⁺ and/or p NO₃⁻ at different land use types in eastern China and its northern and southern regions. The number of sites with the same land use type in each region can be found in Table S1. The error bars are the standard errors of means, and values without same lettersdifferent letters on the bars denote significantly difference between the sites-seasons at $p < 0.05$. U, R, and B denote urban, rural, and background sites, respectively.

Figure S12. Comparison of model simulated NH₄⁺ wet deposition, NO₃⁻ wet deposition for 2010 with surface observations (5-year averages) at twenty-seven sites. The background colors show the model results and the overlotted dots show the observations. The correlation coefficients (r) and normalized mean bias

$(NMB = \sum_{i=1}^N (M_i - O_i) / \sum_{i=1}^N O_i)$ between N observed and corresponding modeled values are shown inset.

Figure S13. HYSPLIT back-trajectories analysis on the path of air parcels (NO_2 , particulate NH_4^+ and particulate NO_3^-) prior to arrival at five selected sites (Nanjing, Baiyun, Taojing, Ziyang and Huinong) in southern region of eastern China during different seasons (January-Winter, April-Spring, July-Summer, October-Autumn).

Figure S14. Annual variations in precipitation amounts at sixteen selected sites.

Figure S1

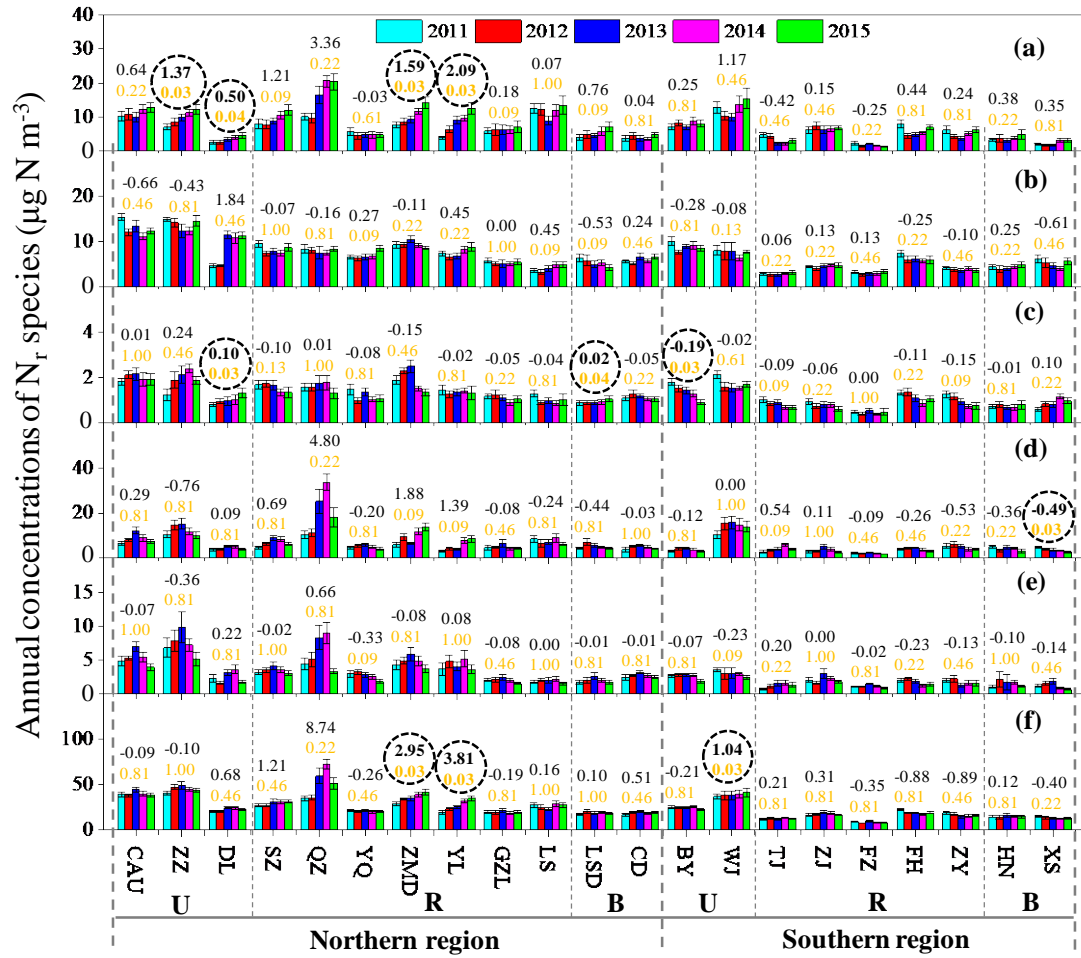


Figure S2

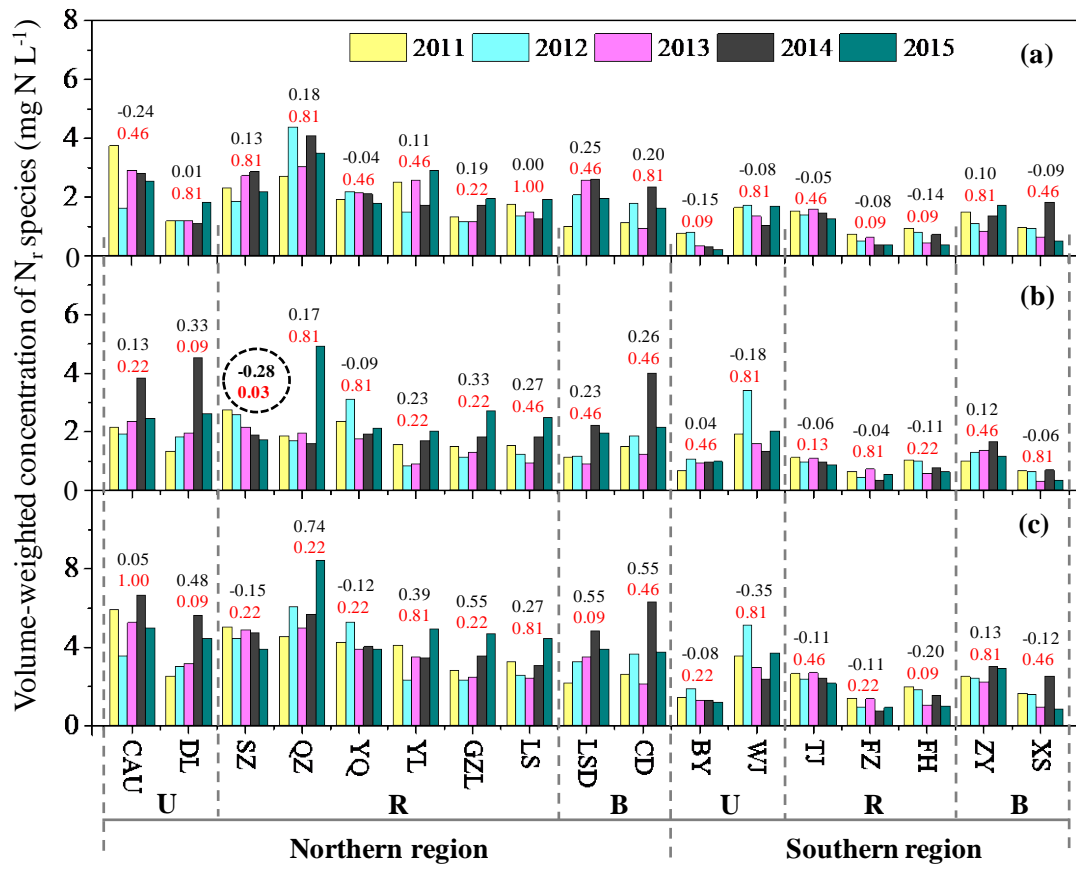


Figure S3

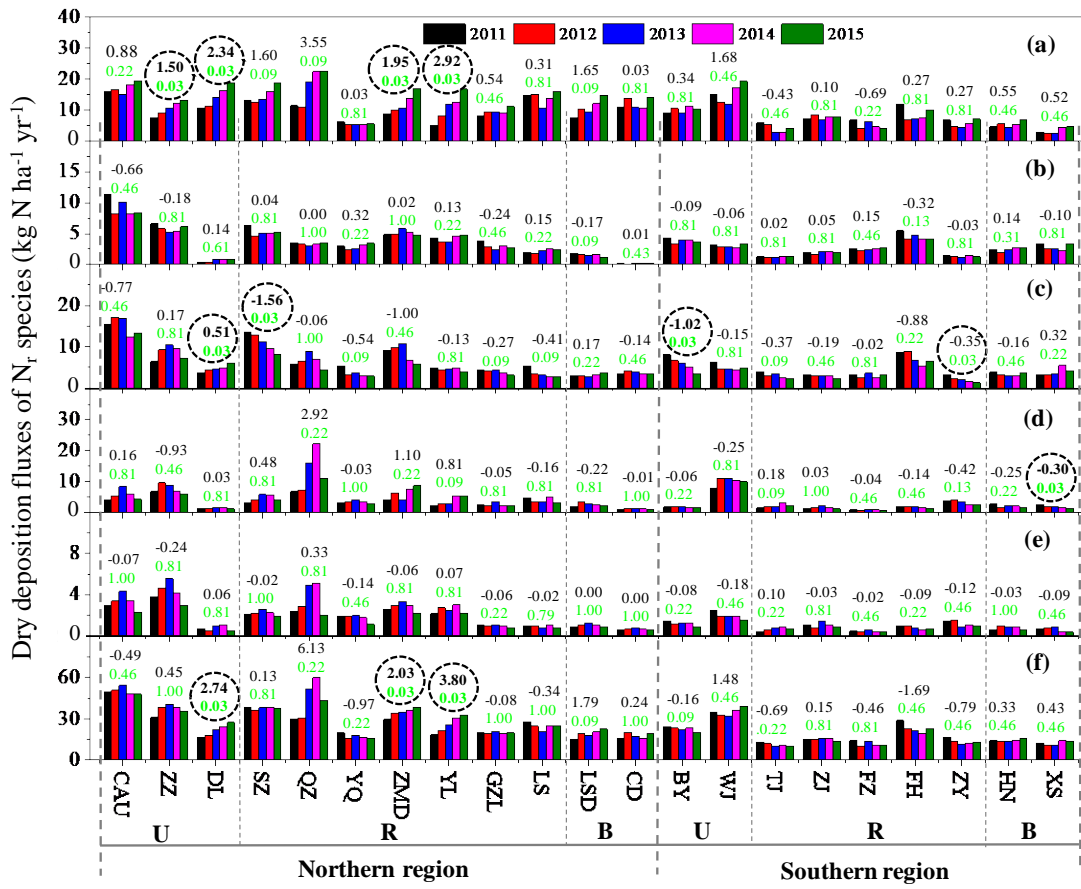


Figure S4

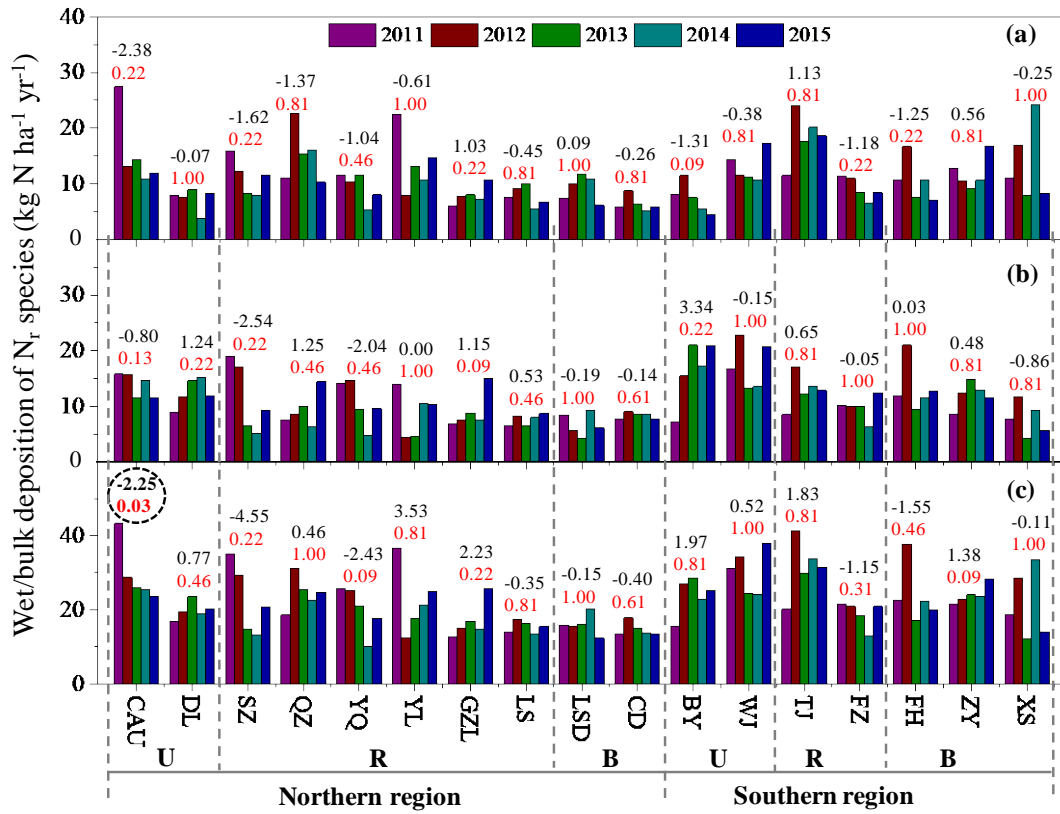


Figure S5

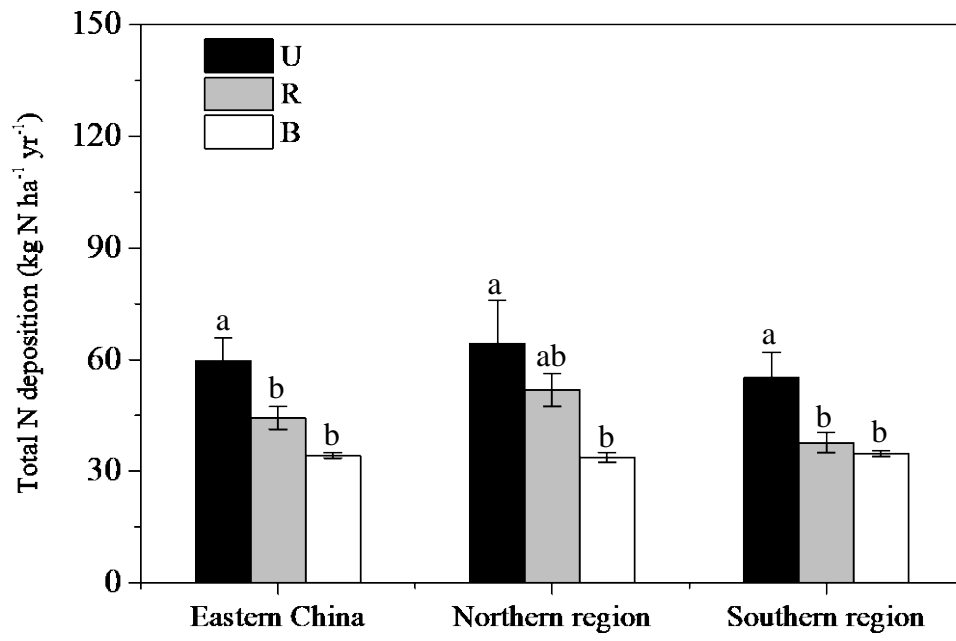


Figure S6

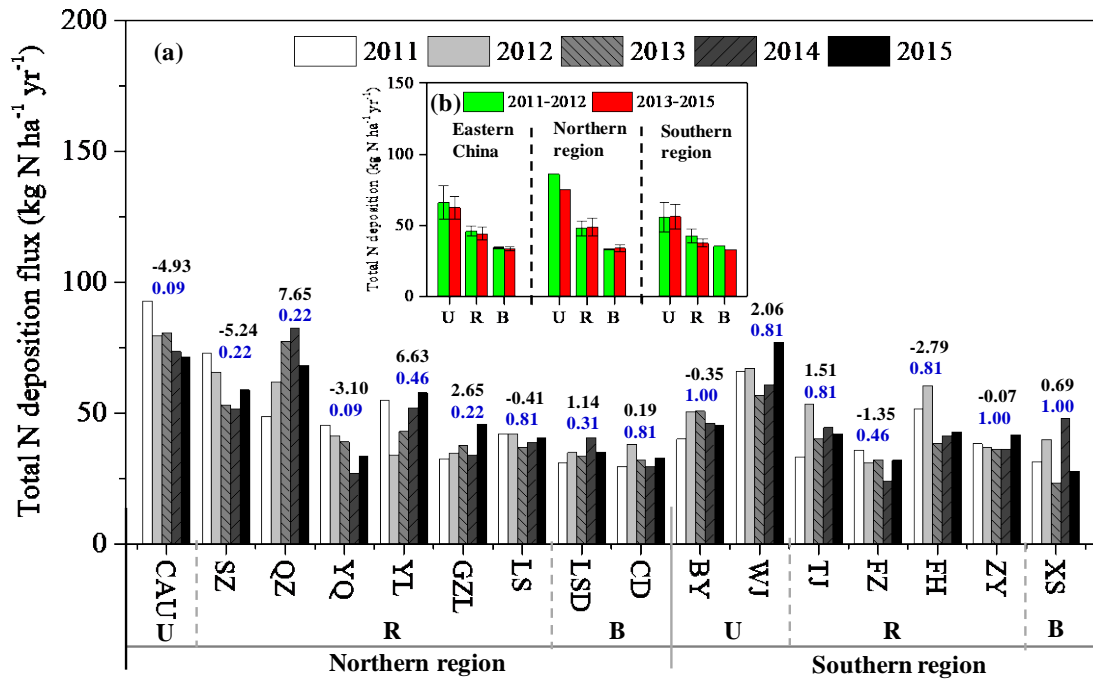


Figure S7

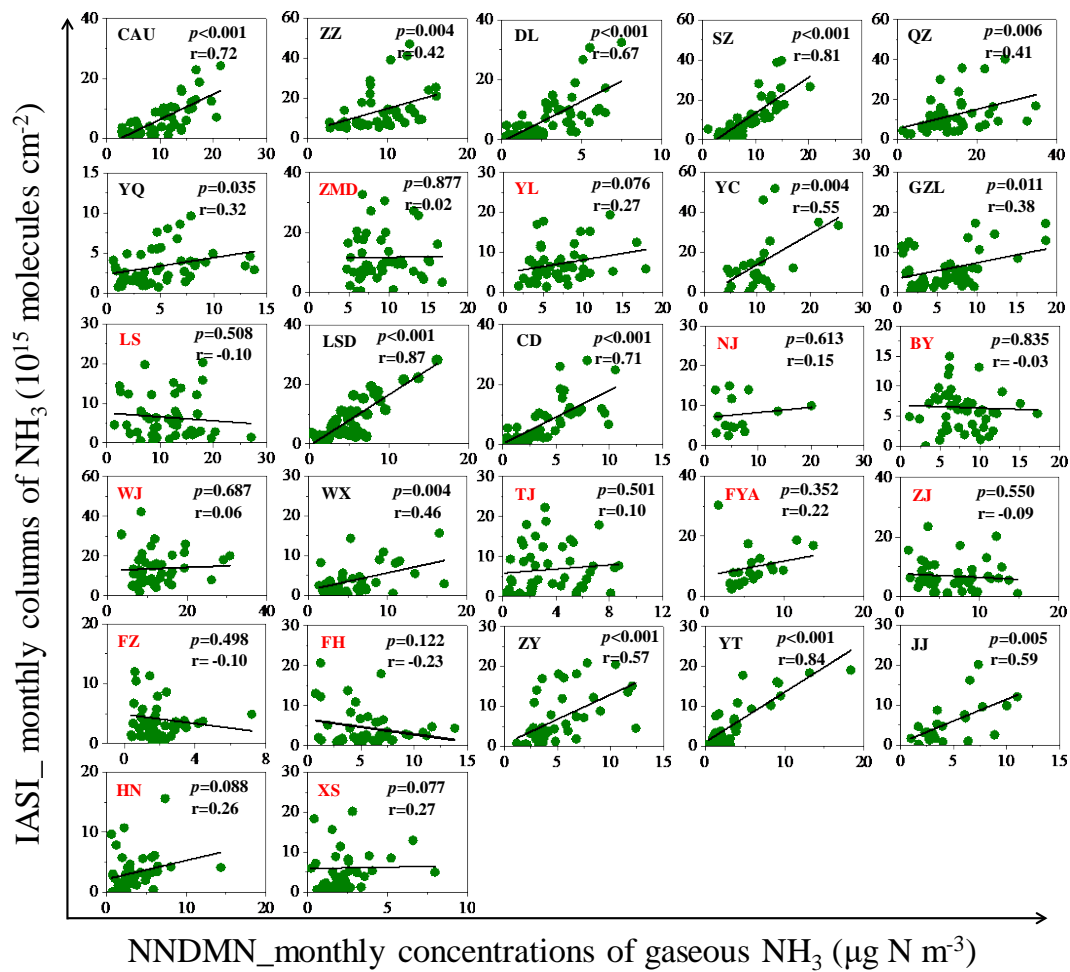


Figure S8

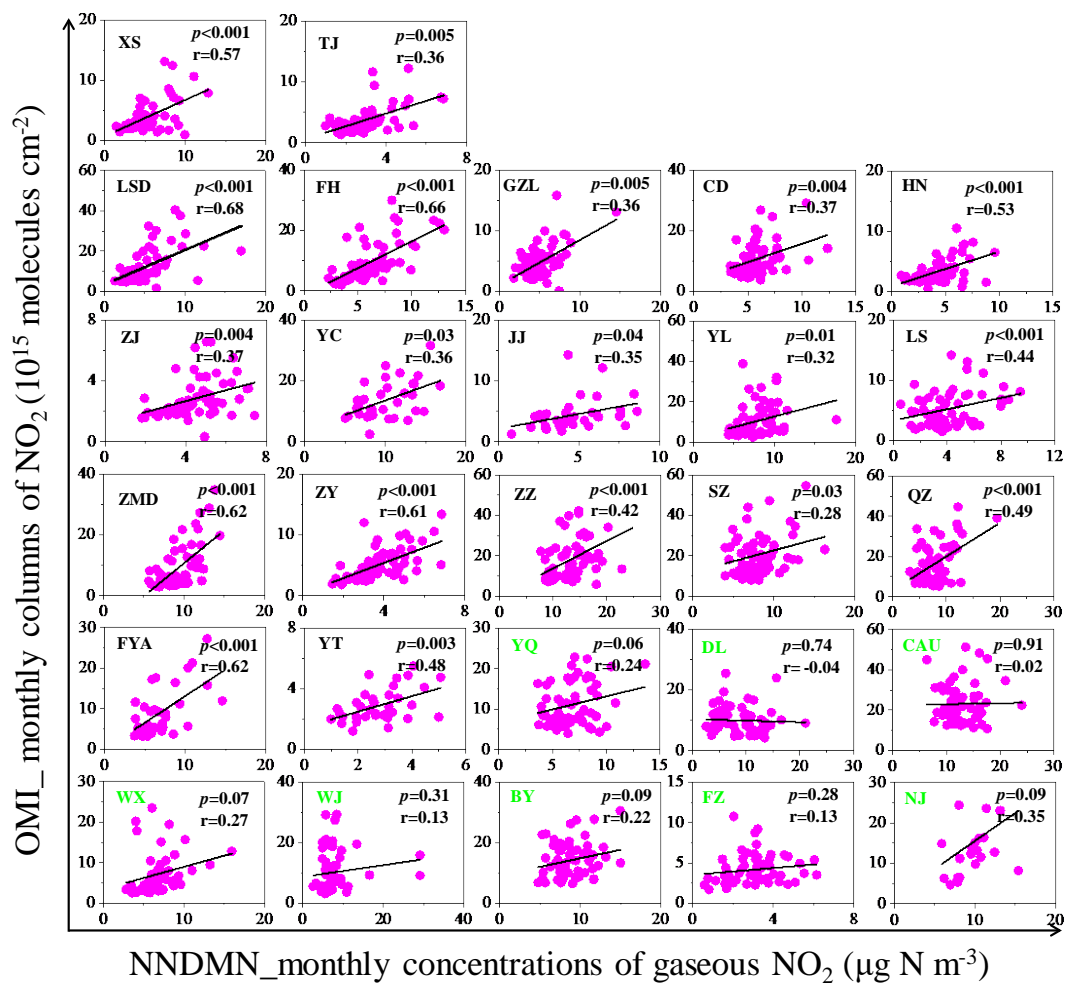


Figure S9

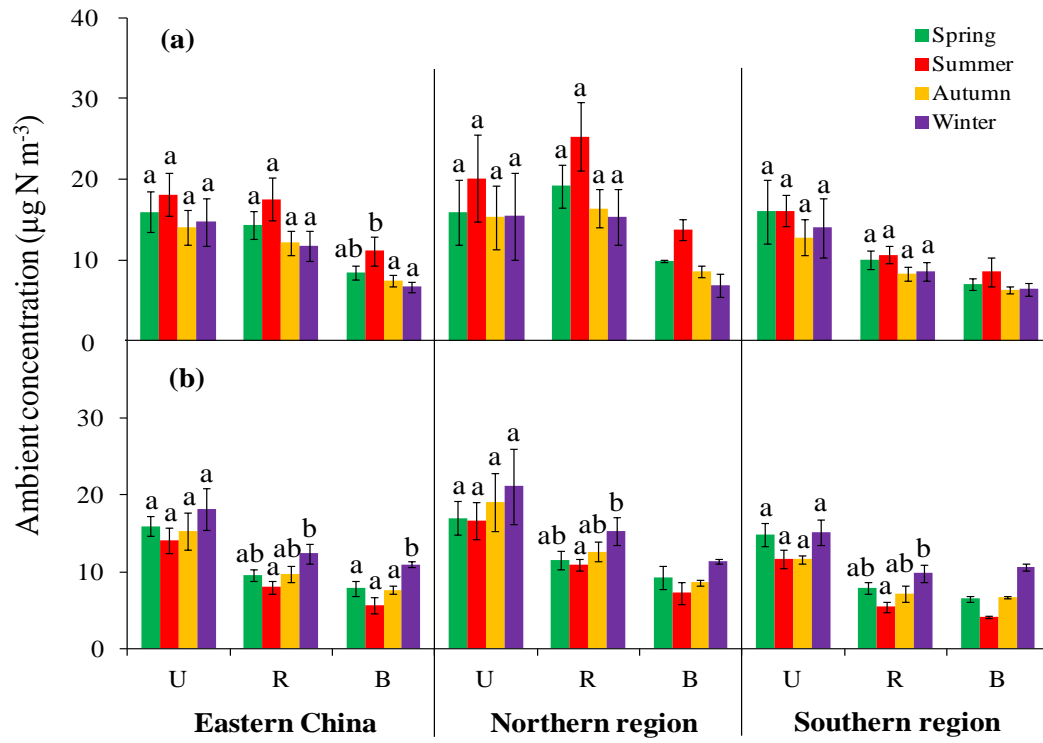


Figure S10

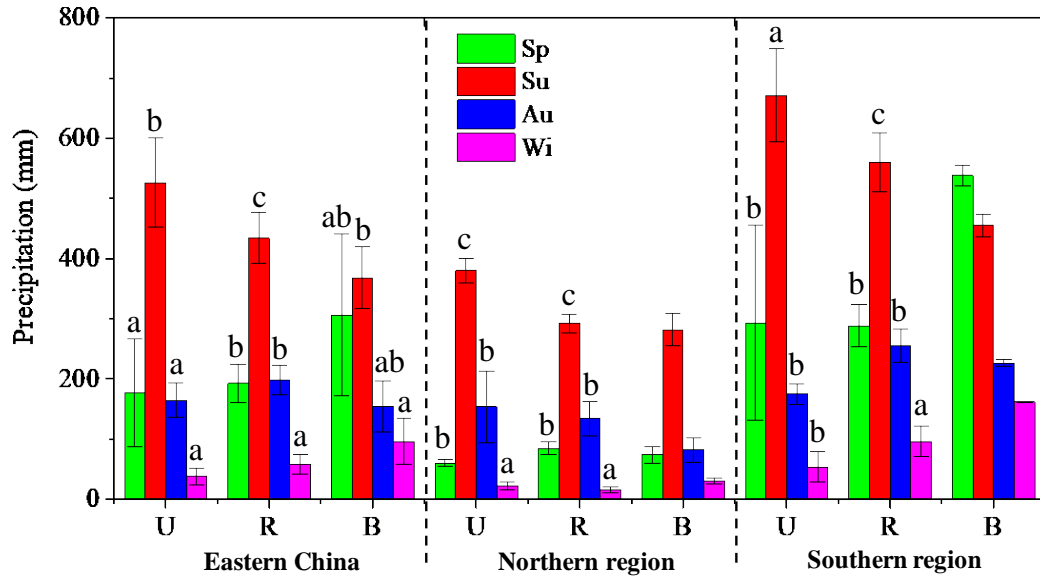


Figure S11

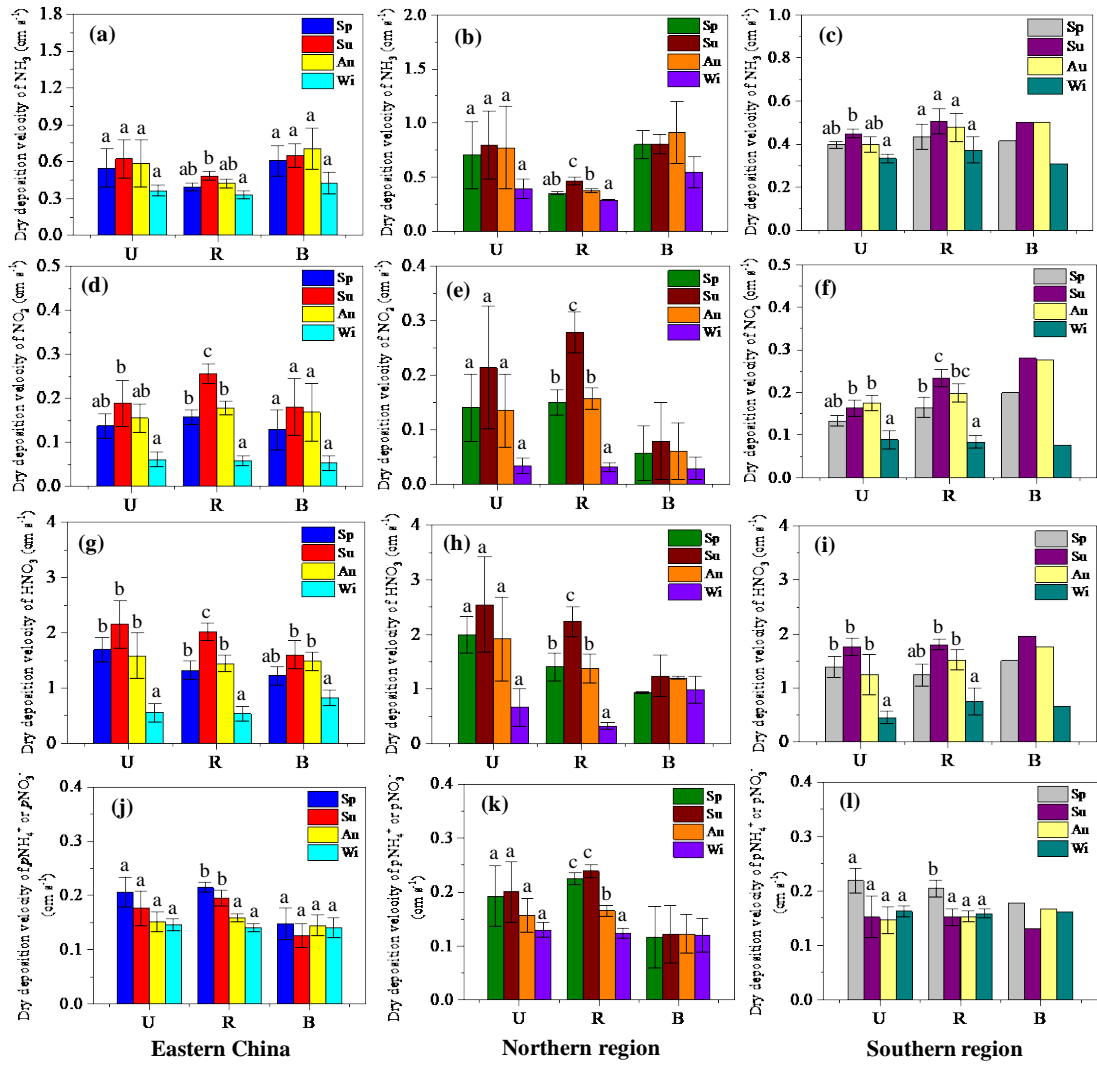


Figure S12

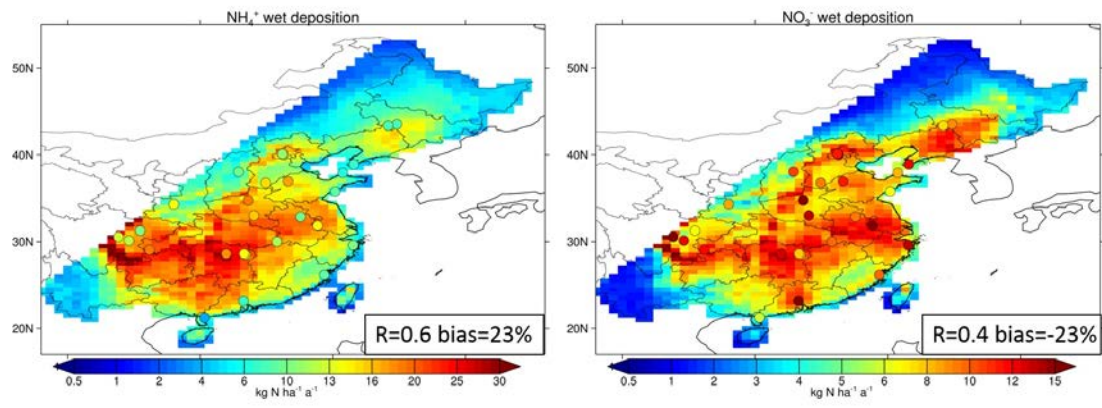


Figure S13

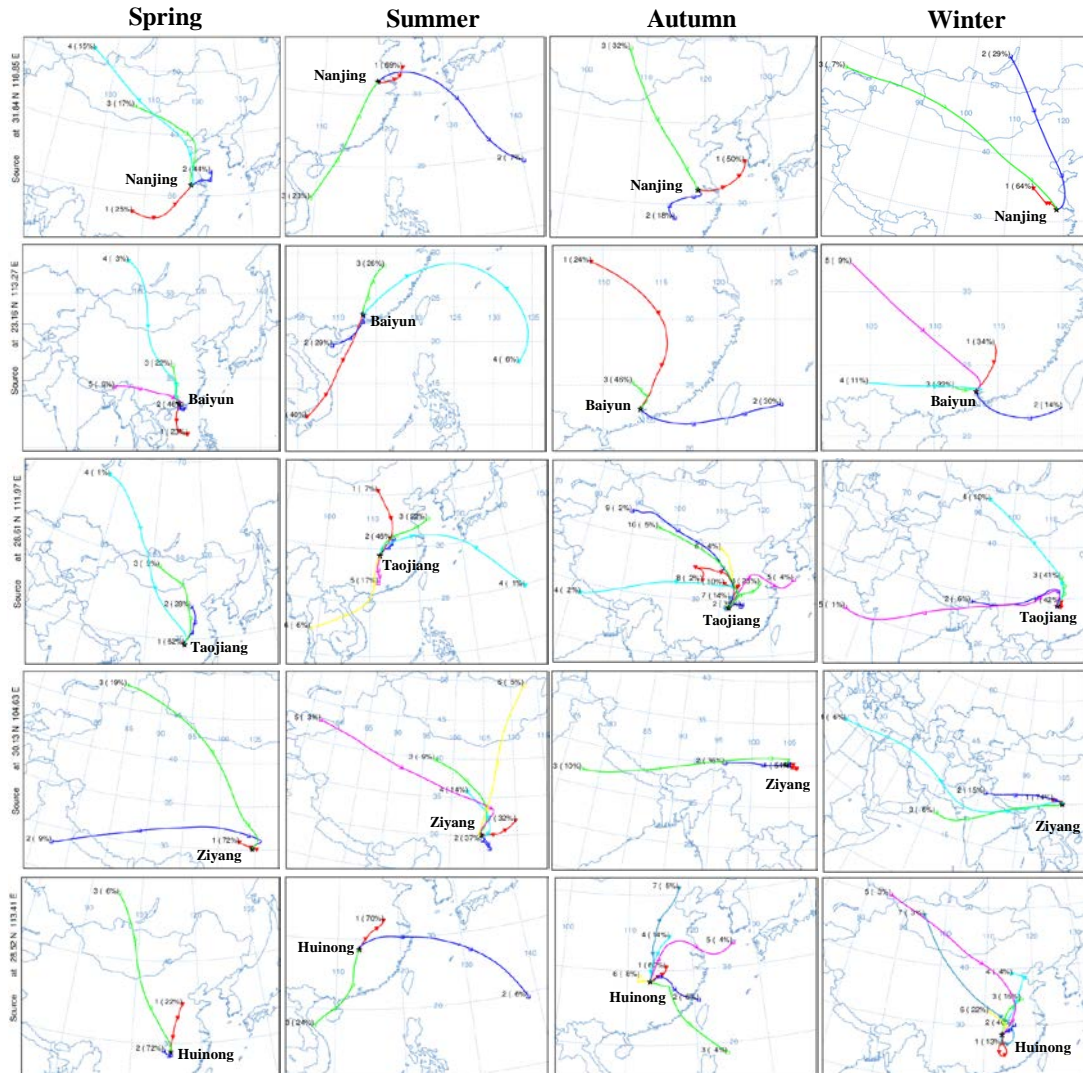


Figure S14

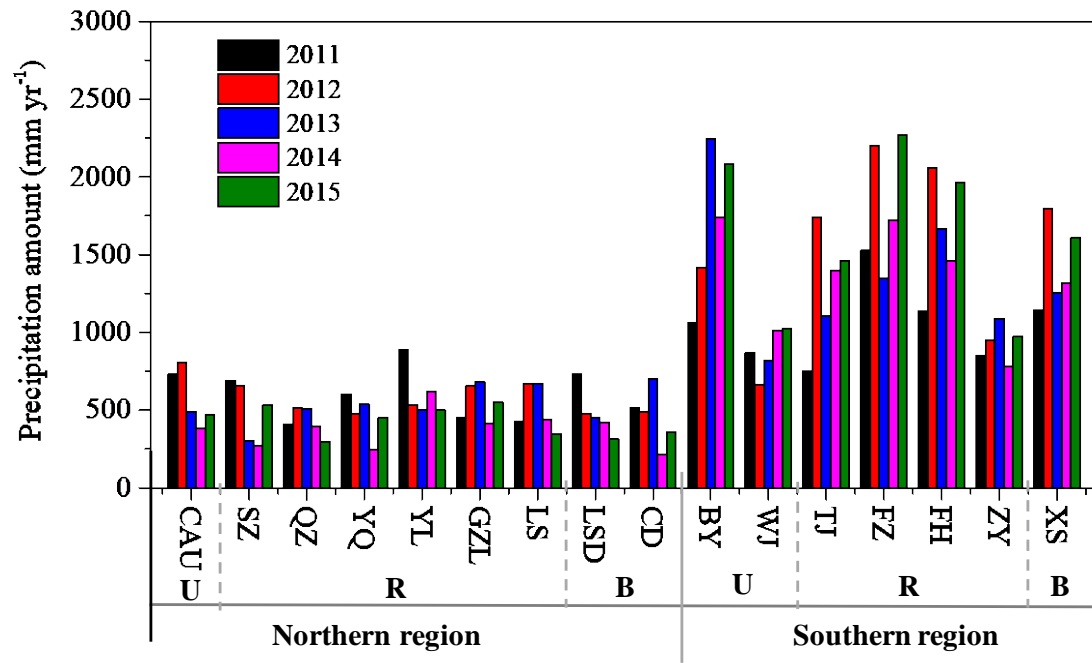


Table S1. Summary of the twenty-seven monitoring sites locations and periods.

Site name	Land use type	Region	Coordinate	Monitoring period	
				Dry deposition	Wet deposition
China Agricultural University (CAU)	Urban	Northern region	116.28 ° E, 40.02 ° N	Jan. 2011-Dec. 2015	Jan. 2011-Dec. 2015
Zhengzhou (ZZ)	Urban	Northern region	113.63 ° E, 34.75 ° N	Jan. 2011-Dec. 2015	Jan. 2011-Dec. 2011
Dalian (DL)	Urban	Northern region	121.58 ° E, 38.92 ° N	Jan. 2011-Dec. 2015	Jan. 2011-Dec. 2015
Shangzhuang (SZ)	Rural	Northern region	116.20 ° E, 40.11 ° N	Jan. 2011-Dec. 2015	Jan. 2011-Dec. 2015
Quzhou (QZ)	Rural	Northern region	114.94 ° E, 36.78 ° N	Jan. 2011-Dec. 2015	Jan. 2011-Dec. 2015
Yangqu (YQ)	Rural	Northern region	112.89 ° E, 38.05 ° N	Jan. 2011-Dec. 2015	Jan. 2011-Dec. 2015
Zhumadian (ZMD)	Rural	Northern region	114.05 ° E, 33.02 ° N	Jan. 2011-Dec. 2015	Jan. 2011-Dec. 2011 Jan. 2014-Dec. 2015
Yanglin (YL)	Rural	Northern region	108.01 ° E, 34.31 ° N	Jan. 2011-Dec. 2015	Jan. 2011-Dec. 2015
Yucheng (YC)	Rural	Northern region	116.63 ° E, 36.94 ° N	Jan. 2013-Dec. 2015	Jan. 2013-Dec. 2015
Gongzhuling (GZL)	Rural	Northern region	124.83 ° E, 43.53 ° N	Jan. 2011-Dec. 2015	Jan. 2011-Dec. 2015
Lishu (LS)	Rural	Northern region	124.17 ° E, 43.36 ° N	Jan. 2011-Dec. 2015	Jan. 2011-Dec. 2015
Lingshandaο (LSD)	Background	Northern region	120.18 ° E, 35.77 ° N	Feb. 2011-Dec. 2015	Feb. 2011-Dec. 2015
Changdao (CD)	Background	Northern region	120.75 ° E, 37.93 ° N	Jan. 2011-Dec. 2015	Jan. 2011-Dec. 2015
Nanjing (NJ)	Urban	Southern region	118.85 ° E, 31.84 ° N	Jan. 2011-Dec. 2011 Jan. 2015-Dec. 2015	Jan. 2011-Dec. 2011 Jan. 2015-Dec. 2015
Baiyun (BY)	Urban	Southern region	113.27 ° E, 23.16 ° N	Jan. 2011-Dec. 2015	Jan. 2011-Dec. 2015
Wenjiang (WJ)	Urban	Southern region	103.84 ° E, 30.55 ° N	Jan. 2011-Dec. 2015	Jan. 2011-Dec. 2015
Wuxue (WX)	Rural	Southern region	115.79 ° E, 30.01 ° N	Jan. 2012-Dec. 2015	Jan. 2012-Dec. 2015
Taojing (TJ)	Rural	Southern region	111.97 ° E, 28.61 ° N	Jan. 2011-Dec. 2015	Jan. 2011-Dec. 2015
Fengyang (FYA)	Rural	Southern region	117.56 ° E, 32.88 ° N	Feb. 2013-Dec. 2015	Feb. 2014-Dec. 2015

Zhanjiang (ZZ)	Rural	Southern region	110.33 ° E, 21.26 ° N	Jan. 2011-Dec. 2015	Jan. 2013-Dec. 2015
Fuzhou (FZ)	Rural	Southern region	119.36 ° E, 26.17 ° N	Jan. 2011-Dec. 2015	Jan. 2011-Dec. 2015
Fenghua (FH)	Rural	Southern region	121.53 ° E, 29.61 ° N	Jan. 2011-Dec. 2015	Jan. 2011-Dec. 2015
Ziyang (ZY)	Rural	Southern region	104.63 ° E, 30.13 ° N	Jan. 2011-Dec. 2015	Jan. 2011-Dec. 2015
Yanting (YT)	Rural	Southern region	105.47 ° E, 31.28 ° N	Jan. 2012-Dec. 2013 Jan. 2015-Dec. 2015	Jan. 2012-Dec. 2013
Jiangjin (JJ)	Rural	Southern region	106.18 ° E, 29.06 ° N	Jan. 2013-Dec. 2015	Jan. 2013-Dec. 2015
Huinong (HN)	Background	Southern region	113.41 ° E, 28.52 ° N	Jan. 2011-Dec. 2015	Jan. 2011-Dec. 2014
Xishan (XS)	Background	Southern region	113.31 ° E, 28.61 ° N	Jan. 2011-Dec. 2015	Jan. 2011-Dec. 2015

Table S2. Summary of monthly mean N_r concentrations measured during the 2011-2015 period.

Site	NH_3 ($\mu g N m^{-3}$)				NO_2 ($\mu g N m^{-3}$)				HNO_3 ($\mu g N m^{-3}$)				pNH_4^+ ($\mu g N m^{-3}$)				pNO_3^- ($\mu g N m^{-3}$)			
	Min	Max	Avg	N	Min	Max	Avg	N ^a	Min	Max	Avg	N	Min	Max	Avg	N	Min	Max	Avg	N
CAU	2.86	22.43	11.21	60	6.35	24.03	12.87	60	0.36	4.93	1.98	60	1.96	19.40	8.72	60	1.01	13.38	5.34	60
ZZ	2.75	18.59	9.76	60	7.74	24.75	13.66	60	0.07	4.30	1.89	60	1.35	33.10	12.53	60	0.44	32.06	7.40	60
DL	0.27	8.53	3.40	60	2.54	21.04	8.60	60	0.10	2.58	1.00	60	0.65	9.54	4.45	60	0.01	7.16	2.53	60
SZ	1.00	21.23	9.44	60	3.96	16.27	8.16	60	0.29	3.50	1.54	60	1.48	15.95	6.95	60	1.00	9.43	3.53	60
QZ	1.36	34.80	15.43	60	3.23	19.48	7.97	60	0.14	4.40	1.59	60	1.89	57.20	19.68	60	0.22	20.78	6.06	60
YQ	0.58	13.81	4.88	60	3.62	13.61	6.98	60	0.04	2.73	1.18	60	0.99	10.69	5.11	60	0.21	7.26	2.72	60
ZMD	4.73	27.30	10.31	60	5.65	14.47	9.36	60	0.22	4.09	1.90	60	0.92	21.87	9.52	60	0.47	14.50	4.75	60
YL	1.91	19.77	8.30	60	4.30	17.64	7.55	60	0.14	3.73	1.35	60	0.59	21.55	5.56	60	1.07	16.22	4.29	60
YC	4.39	25.36	11.88	36	5.02	16.78	9.74	36	0.10	3.82	1.52	36	4.70	46.53	13.66	36	1.00	11.81	4.50	36
GZL	0.48	18.62	6.35	60	1.79	14.52	5.29	60	0.21	2.41	1.09	60	0.40	18.14	4.97	60	0.51	5.52	2.07	60
LS	1.42	38.89	11.79	60	0.55	9.45	4.16	60	0.22	3.27	1.00	60	1.61	26.67	7.51	60	0.29	5.79	1.93	60
LSD	0.30	16.02	5.30	59	1.32	16.97	5.31	59	0.08	1.69	0.92	59	0.39	20.69	5.34	59	0.21	6.15	2.05	59
CD	0.30	10.55	4.04	60	3.40	12.37	5.97	60	0.50	2.92	1.13	60	0.54	12.97	4.91	60	0.97	6.55	2.74	60
NJ	1.57	20.06	6.02	24	5.89	15.38	9.73	24	0.64	3.65	1.80	24	0.56	9.28	5.87	24	1.13	5.64	3.17	24
BY	1.13	17.22	7.86	60	4.75	14.97	8.86	60	0.16	2.58	1.38	60	0.60	8.57	3.81	60	0.73	4.62	2.62	60
WJ	3.53	39.57	12.47	60	2.52	29.06	7.58	60	0.09	3.27	1.70	60	2.00	32.21	14.09	60	1.09	11.50	3.04	60
WX	1.39	17.12	5.91	48	2.82	15.93	6.81	48	0.32	3.24	1.27	48	0.70	12.42	5.22	48	0.10	8.55	1.98	48
TJ	0.16	8.70	3.31	60	1.00	6.85	2.91	60	0.14	1.71	0.82	60	0.24	9.03	4.19	60	0.03	4.41	1.32	60
FYA	1.73	20.25	6.81	35	3.70	14.58	7.01	35	0.18	2.25	1.41	35	0.73	11.85	5.71	35	0.83	9.21	3.01	35
ZJ	1.07	14.80	6.68	60	1.84	7.41	4.52	60	0.09	1.68	0.77	60	0.39	10.23	3.58	60	0.19	9.83	2.23	60
FZ	0.19	7.20	1.77	60	0.57	6.15	3.05	60	0.05	1.62	0.45	60	0.17	3.79	2.22	60	0.22	2.20	1.20	60
FH	0.76	13.83	5.90	60	2.26	13.04	6.24	60	0.29	2.63	1.13	60	0.45	8.01	4.04	60	0.31	3.88	1.81	60

ZY	1.16	12.46	5.12	60	1.45	6.85	3.83	60	0.22	2.24	0.96	60	0.11	16.08	4.99	60	0.11	5.53	1.78	60
YT	0.43	18.31	4.18	36	0.99	5.07	2.75	36	0.08	1.20	0.49	36	0.88	15.80	3.01	36	0.11	2.54	1.01	36
JJ	0.70	12.99	4.48	36	0.82	8.61	4.75	36	0.13	3.09	1.48	36	1.26	16.74	7.85	36	0.34	7.61	3.03	36
HN	0.64	18.86	3.78	60	0.89	9.59	4.31	60	0.12	2.68	0.74	60	0.44	12.58	4.21	60	0.16	14.77	1.62	60
XS	0.21	7.97	2.38	60	1.41	12.81	5.18	60	0.08	1.96	0.87	60	0.43	9.19	3.74	60	0.15	5.27	1.25	60

^aMultiply by 3 to obtain a total numbers of NO₂ samples.

Table S3. Summary of monthly volume-weighted mean N_r concentrations in precipitation measured during the 2011-2015 period.

Site	NH_4^+ -N (mg N L ⁻¹)				NO_3^- -N (mg N L ⁻¹)				TIN (mg N L ⁻¹)			
	Min	Max	Avg	N	Min	Max	Avg	N	Min	Max	Avg	N
CAU	0.16	19.15	3.91	47	0.22	15.75	4.20	47	0.46	32.37	8.10	47
ZZ	1.37	10.67	4.11	10	1.01	27.89	5.30	10	2.38	38.56	9.41	10
DL	0.13	15.93	2.94	53	0.70	14.40	4.22	53	1.13	25.57	7.15	53
SZ	0.44	13.08	3.21	42	0.40	8.99	2.86	42	0.84	19.52	6.08	42
QZ	0.16	16.60	3.76	47	0.21	14.40	3.04	47	0.53	29.27	6.80	47
YQ	0.16	17.56	2.79	48	0.22	12.45	3.18	48	0.69	30.01	5.96	48
ZMD	0.03	9.31	2.66	34	0.07	5.81	2.21	34	0.11	12.29	4.87	34
YL	0.46	10.51	3.29	53	0.07	8.32	2.83	53	0.55	17.86	6.12	53
YC	0.97	26.77	6.80	32	0.84	23.52	4.81	32	2.22	50.29	11.61	32
GZL	0.12	7.34	2.37	60	0.53	10.06	2.67	60	0.81	15.05	5.05	60
LS	0.27	12.72	2.22	48	0.28	9.46	2.61	48	0.55	14.73	4.82	48
LSD	0.29	8.44	2.38	45	0.14	11.10	2.41	45	0.54	17.67	4.80	45
CD	0.34	11.27	2.48	54	0.46	19.92	4.00	54	1.06	29.65	6.47	54
NJ	0.33	2.82	1.27	26	0.28	8.31	2.11	26	0.62	10.06	3.38	26
BY	0.01	13.88	0.97	53	0.11	6.23	1.70	53	0.34	19.98	2.67	53
WJ	0.19	13.62	2.65	52	0.10	28.92	4.75	52	0.91	34.64	7.41	52
WX	0.16	2.88	1.01	44	0.10	7.39	1.30	44	0.31	8.75	2.31	44
TJ	0.24	8.36	2.02	59	0.11	7.23	1.53	59	0.35	15.03	3.55	59
FYA	0.24	9.63	2.32	24	0.34	28.77	3.06	24	0.61	38.40	5.38	24
ZJ	0.10	2.04	0.42	29	0.07	3.77	0.79	29	0.23	4.16	1.21	29
FZ	0.04	4.96	0.74	60	0.09	4.93	0.85	60	0.22	8.88	1.59	60
FH	0.12	5.62	1.03	55	0.34	6.61	1.25	55	0.52	12.23	2.27	55
ZY	0.16	5.08	1.79	53	0.47	11.52	2.20	53	1.20	15.74	3.99	53
YT	0.16	3.81	1.31	32	0.16	3.13	1.17	32	0.54	6.27	2.48	32
JJ	0.35	12.73	3.27	36	0.26	10.31	2.63	36	0.61	23.04	5.89	36
HN	0.19	5.26	1.40	48	0.17	3.74	0.91	48	0.36	8.86	2.30	48
XS	0.03	3.78	1.22	60	0.06	3.52	0.81	60	0.09	6.09	2.03	60

Table S4. Seasonal average concentrations and deposition fluxes of gaseous NH₃ at twenty-seven monitoring sites in eastern China.

Sites	Air concentrations				Dry deposition fluxes			
	Spring	Summer	Autumn	Winter	Spring	Summer	Autumn	Winter
CAU	12.1 ± 1.9b	16.0 ± 2.4a	11.2 ± 1.6b	5.6 ± 1.5c	3.8 ± 0.6b	7.8 ± 1.1a	4.1 ± 0.6b	1.3 ± 0.3c
ZZ	11.7 ± 1.4a	12.2 ± 3.9a	8.9 ± 3.2ab	6.3 ± 1.1b	3.4 ± 0.4a	3.4 ± 1.1a	2.2 ± 0.8ab	1.5 ± 0.3b
DL	3.8 ± 1.0a	5.1 ± 1.2a	3.5 ± 1.3a	1.2 ± 0.4b	4.2 ± 1.1a	5.5 ± 1.3a	4.1 ± 1.5a	0.6 ± 0.2b
SZ	9.7 ± 1.9b	14.9 ± 2.5a	9.0 ± 2.9b	4.2 ± 1.4c	3.1 ± 0.6b	7.3 ± 1.2a	3.4 ± 1.1b	1.0 ± 0.3c
QZ	17.4 ± 5.7a	18.2 ± 4.6a	13.3 ± 3.8a	12.8 ± 8.8a	4.8 ± 1.6a	5.8 ± 1.5a	3.7 ± 1.1a	3.0 ± 2.1a
YQ	7.7 ± 0.8a	6.0 ± 0.6a	3.1 ± 0.7b	2.7 ± 2.1b	2.0 ± 0.2a	2.0 ± 0.2a	0.9 ± 0.2b	0.6 ± 0.5b
ZMD	11.3 ± 4.0a	9.8 ± 4.1a	10.8 ± 2.9a	9.3 ± 0.9a	3.8 ± 1.3a	3.1 ± 1.3a	2.9 ± 0.8a	2.2 ± 0.2a
YL	7.6 ± 2.8a	10.9 ± 6.3a	8.5 ± 3.8a	6.3 ± 2.1a	2.4 ± 0.9ab	4.3 ± 2.5a	2.7 ± 1.3ab	1.5 ± 0.5b
YC	10.9 ± 2.2b	17.0 ± 2.0a	12.2 ± 2.3ab	9.2 ± 2.1b	2.6 ± 0.5b	4.9 ± 0.6a	3.1 ± 0.6b	2.1 ± 0.5b
GZL	7.3 ± 0.6b	11.7 ± 2.4a	5.2 ± 0.3b	1.3 ± 0.6c	1.8 ± 0.2b	5.5 ± 1.2a	1.8 ± 0.1b	0.2 ± 0.1c
LS	17.0 ± 3.5a	13.2 ± 2.5ab	11.9 ± 1.9b	5.1 ± 1.7c	4.0 ± 0.8b	5.5 ± 1.1a	3.6 ± 0.6b	1.0 ± 0.4c
LSD	5.0 ± 0.9b	9.4 ± 2.4a	4.8 ± 2.2bc	1.9 ± 0.4c	2.6 ± 0.5b	5.2 ± 1.4a	2.4 ± 1.1b	0.5 ± 0.1c
CD	4.9 ± 0.7b	6.9 ± 1.2a	3.3 ± 0.9b	1.1 ± 0.5c	3.6 ± 0.5ab	4.8 ± 1.0a	3.0 ± 0.8b	0.6 ± 0.3c
NJ	7.7 ± 1.7	10.2 ± 2.1	3.6 ± 1.1	3.8 ± 0.1	2.6 ± 0.6	3.8 ± 0.8	1.1 ± 0.3	0.9 ± 0.0
BY	7.4 ± 1.2b	9.9 ± 2.0a	9.4 ± 0.8ab	4.7 ± 0.8c	2.2 ± 0.4b	3.1 ± 0.6a	3.3 ± 0.3a	1.4 ± 0.2c
WJ	14.8 ± 3.8a	16.2 ± 6.9a	10.1 ± 3.8a	8.8 ± 1.7a	4.5 ± 1.1ab	5.9 ± 2.5a	2.6 ± 1.0b	2.1 ± 0.4b
WX	6.3 ± 1.9b	9.6 ± 1.7a	5.1 ± 0.9bc	3.2 ± 0.5c	1.9 ± 0.6b	3.3 ± 0.6a	1.8 ± 0.3b	0.8 ± 0.1c
TJ	4.0 ± 2.5ab	5.3 ± 1.4a	2.4 ± 1.2b	1.5 ± 0.8b	1.1 ± 0.7ab	1.8 ± 0.5a	0.9 ± 0.4b	0.4 ± 0.2b
FYA	6.4 ± 1.6ab	11.2 ± 4.9a	5.4 ± 0.2ab	3.8 ± 0.5b	2.1 ± 0.5ab	3.6 ± 1.8a	1.6 ± 0.0ab	0.8 ± 0.3b
ZJ	7.6 ± 1.5a	9.3 ± 1.9a	6.6 ± 1.6a	3.3 ± 1.3b	1.9 ± 0.4a	2.6 ± 0.5a	2.3 ± 0.6a	0.8 ± 0.3b
FZ	1.7 ± 0.5ab	3.0 ± 1.2a	1.4 ± 0.2b	1.0 ± 0.6b	1.2 ± 0.4b	2.2 ± 0.9a	1.1 ± 0.2b	0.7 ± 0.4b
FH	6.9 ± 2.3ab	7.5 ± 2.5a	5.9 ± 1.6ab	3.4 ± 1.5b	2.5 ± 0.9a	3.1 ± 1.0a	2.2 ± 0.6ab	0.8 ± 0.4b
ZY	7.7 ± 1.4a	5.7 ± 2.0ab	4.3 ± 1.2bc	2.9 ± 0.5c	2.0 ± 0.4a	1.9 ± 0.6a	1.1 ± 0.3b	0.7 ± 0.1b

YT	3.3 ± 0.7b	9.3 ± 0.8a	2.6 ± 1.4b	1.5 ± 0.7b	1.0 ± 0.2b	3.4 ± 0.2a	0.8 ± 0.4b	0.4 ± 0.2b
JJ	7.1 ± 1.2a	5.2 ± 2.1ab	3.3 ± 0.8b	2.4 ± 0.4b	2.1 ± 0.4a	1.9 ± 0.8a	1.1 ± 0.3ab	0.6 ± 0.1b
HN	4.1 ± 0.7ab	7.0 ± 2.8a	2.2 ± 0.9b	1.8 ± 0.6b	1.4 ± 0.2b	2.7 ± 1.1a	0.9 ± 0.4b	0.4 ± 0.2b
XS	2.7 ± 1.3ab	3.5 ± 1.3a	1.8 ± 0.7ab	1.5 ± 0.5b	0.9 ± 0.5ab	1.4 ± 0.5a	0.7 ± 0.3ab	0.4 ± 0.1b

The data shown are the seasonal means ± standard deviations of observation periods (sampling period for each site are given in Table S1). Different letters in the columns of “air concentrations” and “dry deposition fluxes” indicate significant difference between the seasons at $p < 0.05$. The full names of all the sites are presented in Table S1.

Table S5. Seasonal average concentrations and deposition fluxes of gaseous NO₂ at twenty-seven monitoring sites in eastern China.

Sites	Air concentrations				Dry deposition fluxes			
	Spring	Summer	Autumn	Winter	Spring	Summer	Autumn	Winter
CAU	12.0 ± 1.7a	12.7 ± 1.7a	14.3 ± 3.3a	12.5 ± 2.1a	1.9 ± 0.2c	4.2 ± 0.6a	2.9 ± 0.8b	0.3 ± 0.0d
ZZ	12.5 ± 1.8a	12.0 ± 2.2a	15.0 ± 2.0a	15.1 ± 2.3a	1.9 ± 0.2a	1.7 ± 0.3ab	1.4 ± 0.2b	0.7 ± 0.1c
DL	9.1 ± 4.2a	8.4 ± 4.4a	8.6 ± 3.7a	8.3 ± 3.8a	0.1 ± 0.1a	0.2 ± 0.1a	0.2 ± 0.1a	0.1 ± 0.0a
SZ	8.8 ± 0.9a	7.4 ± 1.0a	7.4 ± 0.8a	9.0 ± 2.1a	1.4 ± 0.1b	2.4 ± 0.3a	1.3 ± 0.2b	0.2 ± 0.0c
QZ	6.8 ± 1.5b	7.3 ± 1.5ab	8.0 ± 0.9ab	9.7 ± 1.7a	0.9 ± 0.2a	1.2 ± 0.2a	0.9 ± 0.1a	0.3 ± 0.1b
YQ	6.7 ± 1.7a	6.8 ± 1.6a	7.5 ± 0.6a	6.8 ± 1.8a	0.6 ± 0.1b	1.4 ± 0.3a	0.8 ± 0.1b	0.1 ± 0.0c
ZMD	9.3 ± 0.9ab	8.0 ± 0.5b	9.5 ± 1.0ab	10.5 ± 1.6a	1.9 ± 0.2a	1.5 ± 0.1b	1.1 ± 0.1c	0.7 ± 0.1d
YL	7.2 ± 1.9ab	5.9 ± 1.1b	7.8 ± 0.4ab	9.3 ± 1.8a	1.3 ± 0.3a	1.5 ± 0.3a	1.1 ± 0.2a	0.3 ± 0.1b
YC	9.9 ± 2.9a	8.5 ± 2.1a	9.9 ± 2.2a	11.3 ± 3.0a	0.9 ± 0.2ab	1.1 ± 0.3a	0.8 ± 0.2ab	0.3 ± 0.1b
GZL	4.3 ± 1.0a	5.8 ± 1.1a	5.0 ± 0.5a	6.0 ± 1.5a	0.4 ± 0.1b	1.9 ± 0.4a	0.6 ± 0.2b	0.04 ± 0.01c
LS	3.8 ± 1.7a	5.5 ± 0.6a	3.8 ± 0.9a	3.6 ± 1.0a	0.3 ± 0.1b	1.5 ± 0.2a	0.4 ± 0.1b	0.03 ± 0.01c
LSD	4.5 ± 1.4bc	3.4 ± 0.7c	6.0 ± 2.4ab	7.5 ± 0.3a	0.4 ± 0.1a	0.4 ± 0.1a	0.5 ± 0.2a	0.3 ± 0.0a
CD	6.5 ± 0.5ab	5.1 ± 0.5b	5.2 ± 0.7b	7.1 ± 1.6a	0.04 ± 0.00a	0.04 ± 0.00a	0.04 ± 0.00a	0.05 ± 0.01a
NJ	12.0 ± 0.9	7.8 ± 0.7	8.5 ± 1.6	10.9 ± 0.8	1.5 ± 0.2	1.2 ± 0.1	1.1 ± 0.4	0.4 ± 0.0
BY	10.7 ± 2.0a	9.4 ± 2.1ab	7.6 ± 1.0b	7.7 ± 0.7b	1.0 ± 0.2a	1.1 ± 0.2a	1.1 ± 0.1a	0.7 ± 0.1b
WJ	7.4 ± 1.4ab	5.9 ± 1.4b	6.6 ± 0.6b	10.4 ± 3.4a	0.9 ± 0.2a	1.1 ± 0.3a	0.5 ± 0.1b	0.5 ± 0.1b
WX	6.8 ± 0.3a	4.7 ± 0.7a	8.0 ± 2.7a	7.5 ± 1.4a	0.8 ± 0.0ab	0.8 ± 0.1ab	1.2 ± 0.4a	0.4 ± 0.1b
TJ	2.6 ± 0.6bc	1.9 ± 0.2c	2.9 ± 0.3b	4.3 ± 0.4a	0.3 ± 0.1bc	0.3 ± 0.0ab	0.4 ± 0.1a	0.2 ± 0.0c
FYA	6.0 ± 1.3a	5.7 ± 1.0a	8.3 ± 0.8a	8.4 ± 2.4a	0.8 ± 0.2a	0.9 ± 0.1a	0.7 ± 0.2ab	0.3 ± 0.1b
ZJ	5.3 ± 0.4a	3.2 ± 0.8b	4.5 ± 0.8a	5.1 ± 0.6a	0.4 ± 0.0b	0.4 ± 0.1b	0.8 ± 0.1a	0.4 ± 0.0b
FZ	4.1 ± 0.5a	3.4 ± 0.4b	1.7 ± 0.2c	3.0 ± 0.4b	0.9 ± 0.1a	0.8 ± 0.1a	0.4 ± 0.1b	0.4 ± 0.1b
FH	6.7 ± 1.2b	4.4 ± 1.1c	5.5 ± 0.6bc	8.4 ± 0.9a	1.4 ± 0.3a	1.2 ± 0.3ab	1.2 ± 0.2ab	0.8 ± 0.1b
ZY	4.5 ± 0.8ab	2.7 ± 0.4c	3.5 ± 0.6bc	4.6 ± 0.2a	0.4 ± 0.1a	0.4 ± 0.1a	0.3 ± 0.1b	0.2 ± 0.0c

YT	3.2 ± 0.7ab	2.0 ± 0.4b	2.4 ± 0.2ab	3.5 ± 0.4a	0.4 ± 0.1ab	0.4 ± 0.1a	0.3 ± 0.0ab	0.2 ± 0.0b
JJ	5.4 ± 0.7ab	3.5 ± 0.4bc	3.3 ± 0.9c	6.8 ± 0.9a	0.4 ± 0.1ab	0.5 ± 0.1a	0.4 ± 0.1ab	0.2 ± 0.0b
HN	3.8 ± 0.9bc	2.7 ± 0.9c	4.5 ± 0.4b	6.1 ± 0.8a	0.6 ± 0.1bc	0.6 ± 0.2b	0.9 ± 0.1a	0.4 ± 0.0c
XS	4.9 ± 1.2b	2.8 ± 0.9b	4.9 ± 0.8b	8.2 ± 2.1a	0.7 ± 0.2ab	0.6 ± 0.2b	1.0 ± 0.2a	0.5 ± 0.1b

The data shown are the seasonal means ± standard deviations of observation periods (sampling period for each site are given in Table S1). Different letters in the columns of “air concentrations” and “dry deposition fluxes” indicate significant difference between the seasons at $p < 0.05$. The full names of all sites are presented in Table S1).

Table S6. Seasonal average concentrations and deposition fluxes of gaseous HNO₃ at twenty-seven monitoring sites in eastern China.

Sites	Air concentrations				Dry deposition fluxes			
	Spring	Summer	Autumn	Winter	Spring	Summer	Autumn	Winter
CAU	1.9 ± 0.8a	1.9 ± 0.2a	1.8 ± 0.3a	2.3 ± 0.8a	3.5 ± 1.5b	6.3 ± 0.6a	4.6 ± 0.7b	0.6 ± 0.2c
ZZ	2.3 ± 0.5ab	2.8 ± 0.5a	1.5 ± 0.7bc	1.0 ± 0.7c	3.6 ± 0.7a	3.9 ± 0.8a	0.8 ± 0.4b	0.2 ± 0.2b
DL	1.1 ± 0.5a	1.3 ± 0.4a	1.0 ± 0.3a	0.7 ± 0.4a	1.2 ± 0.6a	1.5 ± 0.4a	1.3 ± 0.4a	0.7 ± 0.4a
SZ	1.3 ± 0.3b	1.3 ± 0.5b	1.5 ± 0.3ab	2.0 ± 0.5a	2.7 ± 0.6b	4.3 ± 1.5a	3.5 ± 0.6ab	0.5 ± 0.1c
QZ	1.8 ± 0.3a	1.8 ± 0.8a	1.2 ± 0.4a	1.6 ± 0.6a	2.7 ± 0.6a	2.3 ± 1.0a	1.0 ± 0.3b	0.4 ± 0.2b
YQ	1.3 ± 0.5a	1.0 ± 0.4a	1.0 ± 0.1a	1.3 ± 0.5a	1.0 ± 0.4ab	1.6 ± 0.5a	0.9 ± 0.2b	0.2 ± 0.1c
ZMD	1.6 ± 0.5a	1.8 ± 0.3a	2.0 ± 0.6a	2.2 ± 0.7a	2.9 ± 0.9a	2.9 ± 0.6a	1.5 ± 0.5b	1.2 ± 0.3b
YL	1.1 ± 0.2c	1.2 ± 0.0bc	1.5 ± 0.2ab	1.7 ± 0.3a	1.4 ± 0.2ab	1.6 ± 0.0a	1.1 ± 0.3b	0.4 ± 0.1c
YC	1.2 ± 0.1a	1.9 ± 0.1a	1.9 ± 1.1a	1.3 ± 1.2a	0.4 ± 0.0bc	2.1 ± 0.1a	1.1 ± 0.6b	0.2 ± 0.2c
GZL	0.9 ± 0.0a	0.9 ± 0.1a	1.2 ± 0.4a	1.3 ± 0.4a	0.6 ± 0.1b	1.8 ± 0.1a	1.4 ± 0.5a	0.2 ± 0.0c
LS	0.9 ± 0.2ab	1.0 ± 0.4ab	0.7 ± 0.2b	1.4 ± 0.5a	0.6 ± 0.1b	2.0 ± 0.8a	0.7 ± 0.3b	0.2 ± 0.1b
LSD	1.1 ± 0.1a	0.9 ± 0.3ab	0.7 ± 0.2b	1.0 ± 0.2ab	0.8 ± 0.1ab	1.2 ± 0.4a	0.6 ± 0.2b	0.6 ± 0.2b
CD	1.1 ± 0.2a	1.2 ± 0.2a	1.0 ± 0.2a	1.2 ± 0.2a	0.9 ± 0.2a	0.8 ± 0.1a	1.0 ± 0.2a	1.1 ± 0.2a
NJ	1.6 ± 0.4	1.8 ± 0.5	1.6 ± 0.6	2.2 ± 0.8	2.3 ± 0.3	2.8 ± 0.7	1.3 ± 0.5	0.5 ± 0.2
BY	1.4 ± 0.4a	1.7 ± 0.4a	1.2 ± 0.6a	1.2 ± 0.2a	1.2 ± 0.4bc	2.3 ± 0.6a	1.8 ± 0.8ab	0.6 ± 0.2c
WJ	2.0 ± 0.3a	1.5 ± 0.2b	1.5 ± 0.3ab	1.8 ± 0.3ab	2.0 ± 0.3a	1.7 ± 0.2a	0.7 ± 0.2b	0.6 ± 0.1b
WX	1.3 ± 0.2a	1.3 ± 0.3a	1.1 ± 0.5a	1.4 ± 0.3a	1.0 ± 0.2ab	1.5 ± 0.3a	1.1 ± 0.5a	0.4 ± 0.1b
TJ	0.9 ± 0.3a	0.7 ± 0.1a	0.7 ± 0.2a	0.9 ± 0.1a	0.8 ± 0.4a	1.0 ± 0.2a	0.9 ± 0.3a	0.3 ± 0.0b
FYA	1.3 ± 0.3a	1.4 ± 0.2a	1.4 ± 0.3a	1.5 ± 0.3a	1.9 ± 0.6a	1.7 ± 0.3a	1.0 ± 0.4ab	0.4 ± 0.1b
ZJ	0.8 ± 0.3a	0.4 ± 0.1b	0.9 ± 0.2a	1.0 ± 0.1a	0.5 ± 0.2b	0.5 ± 0.1b	1.4 ± 0.2a	0.6 ± 0.1b
FZ	0.5 ± 0.1ab	0.6 ± 0.2a	0.3 ± 0.2b	0.3 ± 0.1ab	0.8 ± 0.2a	1.0 ± 0.3a	0.6 ± 0.3a	0.6 ± 0.2a

FH	1.1 ± 0.3ab	0.9 ± 0.2b	1.0 ± 0.3b	1.5 ± 0.2a	2.0 ± 0.5a	1.5 ± 0.3a	1.7 ± 0.6a	2.1 ± 0.4a
ZY	1.3 ± 0.5a	0.6 ± 0.2b	0.7 ± 0.3b	1.2 ± 0.2ab	0.7 ± 0.3a	0.8 ± 0.3a	0.5 ± 0.2ab	0.2 ± 0.0b
YT	0.6 ± 0.3a	0.4 ± 0.1a	0.4 ± 0.1a	0.5 ± 0.2a	0.6 ± 0.3a	0.5 ± 0.1a	0.4 ± 0.1a	0.2 ± 0.0a
JJ	1.7 ± 0.7a	1.4 ± 0.8a	1.2 ± 0.6a	1.6 ± 0.4a	0.7 ± 0.3ab	1.9 ± 1.0a	0.9 ± 0.5ab	0.3 ± 0.1b
HN	0.9 ± 0.3a	0.6 ± 0.2a	0.7 ± 0.2a	0.7 ± 0.2a	1.1 ± 0.4a	1.0 ± 0.3a	0.9 ± 0.3a	0.4 ± 0.1b
XS	0.8 ± 0.2a	0.9 ± 0.4a	0.9 ± 0.2a	0.9 ± 0.4a	1.0 ± 0.3ab	1.3 ± 0.5a	1.2 ± 0.3a	0.5 ± 0.2b

The data shown are the seasonal means ± standard deviations of observation periods (sampling period for each site are given in Table S1). Different letters in the columns of “air concentrations” and “dry deposition fluxes” indicate significant difference between the seasons at $p < 0.05$. The full names of all sites are presented in Table S1.

Table S7. Seasonal average concentrations and deposition fluxes of particulate NH₄⁺ at twenty-seven monitoring sites in eastern China.

Sites	Air concentrations				Dry deposition fluxes			
	Spring	Summer	Autumn	Winter	Spring	Summer	Autumn	Winter
CAU	7.9 ± 3.6a	10.4 ± 3.7a	7.8 ± 2.0a	8.8 ± 1.6a	1.5 ± 0.7a	2.0 ± 0.8a	1.2 ± 0.3a	1.0 ± 0.2a
ZZ	8.2 ± 2.1b	12.3 ± 4.5b	10.7 ± 1.7b	18.9 ± 4.6a	1.6 ± 0.4a	2.5 ± 0.9a	1.6 ± 0.3a	2.0 ± 0.5a
DL	3.9 ± 0.8a	4.5 ± 1.6a	3.9 ± 0.3a	5.5 ± 0.9a	0.2 ± 0.1b	0.3 ± 0.1ab	0.3 ± 0.0ab	0.4 ± 0.1a
SZ	6.2 ± 2.2a	8.7 ± 2.1a	6.3 ± 1.9a	6.6 ± 2.0a	1.2 ± 0.4ab	1.7 ± 0.4a	0.9 ± 0.3b	0.7 ± 0.2b
QZ	15.3 ± 10.5a	24.2 ± 12.2a	15.7 ± 9.7a	23.5 ± 12.6a	2.9 ± 1.9a	5.1 ± 2.6a	2.2 ± 1.4a	2.3 ± 1.3a
YQ	4.6 ± 1.4a	5.1 ± 0.6a	5.0 ± 0.6a	5.8 ± 1.4a	0.9 ± 0.3ab	1.2 ± 0.2a	0.7 ± 0.1b	0.6 ± 0.2b
ZMD	11.5 ± 5.4ab	12.7 ± 4.0a	8.8 ± 4.2ab	5.2 ± 0.7b	2.1 ± 1.0a	2.1 ± 0.6a	1.3 ± 0.6ab	0.6 ± 0.1b
YL	4.8 ± 2.7a	6.3 ± 2.4a	4.1 ± 1.8a	7.0 ± 4.2a	0.9 ± 0.5a	1.4 ± 0.6a	0.6 ± 0.3a	0.8 ± 0.5a
YC	8.9 ± 0.8bc	27.9 ± 1.9a	7.3 ± 0.9c	13.1 ± 2.8b	1.6 ± 0.2b	5.0 ± 0.3a	1.0 ± 0.2c	1.3 ± 0.2bc
GZL	4.9 ± 2.3a	6.1 ± 2.6a	3.9 ± 0.8a	5.0 ± 0.5a	0.8 ± 0.3ab	1.0 ± 0.5a	0.4 ± 0.1b	0.4 ± 0.1b
LS	8.3 ± 5.1a	9.8 ± 3.1a	5.9 ± 1.0a	6.0 ± 1.6a	1.3 ± 0.8ab	1.6 ± 0.5a	0.6 ± 0.1b	0.4 ± 0.1b
LSD	4.8 ± 0.7a	5.6 ± 3.3a	4.5 ± 0.8a	6.5 ± 1.4a	0.6 ± 0.1a	0.7 ± 0.4a	0.5 ± 0.1a	0.7 ± 0.2a
CD	5.2 ± 0.8a	5.5 ± 1.0a	4.6 ± 1.5a	4.3 ± 1.4a	0.2 ± 0.0a	0.3 ± 0.0a	0.3 ± 0.1a	0.3 ± 0.1a
NJ	5.6 ± 2.4	4.4 ± 1.8	5.4 ± 0.3	7.8 ± 0.5	0.9 ± 0.3	0.5 ± 0.2	0.5 ± 0.0	0.9 ± 0.1
BY	3.6 ± 0.8a	3.8 ± 0.8a	3.4 ± 1.1a	4.5 ± 0.3a	0.5 ± 0.1a	0.3 ± 0.1b	0.3 ± 0.1b	0.6 ± 0.0a
WJ	8.9 ± 0.5a	3.7 ± 1.5a	6.5 ± 2.7b	12.3 ± 1.3b	4.3 ± 1.0a	3.4 ± 0.6a	1.0 ± 0.2b	1.3 ± 0.5b
WX	4.2 ± 1.3a	4.6 ± 1.7a	5.2 ± 0.6a	6.5 ± 1.0a	0.6 ± 0.2a	0.4 ± 0.2a	0.6 ± 0.1a	0.7 ± 0.1a
TJ	3.6 ± 1.3a	3.3 ± 1.2a	4.5 ± 1.1a	5.4 ± 2.5a	0.5 ± 0.2a	0.4 ± 0.1a	0.6 ± 0.2a	0.7 ± 0.3a
FYA	4.9 ± 1.3b	4.4 ± 0.4b	5.2 ± 1.2b	8.7 ± 1.2a	0.8 ± 0.2a	0.6 ± 0.1a	0.6 ± 0.1a	0.8 ± 0.1a
ZJ	3.6 ± 2.5a	2.0 ± 0.3a	4.1 ± 0.6a	4.6 ± 1.6a	0.5 ± 0.3a	0.1 ± 0.0b	0.4 ± 0.1ab	0.6 ± 0.2a

FZ	2.8 ± 0.7a	1.6 ± 0.3b	2.1 ± 0.5ab	2.4 ± 0.6ab	0.3 ± 0.1a	0.1 ± 0.0b	0.2 ± 0.0ab	0.2 ± 0.1ab
FH	3.6 ± 1.0a	4.2 ± 1.4a	3.9 ± 1.5a	4.5 ± 1.3a	0.5 ± 0.1a	0.4 ± 0.1a	0.4 ± 0.2a	0.5 ± 0.2a
ZY	5.0 ± 2.1ab	3.5 ± 1.3b	4.2 ± 1.4b	7.2 ± 1.4a	1.0 ± 0.4a	0.6 ± 0.2a	0.6 ± 0.2a	1.0 ± 0.2a
YT	2.9 ± 1.1a	2.7 ± 0.8a	2.4 ± 0.9a	2.7 ± 0.6a	0.5 ± 0.2a	0.4 ± 0.1a	0.3 ± 0.1a	0.4 ± 0.1a
JJ	8.9 ± 0.5ab	3.7 ± 1.5c	6.5 ± 2.7bc	12.3 ± 1.3a	1.8 ± 0.1a	0.6 ± 0.2b	0.9 ± 0.4b	1.9 ± 0.2a
HN	3.5 ± 0.6a	3.4 ± 1.4a	4.5 ± 1.2a	5.4 ± 1.3a	0.5 ± 0.1ab	0.3 ± 0.1b	0.6 ± 0.2ab	0.7 ± 0.2a
XS	3.6 ± 0.7a	3.2 ± 0.7a	4.0 ± 1.5a	4.1 ± 1.6a	0.5 ± 0.1a	0.3 ± 0.1a	0.5 ± 0.2a	0.5 ± 0.2a

The data shown are the seasonal means ± standard deviations of observation periods (sampling period for each site are given in Table S1). Different letters in the columns of “air concentrations” and “dry deposition fluxes” indicate significant difference between the seasons at $p < 0.05$. The full names of all sites are presented in Table S1.

Table S8. Seasonal average concentrations and deposition fluxes of particulate NO₃⁻ at twenty-seven monitoring sites in eastern China.

Sites	Air concentrations				Dry deposition fluxes			
	Spring	Summer	Autumn	Winter	Spring	Summer	Autumn	Winter
CAU	4.7 ± 1.6ab	4.2 ± 1.2b	5.9 ± 1.1ab	6.5 ± 0.8a	0.9 ± 0.3a	0.8 ± 0.2a	0.9 ± 0.2a	0.7 ± 0.1a
ZZ	4.8 ± 1.1b	4.3 ± 0.5b	7.1 ± 2.2b	13.3 ± 4.5a	0.9 ± 0.2a	0.9 ± 0.1a	1.0 ± 0.3a	1.4 ± 0.5a
DL	2.5 ± 1.3a	2.1 ± 0.8a	1.8 ± 0.9a	3.6 ± 1.7a	0.2 ± 0.1ab	0.2 ± 0.1ab	0.1 ± 0.1b	0.3 ± 0.1a
SZ	3.3 ± 0.7a	2.9 ± 0.9a	3.9 ± 0.6a	4.0 ± 1.4a	0.6 ± 0.1a	0.5 ± 0.2a	0.6 ± 0.1a	0.5 ± 0.1a
QZ	4.5 ± 2.3b	3.7 ± 1.6b	6.2 ± 2.8ab	9.7 ± 4.0a	0.9 ± 0.4a	0.8 ± 0.3a	0.9 ± 0.4a	0.9 ± 0.4a
YQ	2.7 ± 0.9a	2.2 ± 0.6a	2.9 ± 0.8a	3.1 ± 1.3a	0.5 ± 0.2a	0.5 ± 0.2a	0.4 ± 0.1a	0.3 ± 0.1a
ZMD	3.7 ± 0.7bc	3.1 ± 0.6c	5.4 ± 0.8ab	6.8 ± 2.0a	0.7 ± 0.1ab	0.6 ± 0.1b	0.8 ± 0.1a	0.8 ± 0.2a
YL	3.2 ± 0.7b	2.4 ± 0.3b	4.1 ± 0.7b	7.5 ± 2.2a	0.6 ± 0.1ab	0.5 ± 0.1b	0.5 ± 0.1ab	0.8 ± 0.2a
YC	4.1 ± 0.8ab	3.0 ± 0.3b	3.9 ± 1.2ab	6.6 ± 1.5a	0.7 ± 0.1a	0.6 ± 0.1a	0.5 ± 0.2a	0.6 ± 0.1a
GZL	1.7 ± 0.4a	1.7 ± 0.3a	2.3 ± 0.8a	2.5 ± 0.8a	0.3 ± 0.1a	0.3 ± 0.0a	0.2 ± 0.1a	0.2 ± 0.0a
LS	1.6 ± 0.8a	1.7 ± 0.4a	2.0 ± 0.5a	2.4 ± 0.8a	0.3 ± 0.1a	0.3 ± 0.1a	0.2 ± 0.1a	0.2 ± 0.1a
LSD	2.1 ± 0.4ab	1.5 ± 0.3b	1.5 ± 0.7b	3.1 ± 0.9a	0.3 ± 0.1a	0.2 ± 0.0a	0.2 ± 0.1a	0.3 ± 0.1a
CD	3.1 ± 0.4a	2.4 ± 0.3a	2.7 ± 0.5a	2.7 ± 0.7a	0.1 ± 0.0a	0.1 ± 0.0a	0.2 ± 0.0a	0.2 ± 0.1a
NJ	3.5 ± 0.8	2.5 ± 0.2	2.7 ± 0.9	3.8 ± 0.5	0.6 ± 0.0	0.2 ± 0.0	0.3 ± 0.1	0.4 ± 0.1
BY	3.0 ± 0.7a	2.3 ± 0.4a	2.2 ± 0.6a	2.9 ± 0.2a	0.4 ± 0.1a	0.2 ± 0.0b	0.2 ± 0.1b	0.4 ± 0.0a
WJ	2.7 ± 0.8b	2.0 ± 0.7b	2.8 ± 0.7ab	4.6 ± 1.5a	0.5 ± 0.2a	0.4 ± 0.1a	0.4 ± 0.1a	0.6 ± 0.2a
WX	1.7 ± 0.5a	1.3 ± 0.4a	1.9 ± 1.4a	2.9 ± 0.6a	0.2 ± 0.1ab	0.1 ± 0.0b	0.2 ± 0.2ab	0.3 ± 0.1a
TJ	0.9 ± 0.3b	0.5 ± 0.0b	1.3 ± 0.6b	2.5 ± 1.0a	0.1 ± 0.0b	0.1 ± 0.0b	0.2 ± 0.1ab	0.3 ± 0.1a
FYA	2.8 ± 0.4a	2.1 ± 0.1a	3.0 ± 1.4a	4.5 ± 2.3a	0.4 ± 0.1a	0.3 ± 0.0a	0.3 ± 0.2a	0.4 ± 0.1a
ZJ	2.3 ± 0.7ab	1.1 ± 0.2b	2.2 ± 0.4ab	3.4 ± 1.5a	0.3 ± 0.1ab	0.1 ± 0.0c	0.2 ± 0.0bc	0.4 ± 0.2a

FZ	$1.4 \pm 0.1a$	$1.1 \pm 0.1a$	$1.1 \pm 0.5a$	$1.2 \pm 0.2a$	$0.2 \pm 0.0a$	$0.1 \pm 0.0a$	$0.1 \pm 0.0a$	$0.1 \pm 0.0a$
FH	$1.9 \pm 0.3ab$	$1.1 \pm 0.4c$	$1.6 \pm 0.7bc$	$2.7 \pm 0.4a$	$0.3 \pm 0.0ab$	$0.1 \pm 0.0c$	$0.2 \pm 0.1bc$	$0.3 \pm 0.0a$
ZY	$1.6 \pm 0.4bc$	$0.7 \pm 0.4c$	$1.9 \pm 1.0ab$	$2.9 \pm 0.5a$	$0.3 \pm 0.1a$	$0.1 \pm 0.1b$	$0.3 \pm 0.1ab$	$0.4 \pm 0.1a$
YT	$1.3 \pm 0.4a$	$0.8 \pm 0.1a$	$0.9 \pm 0.6a$	$1.2 \pm 0.3a$	$0.2 \pm 0.1a$	$0.1 \pm 0.0a$	$0.1 \pm 0.1a$	$0.2 \pm 0.0a$
JJ	$2.9 \pm 0.7ab$	$1.7 \pm 0.8b$	$2.5 \pm 1.6ab$	$4.9 \pm 0.8a$	$0.6 \pm 0.1a$	$0.3 \pm 0.1a$	$0.4 \pm 0.2a$	$0.8 \pm 0.1a$
HN	$1.4 \pm 0.3b$	$0.6 \pm 0.2b$	$1.3 \pm 0.5b$	$3.2 \pm 1.9a$	$0.2 \pm 0.0b$	$0.1 \pm 0.0b$	$0.2 \pm 0.1b$	$0.4 \pm 0.2a$
XS	$1.2 \pm 0.6ab$	$0.7 \pm 0.1b$	$1.2 \pm 0.4ab$	$2.0 \pm 1.0a$	$0.2 \pm 0.1a$	$0.1 \pm 0.0a$	$0.2 \pm 0.0a$	$0.2 \pm 0.1a$

The data shown are the seasonal means \pm standard deviations of observation periods (sampling period for each site are given in Table S1). Different letters in the columns of “air concentrations” and “dry deposition fluxes” indicate significant difference between the seasons at $p < 0.05$. The full names of all sites are presented in Table S1.

Table S9. Seasonal average concentrations and deposition fluxes of the total N_r at twenty-seven monitoring sites in eastern China.

Sites	Air concentrations				Dry deposition fluxes			
	Spring	Summer	Autumn	Winter	Spring	Summer	Autumn	Winter
CAU	38.6 ± 4.5ab	45.3 ± 3.6a	40.9 ± 4.2ab	35.7 ± 3.0b	11.7 ± 2.2b	21.0 ± 0.3a	13.6 ± 1.3b	3.9 ± 0.7c
ZZ	39.6 ± 2.9b	43.6 ± 4.1b	43.2 ± 2.0b	54.6 ± 9.2a	11.4 ± 1.2a	12.5 ± 1.3a	7.0 ± 1.0b	5.9 ± 0.9b
DL	20.5 ± 6.5a	21.3 ± 7.1a	18.9 ± 4.8a	19.3 ± 4.7a	5.9 ± 1.6a	7.7 ± 1.7a	6.0 ± 1.4a	2.1 ± 0.2b
SZ	29.4 ± 3.4ab	35.2 ± 2.1a	28.1 ± 5.2ab	25.9 ± 4.4b	9.0 ± 1.1b	16.3 ± 1.3a	9.6 ± 1.2b	2.9 ± 0.6c
QZ	45.9 ± 18.2a	55.2 ± 16.5a	44.5 ± 14.6a	57.3 ± 22.6a	12.2 ± 4.2ab	15.2 ± 4.3a	8.7 ± 2.6ab	7.0 ± 3.6b
YQ	23.0 ± 1.1a	21.2 ± 2.2ab	19.5 ± 1.1b	19.7 ± 2.4b	5.1 ± 0.5b	6.6 ± 0.8a	3.6 ± 0.2c	1.9 ± 0.4d
ZMD	37.4 ± 8.7a	35.4 ± 7.2a	36.6 ± 6.2a	34.0 ± 3.7a	11.3 ± 1.6a	10.1 ± 1.2a	7.7 ± 0.9b	5.5 ± 0.6c
YL	23.9 ± 6.7a	26.6 ± 8.2a	26.0 ± 4.3a	31.7 ± 7.7a	6.6 ± 1.7ab	9.3 ± 2.9a	6.0 ± 1.2b	3.8 ± 1.0b
YC	34.9 ± 5.2b	58.4 ± 5.0a	35.2 ± 3.1b	41.6 ± 3.1b	6.2 ± 0.7bc	13.8 ± 0.8a	6.5 ± 0.5b	4.6 ± 0.2c
GZL	19.1 ± 2.6b	26.3 ± 3.0a	17.5 ± 2.2b	16.1 ± 1.7b	3.9 ± 0.3b	10.5 ± 1.0a	4.4 ± 0.7b	1.0 ± 0.1c
LS	31.6 ± 8.0a	31.2 ± 4.4a	24.3 ± 2.9ab	18.4 ± 2.3b	6.5 ± 1.2b	10.8 ± 1.7a	5.5 ± 0.8b	1.8 ± 0.3c
LSD	17.5 ± 1.0a	20.8 ± 4.4a	17.5 ± 2.5a	20.1 ± 2.3a	4.7 ± 0.4b	7.7 ± 1.8a	4.2 ± 0.7bc	2.4 ± 0.4c
CD	20.7 ± 1.2ab	21.1 ± 1.8a	16.9 ± 2.6ab	16.4 ± 3.4b	4.9 ± 0.4ab	6.0 ± 1.1a	4.5 ± 0.7b	2.3 ± 0.3c
NJ	30.5 ± 2.0	26.8 ± 1.7	21.7 ± 1.4	28.5 ± 1.0	7.8 ± 0.4	8.6 ± 1.5	4.2 ± 0.8	3.1 ± 0.3
BY	26.2 ± 3.0a	27.1 ± 1.8a	23.8 ± 1.7ab	21.0 ± 0.9b	5.3 ± 0.8b	7.0 ± 0.5a	6.8 ± 0.6a	3.6 ± 0.2c
WJ	48.5 ± 4.1a	44.7 ± 11.2a	27.6 ± 3.9b	34.7 ± 9.0ab	12.2 ± 0.8a	12.5 ± 3.3a	5.2 ± 1.2b	5.1 ± 1.2b
WX	20.3 ± 2.6a	21.4 ± 2.4a	21.2 ± 4.2a	21.6 ± 1.1a	4.5 ± 0.8b	6.2 ± 0.6a	4.9 ± 0.6b	2.6 ± 0.2c
TJ	12.0 ± 2.3a	11.8 ± 1.1a	11.8 ± 2.3a	14.6 ± 2.7a	2.9 ± 0.8ab	3.7 ± 0.4a	3.0 ± 0.8a	1.8 ± 0.3b
FYA	21.5 ± 3.7a	24.8 ± 4.2a	23.3 ± 3.2a	26.9 ± 3.8a	6.0 ± 0.2ab	7.0 ± 1.5a	4.1 ± 0.7bc	2.7 ± 0.4c
ZJ	19.6 ± 4.3a	15.9 ± 1.6a	18.2 ± 2.7a	17.4 ± 3.1a	3.5 ± 0.8b	3.7 ± 0.5b	5.0 ± 0.7a	2.8 ± 0.4b
FZ	10.6 ± 1.3a	9.6 ± 1.3ab	6.7 ± 0.6c	7.9 ± 1.5bc	3.3 ± 0.6ab	4.3 ± 1.0a	2.4 ± 0.3bc	2.0 ± 0.6c
FH	20.2 ± 3.7a	18.0 ± 2.2a	17.9 ± 2.1a	20.5 ± 1.9a	6.6 ± 1.5a	6.2 ± 1.2ab	5.6 ± 0.7ab	4.5 ± 0.4b

ZY	20.1 ± 2.3a	13.2 ± 3.4c	14.6 ± 3.0bc	18.8 ± 1.8ab	4.5 ± 0.6a	3.8 ± 1.1ab	2.8 ± 0.7b	2.6 ± 0.3b
YT	11.2 ± 2.1b	15.2 ± 1.3a	8.6 ± 0.3b	9.6 ± 0.6b	2.7 ± 0.8b	4.9 ± 0.4a	1.9 ± 0.2bc	1.2 ± 0.1c
JJ	25.9 ± 1.4ab	15.5 ± 4.6c	16.8 ± 5.3bc	28.0 ± 1.6a	5.5 ± 0.5a	5.2 ± 1.9a	3.6 ± 1.2a	3.7 ± 0.3a
HN	13.7 ± 1.3b	14.3 ± 2.2ab	13.2 ± 2.1b	17.3 ± 1.5a	3.7 ± 0.5a	4.6 ± 1.0a	3.5 ± 0.9ab	2.2 ± 0.2b
XS	13.2 ± 1.3ab	11.0 ± 2.4b	12.7 ± 1.7ab	16.7 ± 3.6a	3.3 ± 0.7ab	3.7 ± 1.1a	3.6 ± 0.5a	2.1 ± 0.2b

The data shown are the seasonal means ± standard deviations of observation periods (sampling period for each site are given in Table S1). Different letters in the columns of “air concentrations” and “dry deposition fluxes” indicate significant difference between the seasons at $p < 0.05$. The full names of all sites are presented in Table S1.

Table S10. Seasonal volume-weighted mean concentrations and wet/bulk deposition fluxes of $\text{NH}_4^+\text{-N}$ in precipitation at twenty-seven monitoring sites in eastern China.

Sites	Volume-weighted mean concentrations				Wet/bulk deposition fluxes			
	Spring	Summer	Autumn	Winter	Spring	Summer	Autumn	Winter
CAU	2.8	2.6	2.9	3.9	$1.7 \pm 0.9\text{b}$	$10.8 \pm 6.8\text{a}$	$2.5 \pm 2.0\text{b}$	$0.4 \pm 0.3\text{b}$
ZZ	4.5	3.2	1.6	3.8	2.6	8.0	4.5	1.3
DL	2.5	0.8	1.1	5.2	$1.8 \pm 0.9\text{ab}$	$3.1 \pm 0.7\text{a}$	$1.2 \pm 0.4\text{b}$	$1.2 \pm 1.1\text{b}$
SZ	3.2	2.2	1.8	6.1	$1.5 \pm 1.0\text{b}$	$7.6 \pm 3.9\text{a}$	$1.8 \pm 1.6\text{b}$	$0.3 \pm 0.4\text{b}$
QZ	3.0	4.0	2.6	3.8	$2.2 \pm 1.5\text{b}$	$10.5 \pm 5.4\text{a}$	$1.9 \pm 0.9\text{b}$	$0.5 \pm 0.9\text{b}$
YQ	2.8	2.1	1.5	2.7	$2.0 \pm 0.6\text{b}$	$5.0 \pm 1.6\text{a}$	$2.2 \pm 1.4\text{b}$	$0.2 \pm 0.1\text{b}$
ZMD	2.0	2.2	2.1	3.8	$2.6 \pm 0.2\text{a}$	$5.8 \pm 3.8\text{a}$	$5.8 \pm 5.9\text{a}$	$1.5 \pm 0.9\text{a}$
YL	2.2	2.3	2.1	6.6	$2.8 \pm 0.9\text{ab}$	$5.6 \pm 3.9\text{a}$	$4.9 \pm 3.7\text{ab}$	$0.5 \pm 0.4\text{b}$
YC	4.5	3.3	2.8	10.7	$2.5 \pm 1.8\text{b}$	$10.4 \pm 3.1\text{a}$	$1.5 \pm 0.6\text{b}$	$3.2 \pm 3.1\text{b}$
GZL	2.6	1.1	1.1	2.9	$2.4 \pm 1.3\text{ab}$	$3.7 \pm 0.8\text{a}$	$1.1 \pm 0.2\text{bc}$	$0.7 \pm 0.1\text{c}$
LS	2.0	1.3	1.9	4.2	$1.6 \pm 0.5\text{b}$	$4.2 \pm 0.9\text{a}$	$1.7 \pm 1.4\text{b}$	$0.3 \pm 0.2\text{b}$
LSD	2.1	1.9	1.9	1.6	$1.9 \pm 2.4\text{b}$	$4.8 \pm 0.4\text{a}$	$2.0 \pm 1.9\text{b}$	$0.6 \pm 0.4\text{b}$
CD	2.0	1.2	0.9	3.9	$1.2 \pm 0.3\text{b}$	$3.7 \pm 1.3\text{a}$	$0.5 \pm 0.3\text{b}$	$1.0 \pm 0.8\text{b}$
NJ	1.1	1.6	0.7	0.9	1.1 ± 0.3	11.0 ± 1.2	1.0 ± 0.2	0.6 ± 0.1
BY	0.6	0.3	0.4	1.0	$3.5 \pm 1.3\text{a}$	$2.2 \pm 0.6\text{ab}$	$0.7 \pm 0.4\text{b}$	$1.1 \pm 1.0\text{b}$
WJ	2.0	1.2	1.3	6.7	$3.2 \pm 1.4\text{b}$	$6.4 \pm 2.7\text{a}$	$2.4 \pm 0.9\text{b}$	$1.0 \pm 0.9\text{b}$
WX	1.0	1.2	1.0	1.0	$3.8 \pm 0.8\text{ab}$	$5.1 \pm 2.1\text{a}$	$2.0 \pm 1.3\text{bc}$	$0.8 \pm 0.6\text{c}$
TJ	2.8	2.6	2.9	3.9	$5.7 \pm 1.4\text{a}$	$3.7 \pm 1.4\text{a}$	$3.7 \pm 1.4\text{a}$	$5.3 \pm 2.8\text{a}$
FYA	1.2	0.8	2.0	3.4	2.2 ± 0.2	3.3 ± 0.6	2.5 ± 3.3	1.7 ± 0.6
ZJ	0.3	0.3	0.5	0.3	$0.7 \pm 0.6\text{ab}$	$1.7 \pm 0.3\text{a}$	$1.5 \pm 0.6\text{a}$	$0.1 \pm 0.1\text{b}$

FZ	0.7	0.4	0.5	0.5	3.1 ± 1.2a	3.1 ± 1.1a	1.8 ± 2.3a	1.1 ± 0.4a
FH	0.9	0.4	0.4	1.6	2.8 ± 0.8a	2.8 ± 0.6a	1.5 ± 1.0a	3.4 ± 2.2a
ZY	1.9	1.0	1.0	3.3	3.7 ± 2.3ab	5.5 ± 2.0a	1.8 ± 1.0b	1.0 ± 1.0b
YT	1.0	1.0	0.8	1.1	2.2 ± 0.2	5.8 ± 0.8	2.2 ± 0.1	0.3 ± 0.3
JJ	2.5	1.3	1.5	5.6	6.0 ± 1.5a	6.4 ± 2.4a	2.9 ± 1.8a	3.7 ± 3.3a
HN	1.0	0.9	0.9	1.4	5.1 ± 1.3b	3.9 ± 2.3ab	2.1 ± 1.1a	2.4 ± 1.3a
XS	1.1	0.5	1.0	1.6	6.3 ± 4.8b	2.4 ± 1.2a	2.3 ± 1.4a	2.6 ± 0.7ab

The data on wet/bulk deposition fluxes are the seasonal means ± standard deviations of observation periods (sampling periods at all sites are given in Table S1). Different letters in the “wet/bulk deposition fluxes” column indicate significant difference between the seasons at $p < 0.05$.

The full names of all sites are presented in Table S1.

Table S11. Seasonal volume-weighted mean concentrations and wet/bulk deposition fluxes of NO₃⁻-N in precipitation at twenty-seven monitoring sites in eastern China.

Sites	Volume-weighted mean concentrations				Wet/bulk deposition fluxes (Mean ± SD)			
	Spring	Summer	Autumn	Winter	Spring	Summer	Autumn	Winter
CAU	3.5	2.0	3.5	4.0	2.1 ± 0.6bc	8.3 ± 2.2a	3.1 ± 1.5b	0.4 ± 0.3c
ZZ	4.6	2.1	1.6	2.8	2.7	5.1	4.4	0.9
DL	2.7	1.6	3.3	5.5	1.9 ± 0.7bc	6.0 ± 1.8a	3.3 ± 0.9b	1.3 ± 0.9c
SZ	2.3	2.4	1.8	3.0	1.1 ± 0.6b	8.4 ± 6.1a	1.8 ± 1.4b	0.1 ± 0.2b
QZ	2.7	2.1	2.0	4.5	1.9 ± 2.0b	5.5 ± 1.6a	1.5 ± 1.0b	0.6 ± 1.1b
YQ	2.7	1.9	2.7	3.6	2.0 ± 0.5ab	4.5 ± 1.5a	3.8 ± 2.7a	0.2 ± 0.2b
ZMD	2.2	1.7	1.9	2.6	2.9 ± 1.5a	4.5 ± 1.8a	5.3 ± 6.2a	1.0 ± 0.2a
YL	1.8	1.4	1.3	4.3	2.3 ± 0.9a	3.2 ± 2.7a	3.0 ± 1.7a	0.3 ± 0.3a
YC	4.0	2.0	2.7	4.2	2.3 ± 1.8ab	6.4 ± 3.2a	1.5 ± 0.9ab	1.3 ± 0.8b
GZL	2.6	1.4	1.5	2.8	2.5 ± 1.0ab	4.6 ± 2.5a	1.5 ± 0.5b	0.6 ± 0.1b
LS	2.8	1.1	1.5	6.0	2.3 ± 0.6b	3.6 ± 0.9a	1.4 ± 0.4bc	0.4 ± 0.5c
WW	3.8	1.4	1.6	2.8	0.8 ± 0.8ab	1.0 ± 0.4a	0.3 ± 0.2ab	0.1 ± 0.1b
LSD	1.4	1.2	1.9	1.2	1.2 ± 0.7ab	3.1 ± 1.6a	2.0 ± 1.7ab	0.4 ± 0.2b
CD	3.2	1.3	1.6	6.1	1.9 ± 0.6b	3.9 ± 0.9a	1.0 ± 0.5b	1.6 ± 1.0b
NJ	1.4	1.7	1.2	1.4	1.4 ± 0.7	11.6 ± 2.1	1.7 ± 0.9	1.4 ± 0.2
BY	0.8	0.9	1.5	1.7	4.7 ± 1.8ab	6.9 ± 2.8a	3.0 ± 1.1b	1.7 ± 0.6b
WJ	4.8	1.0	1.8	7.3	7.8 ± 2.2a	5.4 ± 3.2ab	3.2 ± 0.8bc	1.1 ± 0.7c
WX	0.9	1.0	0.8	1.0	3.4 ± 0.7a	4.1 ± 3.9a	1.7 ± 0.5a	0.8 ± 0.6a
TJ	3.5	2.0	3.5	4.0	4.0 ± 1.1a	1.9 ± 0.7a	3.1 ± 1.4a	4.0 ± 2.0a
FYA	1.0	0.9	1.9	2.5	1.8 ± 0.5	3.8 ± 1.7	2.4 ± 2.2	1.3 ± 0.6

ZJ	0.6	0.3	0.7	2.3	$1.2 \pm 0.9a$	$1.9 \pm 0.3a$	$2.1 \pm 0.6a$	$0.8 \pm 1.0a$
FZ	0.8	0.3	0.6	0.6	$3.6 \pm 2.0a$	$2.8 \pm 1.5a$	$2.1 \pm 1.8a$	$1.3 \pm 0.6a$
FH	1.0	0.5	0.7	1.9	$3.1 \pm 1.2a$	$3.7 \pm 0.7a$	$2.5 \pm 0.4a$	$4.0 \pm 2.9a$
ZY	2.0	1.0	1.3	3.5	$3.8 \pm 1.2ab$	$5.1 \pm 1.8a$	$2.2 \pm 0.6bc$	$1.0 \pm 0.7c$
YT	0.7	0.5	0.5	2.2	1.5 ± 0.4	3.0 ± 0.2	1.5 ± 0.6	0.7 ± 0.6
JJ	1.5	0.7	1.0	4.4	$3.6 \pm 0.3a$	$3.4 \pm 1.4a$	$2.0 \pm 1.2a$	$3.0 \pm 1.2a$
HN	0.6	0.4	0.6	1.1	$2.9 \pm 0.8a$	$1.6 \pm 0.4a$	$1.5 \pm 0.8a$	$1.9 \pm 1.0a$
XS	0.5	0.3	0.6	1.2	$3.1 \pm 1.8a$	$1.3 \pm 0.5a$	$1.5 \pm 0.8a$	$1.9 \pm 0.8a$

The data on wet/bulk deposition fluxes are the seasonal means \pm standard deviations of observation periods (sampling periods at all sites are given in Table S1). Different letters in the “wet/bulk deposition fluxes” column indicate significant difference between the seasons at $p < 0.05$.

The full names of all sites are presented in Table S1.

Table S12. Seasonal volume-weighted mean concentrations and wet/bulk deposition fluxes of TIN (the sum of NH₄⁺-N and NO₃⁻-N) in precipitation at twenty-seven monitoring sites in eastern China.

Sites	Volume-weighted mean concentrations				Wet/bulk deposition fluxes (Mean ± SD)			
	Spring	Summer	Autumn	Winter	Spring	Summer	Autumn	Winter
CAU	6.3	4.6	6.4	7.9	3.9 ± 1.2b	19.1 ± 8.9a	5.6 ± 2.9b	0.8 ± 0.6b
ZZ	9.1	5.3	3.2	6.6	5.2	13.1	8.9	2.2
DL	5.2	2.4	4.4	10.7	3.7 ± 1.1b	9.2 ± 1.3a	4.5 ± 1.3b	2.4 ± 1.9b
SZ	5.5	4.6	3.6	9.1	2.7 ± 1.5b	16.0 ± 9.8a	3.6 ± 3.0b	0.4 ± 0.6b
QZ	5.7	6.1	4.6	8.3	4.1 ± 3.0b	16.0 ± 6.3a	3.4 ± 1.7b	1.1 ± 2.0b
YQ	5.5	4.0	4.2	6.3	4.0 ± 1.0bc	9.6 ± 2.9a	6.0 ± 3.8ab	0.4 ± 0.3c
ZMD	4.2	3.9	4.0	6.4	5.5 ± 1.3a	10.3 ± 5.3a	11.0 ± 12.0a	2.5 ± 1.1a
YL	4.0	3.7	3.4	10.9	5.0 ± 1.6ab	8.8 ± 6.6a	7.9 ± 5.1ab	0.7 ± 0.7b
YC	8.5	5.3	5.5	14.9	4.8 ± 3.6b	16.8 ± 6.0a	3.0 ± 1.4b	4.4 ± 3.9b
GZL	5.2	2.5	2.6	5.7	4.9 ± 2.3ab	8.3 ± 3.0a	2.6 ± 0.5bc	1.3 ± 0.2c
LS	4.8	2.4	3.4	10.2	3.9 ± 1.0b	7.8 ± 0.6a	3.1 ± 1.7b	0.6 ± 0.8c
WW	8.9	4.9	4.9	7.4	1.8 ± 1.5ab	3.6 ± 1.2a	1.1 ± 0.7b	0.3 ± 0.3b
LSD	3.5	3.1	3.8	2.8	3.1 ± 2.7b	7.9 ± 1.8a	4.0 ± 3.6ab	1.0 ± 0.5b
CD	5.2	2.5	2.5	10.0	3.1 ± 0.9b	7.6 ± 2.0a	1.5 ± 0.7b	2.6 ± 1.8b
NJ	2.5	3.3	1.9	2.3	2.6 ± 1.0	22.6 ± 3.3	2.6 ± 0.7	2.0 ± 0.3
BY	1.4	1.2	1.9	2.7	8.2 ± 2.2a	9.1 ± 2.8a	3.8 ± 1.3b	2.7 ± 0.8b
WJ	6.8	2.2	3.1	14.0	11 ± 2.9a	11.8 ± 4.1a	5.6 ± 1.5b	2.1 ± 1.6b
WX	1.9	2.2	1.8	2.0	7.3 ± 1.5ab	9.1 ± 4.9a	3.7 ± 1.8ab	1.6 ± 1.2b
TJ	6.3	4.6	6.4	7.9	9.7 ± 2.5a	5.6 ± 2.0a	6.8 ± 2.8a	9.2 ± 4.8a
FYA	2.2	1.7	3.9	5.9	4.1 ± 0.6	7.1 ± 2.3	4.9 ± 5.4	3.0 ± 1.2
ZJ	0.9	0.6	1.2	2.6	1.9 ± 0.9ab	3.6 ± 0.3a	3.5 ± 1.0a	0.9 ± 1.1b
FZ	1.5	0.7	1.1	1.1	6.7 ± 3.0a	5.9 ± 2.5a	3.9 ± 4.1a	2.4 ± 0.9a

FH	1.9	0.9	1.1	3.5	$5.9 \pm 1.8a$	$6.6 \pm 1.1a$	$4.0 \pm 1.0a$	$7.5 \pm 5.0a$
ZY	3.9	2.0	2.3	6.8	$7.5 \pm 2.4ab$	$10 \pm 3.0a$	$4.3 \pm 1.0bc$	$2.0 \pm 1.7c$
YT	1.7	1.5	1.3	3.3	$3.7 \pm 0.6b$	$8.8 \pm 1.0a$	$3.7 \pm 0.7b$	$1.0 \pm 0.9b$
JJ	4.0	2.0	2.5	10.0	$9.6 \pm 1.8a$	$9.8 \pm 3.7a$	$4.9 \pm 3.0a$	$6.7 \pm 3.3a$
HN	1.6	1.3	1.5	2.5	$8.1 \pm 2.0a$	$5.5 \pm 2.7a$	$3.6 \pm 1.8a$	$4.3 \pm 2.2a$
XS	1.6	0.8	1.6	2.8	$9.4 \pm 6.4a$	$3.7 \pm 1.6a$	$3.8 \pm 1.9a$	$4.5 \pm 1.5a$

The data on wet/bulk deposition fluxes are the seasonal means \pm standard deviations of observation periods (sampling periods at all sites are given in **Table S1**). Different letters in the “wet/bulk deposition fluxes” column indicate significant difference between the seasons at $p < 0.05$.

The full names of all sites are presented in **Table S1**.

Table S13. Annual NH₃ and NO_x emissions over Eastern China and its contribution to total emissions in China (Tg N a⁻¹)

	Source Type	Eastern China	Eastern China/China
NH ₃	Fertilizer ^a	7.3	93%
	Livestock	1.8	76%
	Human waste	1.4	93%
	Fuel combustion ^b	0.6	93%
	Natural	0.4	81%
	Total	11.6	90%
NO _x	Industry	3.1	92%
	Power	2.5	88%
	Transportation	2.1	91%
	Residential	0.3	90%
	Natural ^c	0.5	68%
	Total	8.5	89%

^aFertilizer NH₃ emissions include both chemical fertilizer and manure fertilizer.

^bNH₃ emissions from fuel combustion in power plant, industry, transportation and residential.

^cNatural NO_x emissions from soil, lighting and biomass burning.